The search for the liquid-gas phase transition in nuclei

Josef Pochodzalla [a]

[a] *Max-Planck Institut für Kernphysik,Saupfercheckweg 1, 69177 Heidelberg, Germany*

Abstract

More than two decades ago, the van der Waals behavior of the nucleon - nucleon force inspired the idea of a liquid-gas phase transition in nuclear matter. Heavy-ion reactions at relativistic energies offer the unique possibility for studying this phase transition in a finite, hadronic system. A general overview of this subject is given emphasizing the most recent results on nuclear calorimetry.

1 The Essence of Nuclei

The dramatic changes of the properties of a substance undergoing a phase transition fascinated mankind since the early beginnings of science. Empedocles of Acragas – the Greek philosopher, statesman and poet – suggested nearly 2500 years ago that the world is composed of four primal elements: *earth, water, air* and *fire* [Empedocles, 440BC]. Indeed, a glass of liquid water cooled below 0^oC will freeze to ice showing the solid character of earth. Water heated above 100^oC will build an airy gas. Finally, at high temperatures atoms disintegrate into a plasma of electrons and ions which – loosely speaking –may be considered as the analog to fire. In that sense the four roots *earth, water, air* and *fire* can be considered as a symbol for what we call now the *solid, liquid, gas* and *plasma* phases.

The prospect of creating a phase of matter resembling that of the pre-hadronic phase of the early universe or of the core of today's neutron stars [Glendenning, 1992] is one of the prime motivations to study relativistic heavy ion collisions [Harris and Müller, 1996]. Unquestionable, the transition to the quark-gluon plasma represents the most spectacular example of a phase transition in nuclear matter. The complex structure of the hadronic components and the many facets of their interaction [Tamagaki, 1993], however, offer the opportunity to observe in addition several other, exciting nuclear state transitions [Siemens, 1984]. Already two decades ago, the van der Waals behavior of the nucleon - nucleon force inspired the idea of a liquid-gas phase transition in nuclear matter [Lamb *et al.*, 1978; Jaqaman *et al.*, 1983; Siemens, 1983; Goodman *et al.*, 1984]. For an infinite nuclear system the critical point should be located at a critical temperature of 15 - 20 MeV and a critical density of about 1/3 - 1/2 normal nuclear matter density. What makes this nuclear liquid gas phase transition stand out from all other conceivable nuclear phase transitions though, is the fact that both phases, cold nuclear Fermi liquids on the one hand and a nuclear gas consisting of free nucleons and a few light clusters on the other hand, are known to exist in nature, and, what may perhaps be even more important, that both are experimentally accessible. This unique feature makes the nuclear liquid-gas phase transition an ideal and relevant test case for our ability to identify and quantify a phase transition in a finite hadronic system.

Probing the phase diagram of a substance two main topics arise. The first concerns the location of the critical point and the properties of the system when the critical point is approached, i.e. the critical exponents. The second question deals with the boundaries between the liquid and the gas phase. While the question of criticality is strongly related with the fragment size distribution, the exploration of the phase boundaries is possible via calorimetric studies.

In the nuclear physics case, the only directly measurable quantities are the size and momenta of the clusters produced in an interaction. Using Fishers droplet model of condensation [Fisher, 1967] the cluster size distribution can be related to thermodynamic quantities. For example, the second moment of the cluster size distribution reflects the isothermal compressibility. Another prediction of this theory is that in case of a second order phase transition *at* the critical point the distribution of the fragment size s should follow a simple power law. According to the theory of critical phenomena the critical exponent τ which describes this self-similar distribution ($n_s \propto s^{-\tau}$) lie between 2 and 3 for many universality classes [Stauffer and Aharony, 1992]. Consequently, the first observation of a power law for the fragment mass distribution in proton induced reactions on Kr and Xe targets [Finn *et al.*, 1982; Hirsch *et al.*, 1984] was – supported by the early predictions of nuclear multifragmentation [Gross and Meng Ta-chung, 1981; Bondorf, 1981] – interpreted as an indication for a critical phenomenon [Fisher, 1967; Siemens, 1983]. This observation has initiated an intensive search for signatures of criticality [Panagiotou *et al.*, 1984; Porile *et al.*, 1989; Campi, 1988]. The systematic investigation of inclusive studies during the subsequent years showed that the power law exponent τ approaches a value of ≈ 2.5 at high bombarding energies [Trautmann *et al.*, 1993].

While the interpretation of inclusive mass spectra was criticized [Aichelin *et al.*, 1988], it was shown in exclusive measurements that the mass or charge distributions may approach the pure power law for certain values of the chosen sorting variable. In this case, the sorting variable may serve as the parameter controlling the distance to the critical point or critical region. Indeed even minima of the exponent τ could be identified which were found to be close to the maximum fragment production [Ogilvie *et al.*, 1991; Li *et al.*, 1993b; Kreutz *et al.*, 1993; Schüttauf *et al.*, 1996]. Within Fisher's droplet model this minimum would allow to locate the critical point. It was, however, realized that in some cases the minimum value of τ was far below the expected value of about 2.2 [Milkau *et al.*, 1993; Li *et al.*, 1993b; D'Agostino *et al.*, 1995]. Such low values may signal the influence of the large Coulomb fields of highly charged systems [D'Agostino *et al.*, 1995], the finite size of the system [Li *et al.*, 1994], the geometry of the source [Phair *et al.*, 1993] and/or the dynamics of the nucleation process [Pratt *et al.*, 1995; Zabrodin, 1995; Bravina and Zabrodin, 1996] .

A further step was taken by the EOS collaboration who have reported values for critical-point exponents from the charge correlations measured for the ^{197}Au on C reaction at 1 GeV per nucleon [Gilkes *et al.*, 1994; Hauger *et al.*, 1996; Elliott *et al.*, 1996]. The analysis takes extensive recourse to results obtained for percolation. Below the critical point, the largest cluster of the partition is associated with the percolating cluster which corresponds to the liquid phase in a liquid-gas transition. It grows in proportion to t^β with the relative distance t=(T_c-T)/T_c from the critical point. The role of the susceptibility in magnetic systems or the isothermal compressibility in a liquid, i.e. the response to the external field, is assumed by the second moment M_2 of the fragment size distributions. It diverges with the power of -γ as the critical point is approached (both critical-point exponents β and γ are positive numbers).

With the guidance provided by percolation studies on small lattices, recipes were developed on how to extract critical exponents from the data [Elliott *et al.*, 1994]. The reported results $\beta = 0.29 \pm 0.02$ and $\gamma = 1.4 \pm 0.1$ are close to those of liquid-gas systems ($\beta_{LG} = 0.32$, $\gamma_{LG} = 1.24$) and significantly different from those of percolation or mean-field theory [Gilkes *et al.*, 1994]. This conclusion relies on the correct assessment of the systematic errors inherent to the procedure which, however, has been questioned by

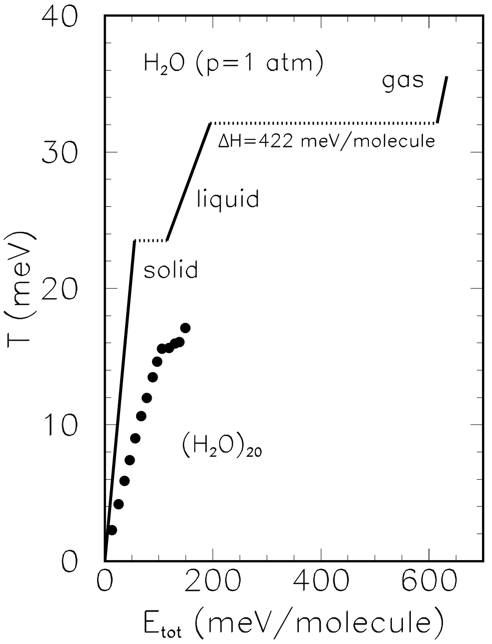

Fig. 1. *Caloric curve of bulk water at atmospheric pressure (line) and of a water clusters consisting of 20 H_2O molecules predicted [Wales and Ohmine, 1993] by molecular dynamics calculations (dots).*

other authors [Bauer and Botvina, 1995; Bauer and Friedmann, 1995]. A critical discussion – including results for Ising models on small lattices – may also be found in Refs. [Hüfner, 1985; Wörner, 1995; Hüller and Promberger, 1996; Müller *et al.*, 1996]. Using the same experimental recipe, the results of the EOS collaboration could be reproduced in ^{208}Pb induced reactions on emulsions at 160A GeV [Jain and Singh, 1996], while an analysis of Au+emulsion reactions at 10.6A GeV gave significantly different critical exponents [Cherry *et al.*, 1995]. This illustrates that – despite enormous effort – the attempts to deduce critical parameters and critical point exponents remained elusive.

An alternative approach to explore the liquid-gas phase diagram is possible via nuclear calorimetry. While this method is not restricted to second order phase transitions, the interpretation of caloric information on nuclei has also to cope with several complications: Excited nuclei are transient systems which have to be generated in nuclear collisions. We are, therefore, facing the difficulty to produce isolated nuclear systems which have reached the highest possible degree of equilibration. Nuclei are composed of a limited number of constituents. In a finite system, fluctuations are limited. Singularities of phase transitions get, therefore, rounded and shifted with respect to their bulk values [Imry, 1980; Labastie and Whetten, 1990]. Moreover, the long-range Coulomb-repulsion between the constituent protons introduces additional instabilities [Gross *et al.*, 1982; Levit and Bonche, 1985] which may lead to a further downward shift of the apparent 'critical' temperature [Satpathy *et al.*, 1989; Bondorf *et al.*, 1985; Gross *et al.*, 1986]. Since no external fields (e.g. pressure) can be applied to excited nuclei in the laboratory, they may expand prior to their disassembly [Bertsch and Siemens, 1983; Lopez and Siemens, 1984; Friedman, 1990; Friedman, 1992; Papp and Nörenberg, 1995]. Eventually, the expanded systems may aggregate into clusters. Velocity gradients built up during this process and may also alter the phase diagram [Dhont, 1996].

Although all these difficulties are inherent in nuclear systems, they do also apply to other fields where finite systems are involved [Blink and Hoover, 1985; Blümel *et al.*, 1988; Hervieux and Gross, 1995]. This is illustrated in figure 1 for the case of water. The solid line shows the well-known caloric curve of water at normal pressure of 1 atmosphere. Comparing this paradigm of first-order phase transitions to the predicted [Wales and Ohmine, 1993] caloric curve of a finite H_2O cluster (dots in figure 1) we still recognize the characteristic 'plateau' signaling the solid-to-liquid transition. However, the transition

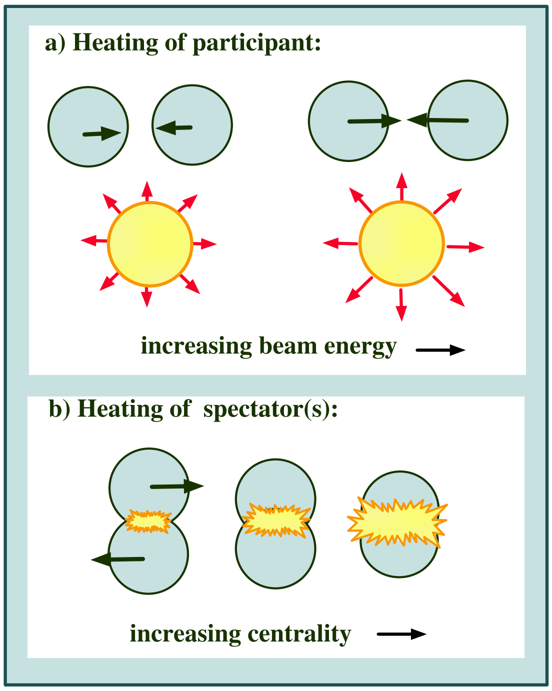

Fig. 2. *Pictorial view of the two different ways to produce boiling nuclei.*

temperature is reduced and distributed over a finite temperature range. Nevertheless, this example illustrates that phase transitions of rather small clusters (∼10 constituents) are still well defined, distinguishable [Labastie and Whetten, 1990; Wales and Ohmine, 1993; Cheng *et al.*, 1992; Hüller, 1992] and – in case of atomic clusters [Blümel *et al.*, 1988] – even detectable via a caloric curve, thus nourishing the hope that nuclear systems produced in energetic heavy ion collisions may also exhibit sufficiently clear signatures of a phase transition.

2 The Making of Boiling Nuclei

In order to explore the liquid-gas phase transition in nuclei we have to deposit excitation energies which are around or a few times the nuclear binding energy. Heavy-ion reactions at relativistic bombarding energies offer a wide range of possibilities to produce nuclear systems with such excitation energies. In the following we will discuss two ideal cases (figure 2): central collisions in symmetric systems forming a nuclear fireball and peripheral collisions at relativistic energies producing highly excited spectator nuclei. While the two types of reactions result in very different collective phenomena, we will see in section 5.1.2 that the thermodynamic behaviour is in qualitative agreement once the underlying collective motion is taken into account.

In head on collisions between equally heavy nuclei the excitation is determined by the incident beam energy. The clear advantage of this method is that, for a given target-beam combination, systems with nearly constant mass number can be produced. However, a significant fraction of the energy is not converted into heat but in collective explosive motion, thus introducing an additional degree of freedom which also depends on the incident energy.

Spectator nuclei produced in more peripheral collisions do not show this collective motion in the *initial* stage, though some radial flow may arise during the thermally driven expansion prior to breakup [Bondorf *et al.*, 1978; Cugnon, 1984; Aguiar *et al.*, 1992; Papp and Nörenberg, 1995; Barz *et al.*, 1996] and may contribute to the kinetic energies of the fragments [Warren *et al.*, 1996] (see also chapter 3.5). As it is illustrated in the bottom part of figure 2, in these collisions the heating is controlled by the size of the fireball and, hence, by the impact parameter.

As mentioned before so called intermediate mass fragments (IMFs) with charge greater 2 and smaller

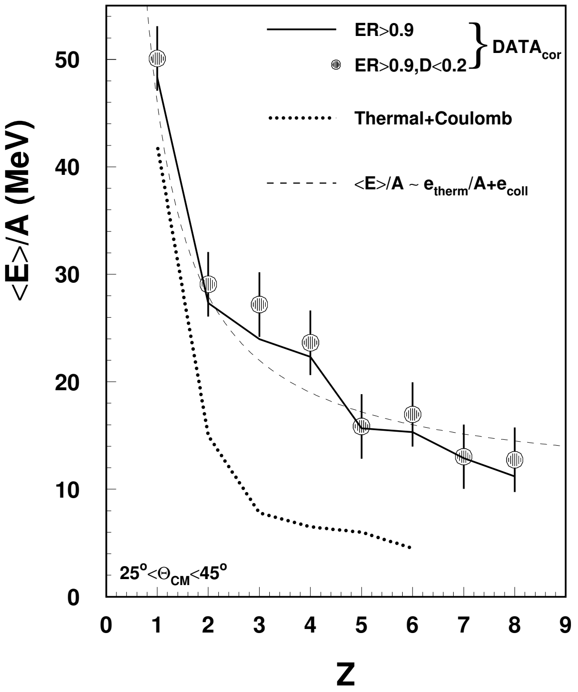

Fig. 3. *Dependence of the mean kinetic energy per nucleon as a function of the fragment charge in central Au+Au collisions at E/A=150 MeV measured by the* FOPI *collaboration [Jeong et al., 1994].*

than $\approx$1/3 of the system size play a keyrole in many studies in this field. These fragments – larger than typical evaporated light particles and smaller than evaporation residues or fission products – can be considered as the nuclear fog. Therefore, the production of many of such fragments may be intimately related with the occurrence of a phase transition. Multifragment events have been observed in emulsion studies shortly after the first heavy-ion beams with relativistic energies became available [Heckmann *et al.*, 1978; Friedlander and Heckmann, 1985; Heckmann *et al.*, 1986]. It was noticed early on that reactions of a peripheral type may lead to rather violent disintegration processes (see e.g. Figure 5 of ref. [Friedlander and Heckmann, 1985]). In addition to many emulsion studies [Jain and Singh, 1992; Jain *et al.*, 1994; Cherry *et al.*, 1994; Jain and Singh, 1995; Cherry *et al.*, 1995], the decay of heavy projectiles was investigated with plastic nuclear-track detectors [Dreute *et al.*, 1991; Lewenkopf *et al.*, 1991] during the subsequent years up to the highest available energies. An important feature of these experiments is the high charge resolution for heavy fragments. The main drawback, however, is that they do not provide complete information on the momenta of the produced fragments.

To overcome this drawback, first large solid angle electronic detectors were built in the early eighties [Warwick *et al.*, 1983]. These studies concentrated on fragments emitted from the nuclear fireball and to some degree also on the target spectator. However, the high identification threshold did not permit a complete detection of the produced target fragments. To bypass this limitation high resolution tracking devices for the detection of projectile fragments were built at the Bevalac of the Lawrence Berkeley Laboratory (EOS [Gilkes *et al.*, 1994]) and at the Schwerionen Synchrotron (SIS) of the Gesellschaft für Schwerionenforschung (GSI) Darmstadt (ALADIN). In parallel, a new generation of low threshold 4π detectors were developed at MSU (MINIBALL/-WALL [de Souza *et al.*, 1990]), GANIL (INDRA[Pouthas *et al.*, 1995]) and Indiana University (ISIS [Kwiatkowski *et al.*, 1995a]). These detection arrays enable nearly complete studies of the nuclear fireball produced in symmetric collisions at intermediate beam energies around 100 MeV per nucleon or even of target spectators produced in light-ion induced reactions at relativistic energies.

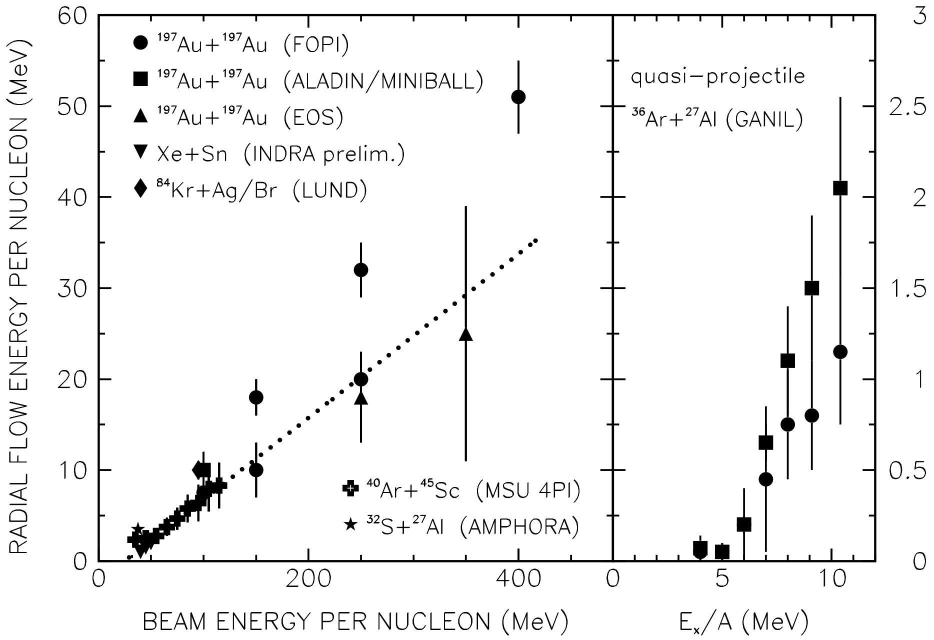

Fig. 4. *Left part: systematics of radial flow energies in (nearly) symmetric nucleus-nucleus collisions as a function of the beam energy per nucleon.*
Right part: mean radial flow energy per nucleon versus the excitation energy per nucleon of quasi-projectiles in ^{36}Ar+^{27}Al reactions (from [Jeong et al., 1996]; note the different vertical scale).

2.1 Nuclear fireballs: the little big-bang

The largest fragment multiplicities measured so far were observed in central ^{197}Au on ^{197}Au collisions at a bombarding energy of 100 MeV per nucleon [Tsang *et al.*, 1993]. In these collisions the system of nearly 400 nucleons disintegrates completely into nuclear fragments and light particles. An analysis of the kinetic energy spectra in these reactions has revealed a considerable collective outward motion superimposed on the random motion of the constituents at the breakup stage (radial flow) which represents a significant fraction of the energy available in the center-of-mass frame [Jeong *et al.*, 1994; Hsi *et al.*, 1994].

The effect of radial flow can be visualized by plotting the mean kinetic energies of the produced fragments as a function of their charge (or mass) number. For a purely thermal emission process and neglecting e.g. recoil effects [Aichelin, 1994] or finite size effects [Kunde *et al.*, 1995], the kinetic energy per nucleon should be proportional to T/A or – for light fragments where A≈2Z – to T/Z. Collective radial motion which adds a velocity field common to all fragments will show up as a constant offset in such a diagram. Thus flow can be identified more easily by analyzing heavier fragments.

Figure 3 shows the mean kinetic energy as a function of the fragment charge Z for central Au+Au collisions measured at E/A = 150 MeV by the FOPI collaboration [Jeong *et al.*, 1994]. Model calculations considering only thermal+Coulomb motion (figure 3 dotted line) can obviously not describe the trend of the data. Adding a collective radial flow of about 10 MeV per nucleon (dashed line), however, the data are nicely reproduced.

This feature prevails, with monotonously increasing flow values, over the range of bombarding energies up to 1000 MeV per nucleon [Jeong *et al.*, 1994; Hsi *et al.*, 1994; Bauer *et al.*, 1993; Reisdorf, 1994; Heuer *et al.*, 1994; Poggi *et al.*, 1995; Lisa *et al.*, 1995; Pak *et al.*, 1996; Marie *et al.*, 1997] (left part of figure 4) and demonstrates the strong dynamical coupling between entrance and exit channels in central collisions. At beam energies below about 500A MeV the energy dependence of the average radial flow energy can be approximated by a linear relation $\langle E/A\rangle_{FLOW} = 0.09 \cdot [(E/A)_{BEAM} - 25MeV]$ indicating that about 1/3 of the available center-of-mass energy is stored in radial flow energy. (Potential systematic uncertainties in the determination of the radial flow are apparent from the various analyses [Jeong *et al.*, 1994; Reisdorf, 1994; Poggi *et al.*, 1995] which are based on the same reaction. Since the various experiments focus on different particle species this may reflect also a fragment mass dependent flow.) The offset of about 25±5 MeV corresponds to an available excitation energy of about 5-7 MeV per nucleon. It is, therefore, interesting to note that also for quasi-projectiles produced in ^{36}Ar+^{27}Al reactions in the range from 55 to 90 MeV per nucleon beam energy [Jeong *et al.*, 1996] the onset for thermally induced collective expansion occurs at an excitation energy of about 6 MeV per nucleon (right part of figure 4).

2.2 Experimental study of projectile decays

Although the two forward spectrometers mentioned before – the EOS experiment at LBL and the ALADIN spectrometer at the GSI – differ with respect to many details, the general layout is quite similar. In either case the main components are (1) a multiple sampling ionization chamber, (2) a time-of-flight wall, (3) a detection device for particles emitted from the fireball and (4) a neutron detector. Since many of the data presented hereafter were obtained with the ALADIN spectrometer, I will discuss this device now in more detail.

2.2.1 The ALADIN *spectrometer*

In a series of experiments, multi-fragment decays of ^{129}Xe, ^{197}Au, and ^{238}U projectiles in collisions with Be, C, Al, Cu, In, Au, and U targets at energies between E/A = 400 MeV and 1000 MeV have been studied with the ALADIN forward-spectrometer at SIS. A schematic layout of the experimental setup is shown in figure 5. For each beam particle, its arrival time and its position in the plane perpendicular to the beam direction were measured upstream of the target with two thin plastic scintillators. The geometric acceptance of the spectrometer of $\theta_{lab} \approx \pm 9.2°$ horizontally and ±4.3° vertically was matched by the dimensions of the multiple sampling ionization chamber TP-MUSIC III and by the time-of-flight (TOF) wall. At E/A = 1000 MeV, these detector systems permitted the detection of close to 100% of all projectile fragments with atomic number $Z \geq 2$. At the lower bombarding energies, the angular distributions of some lighter fragments extended beyond the acceptance of the spectrometer but stayed within the acceptance of the Si-CsI(Tl) hodoscope array that surrounded the entrance to the field gap of the magnet. The primary beam and projectile fragments emitted along directions close to that of the beam were detected with a plastic detector with light-fiber readout (denoted ZDF-detector in figure 5). The large-area neutron detector LAND [Blaich *et al.*, 1992] was positioned close to zero degrees with respect to the incident beam direction and operated in a calorimetric mode.

The atomic numbers Z and the velocities of nuclear fragments were determined with the TOF wall, located at the end of the ALADIN spectrometer and extending over 2.4 m in horizontal and 1.0 m in vertical directions. It consisted of two layers of vertically mounted scintillator strips of 2.5 cm width and 1.0 cm thickness, viewed by photomultiplier tubes at both ends [Hubele *et al.*, 1991]. The two layers were offset by half a width with respect to each other. The primary beam was directed through a hole of cut into the middle sections of the central slats. The upper and lower halves of these central slats were optically connected by a hollow light guide built from aluminized mylar foil. An overall time resolution of about 400 ps and 180 ps (FWHM) for fragments of $Z = 2$ and $Z \approx Z_P$, respectively, was achieved (Z_P denotes the atomic number of the projectile). These values include the systematic uncertainty of the calibration. The intrinsic time-of-flight resolution measured for beam particles was 120 ps.

Elements with $Z \leq 12$ were resolved individually. For heavier fragments the resolution assumed values

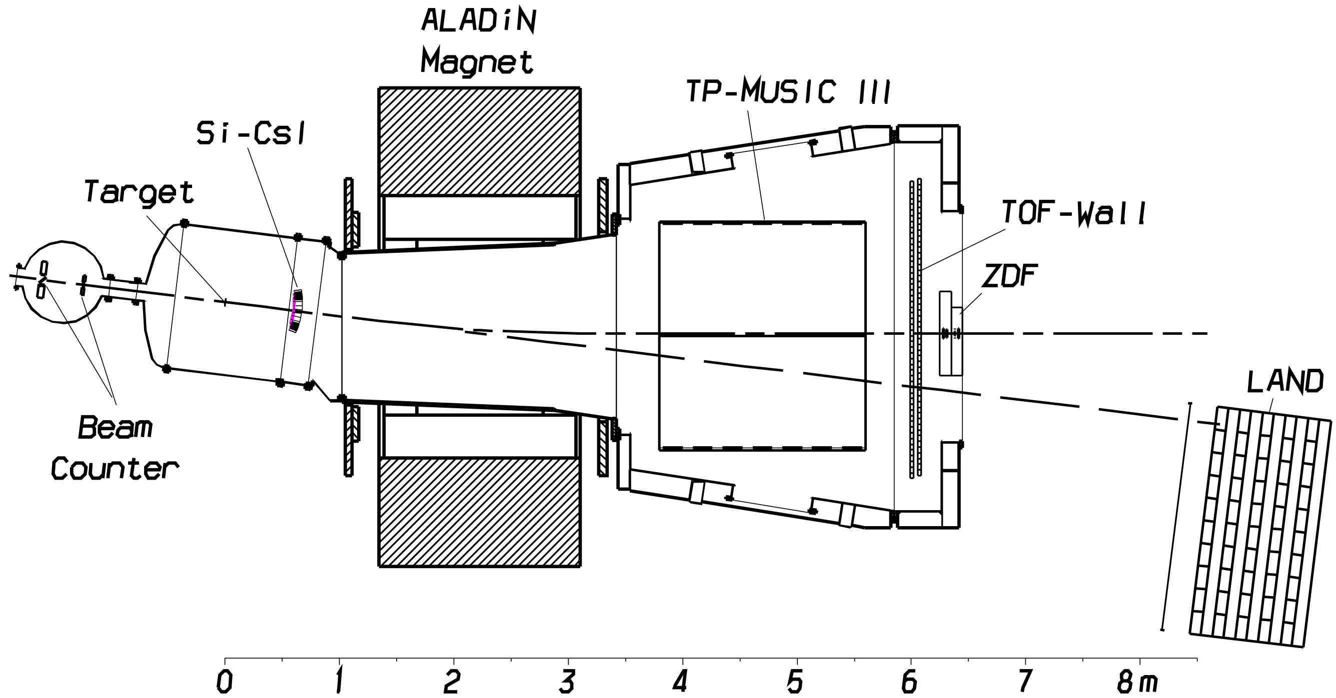

Fig. 5. *Cross sectional view of the* ALADIN *facility. The beam enters from the left and is monitored by two beam detectors before reaching the target. Projectile fragments entering into the acceptance of the magnet are tracked and identified in the TP-MUSIC III detector and in the time-of-flight (TOF) wall. The Central Plastic detector covers the hole in the TOF wall at the exit for the beam. Fragments and particles emitted in forward directions outside the magnet acceptance and up to* $\theta_{lab} = 16°$ *are detected in the Si-CsI array. Neutrons emitted in directions close to 0° are detected with the large-area neutron detector (LAND) [Blaich et al., 1992]. The dashed line indicates the direction of the incident beam. The dash-dotted line represents the trajectory of beam particles after they were deflected by an angle of 7.3°.*

of up to $\Delta Z \approx 1.5$ (FWHM). For this analysis, the TP-MUSIC III detector, capable of identifying the individual elements for $Z \geq 8$ with a resolution between $\Delta Z \approx 0.8$ (FWHM, $Z \approx 20$) and $\Delta Z \approx 0.4$ ($Z \approx 60$), served to calibrate the charge response of the TOF wall. The main purpose of the TP-MUSIC, in these experiments, was to provide the tracking information for other analyses that involved the fragment momenta. The dynamic range for tracking had been extended down to $Z = 2$ by collecting and amplifying their ionization charges with proportional counters mounted in three positions at the anode plane of the drift volume. This low threshold permitted the measurement of isotopic yield ratios of light fragments.

The Z resolution achieved with the two detector systems after off-line calibration is demonstrated in figure 6. A good separation of $Z = 2$ and 3 fragments is crucial for the reliable determination of the multiplicity of intermediate-mass fragments with $Z \geq 3$. Therefore, the $Z = 2$ and 3 distributions in the Z-identification spectrum were fitted individually and, after evaluation of their overlapping tails, the position of an equivalent sharp Z-cut was determined (figure 6).

2.2.2 Definition of the spectator source

The fragments emerging from the decay of the projectile spectators are well localized in rapidity. This is illustrated in figure 7 where rapidity spectra of light fragments detected with the TOF wall in the reaction ^{197}Au on ^{197}Au at $E/A = 1000$ MeV are shown. The distributions are concentrated around a rapidity value very close to the beam rapidity and become increasingly narrower with increasing mass of the fragment. The deviation of the most probable rapidity $y = 1.32$ of light fragments (full line in figure 7) from the rapidity $y_P = 1.35$ of the beam, after it has passed through half of the Au

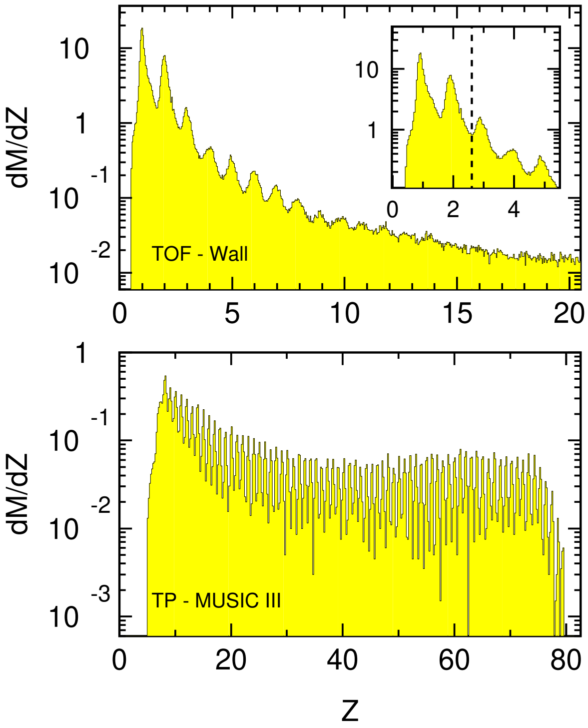

Fig. 6. *Z-identification spectra measured with the TOF wall (top) and the TP-MUSIC (bottom) for the reaction* ^{197}Au *on* ^{197}Au *at* E/A = *600 MeV. Note that the element yield at* $Z > 65$ *is affected by the experimental trigger.*
Insert: Low-Z part of the TOF-wall spectrum. The dashed line indicates the equivalent sharp cut which was used for selecting fragments with $Z \geq 3$.

target, is within the uncertainty of the absolute time-of-flight calibration. For the lighter fragments, the distributions are wider and extend into the mid-rapidity region. The widths and shapes of the distributions also depend on the impact parameter, as demonstrated for helium fragments in the two lower panels of figure 7. Both the dispersion around the projectile rapidity and the relative intensity at mid-rapidity increase with increasing centrality.

The bump in the peripheral He spectrum (lower part in figure 7), located at a rapidity y between 0.8 and 0.9, originates from mid-rapidity emission. This was confirmed by simulating the emission with two Maxwellian sources centered at projectile rapidity and at mid-rapidity. The restriction of the acceptance to forward angles causes the maximum of the observed mid-rapidity yield to appear at this somewhat larger rapidity. For this reason, the two sources can only be discerned in the peripheral collisions with lower emission temperatures. In more central collisions, the mid-rapidity source no longer produces an identifiable bump in the rapidity spectrum. Indications of a mid-rapidity source are only observed for light fragments up to $Z \approx 4$ (figure 7, top), in agreement with the rapid drop of the element yields in central collisions at relativistic bombarding energies [Reisdorf, 1994]. Finally let us note, that for a symmetric system the separation between the (heavy) projectile source and the fireball in rapidity space is largest for a given beam energy and does also not depend on the impact parameter. In reaction with light targets, e.g. ^{12}C, the fireball produced in the overlap region is shifted towards larger rapidity for more central collisions, making a separation between the two sources more difficult in asymmetric reactions.

Guided by these observations, we chose a lower limit in rapidity of $y \geq 0.75 \cdot y_P$ where y_P is the projectile rapidity, so as to define the spectator source. This condition was applied to fragments detected with the TOF wall. For those detected with the hodoscope, for which an equivalent time-of-flight information does not exist, angular limits were set with the same purpose of selecting the spectator source.

Transverse momentum distributions were constructed from the vertical position distributions of fragments measured with the TOF wall. The vertical coordinate is perpendicular to the bending plane of

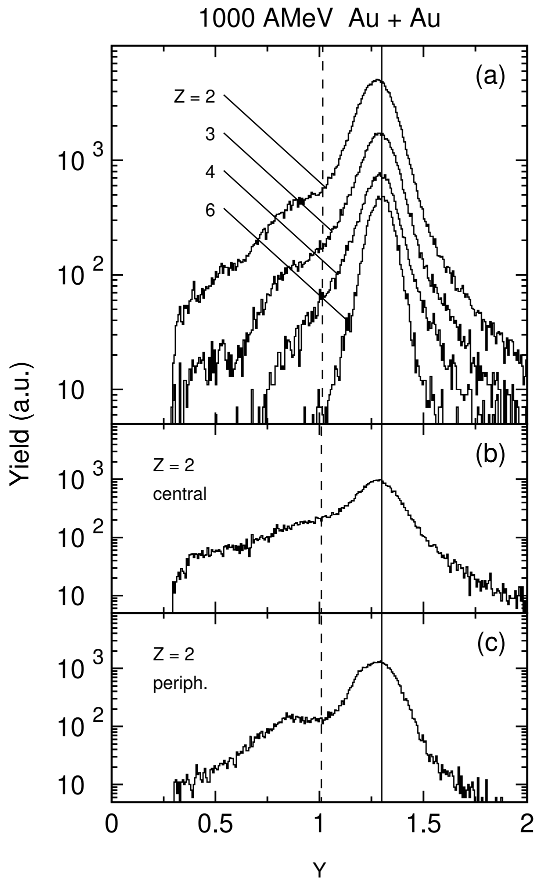

Fig. 7. *(a): Rapidity spectra measured in the reaction* ^{197}Au *on* ^{197}Au *at* $E/A = 1000$ *MeV for fragments with* $Z = 2, 3, 4$, *and 6. The solid and dashed lines indicate the measured most probable rapidity* $y = 1.32$ *of the light fragments and the condition* $y \geq 0.75 \cdot y_P$ *adopted for fragments from the projectile spectator, respectively.*
(b): Rapidity spectra of helium fragments, measured in central collisions ($Z_{bound} \leq 30$) *for the same reaction.*
(c): Same as (b) for peripheral collisions ($Z_{bound} \geq 50$).

the magnet. In figure 8 we show the transverse widths as a function of Z for the reactions ^{197}Au on ^{197}Au at $E/A = 600$, 800, and 1000 MeV. The widths $\sigma(p_t)$ rise approximately in proportion to $\sqrt{Z}$, i.e. the mean transverse energies are independent of Z which is expected for emission from an equilibrated source. Inspecting figure 8, it is, furthermore, evident that the transverse momentum distributions of the emitted projectile fragments do virtually not change with the bombarding energy. There are no indications of any dynamical contributions to the fragment velocities in the moving frame which could be related to the incident energy. Therefore, in order to select the spectator source, upper limits of the laboratory angle were imposed on the hodoscope data that were inversely proportional to the projectile momentum per nucleon. The same limits were used for all projectiles used because the dependence of the p_t distributions on the projectile mass was found to be insignificant for the light fragments. Together with the constraints on the rapidity described before, these definitions allow a comparison of data measured at different bombarding energies on a quantitative level [Schüttauf *et al.*, 1996].

3 Properties of Spectator Nuclei

The interpretation of the fragment distributions observed in violent heavy-ion collisions relies – in many cases – on the simplifying assumption that a thermodynamical equilibrium has been established prior to the disassembly of the system. In this section we will examine several observables which are *necessary*, model independent prerequisites for an equilibrium being reached. The isotropy of the decay and a 1/mass dependence of the mean kinetic energies represent two conditions for kinetic equilibrium.

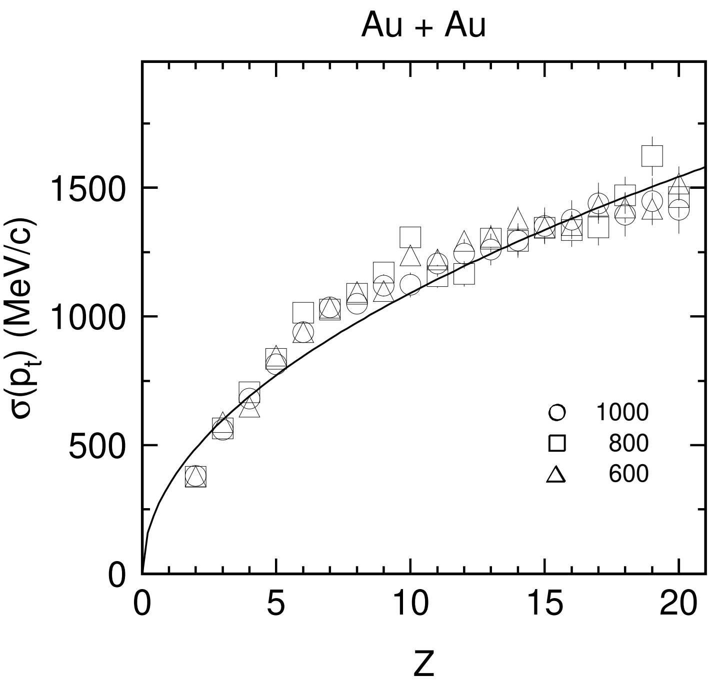

Fig. 8. *Widths of the transverse-momentum distributions $\sigma(p_t)$ as a function of Z for the reactions ^{197}Au on ^{197}Au at E/A = 600, 800, and 1000 MeV and for 20 $\leq Z_{bound} \leq$ 60. The line is proportional to $\sqrt{Z}$.*

In a subsequent section we will then discuss the degree to which the observed fragmentation pattern remember on the entrance channel, i.e. the size of the colliding system and the incident energy.

3.1 Kinetic equilibrium

The times and positions measured with the TOF wall were used to calculate the components of the fragment velocities in the reference frame of the original projectile. These intrinsic velocities have been used to determine the fragment kinetic energies in the frame of the decaying spectator. Results for the reaction ^{197}Au on ^{197}Au at 600 MeV per nucleon, integrated over $20 \leq Z_{bound} \leq 60$, are shown in figure 9. It was assumed that either the longitudinal (squares) or the vertical transverse (circles) degrees of freedom represent one third of the total kinetic energies in the moving frame. The agreement between the two sets of results reflects the isotropy of the kinetic degrees of freedom. The intrinsic kinetic energies do not depend on the bombarding energy and thus are representative for the whole energy range over which the universal spectator decay prevails [Schüttauf *et al.*, 1996].

The mean kinetic energies per unit fragment mass $\langle E_{kin}/A\rangle$ decrease rapidly with atomic number Z (figure 9). As expected for purely thermal decay the kinetic energies, $\langle E_{kin}/A\rangle$ show approximately a $1/A$ dependence. With this assumption the magnitude of the kinetic temperature $T = 2/3 \cdot 1/2 \cdot \langle E_{kin}\rangle$ assumes a value of approximately 15 MeV as indicated by the solid line in figure 9. (Note, however, that for heavy fragments on the order of one half of the kinetic energies in the rest frame of the decaying system may originate from Coulomb repulsion and sequential decays of excited fragments [Lindenstruth, 1993].) As will be shown in section 5.3 this "temperature" exceeds considerably the emission temperatures $T \approx 5$ MeV derived from the relative isotopic abundance or from relative yields of particle unbound states [Kunde *et al.*, 1991; Schwarz *et al.*, 1993] which represents a well known but up to now not fully resolved problem [Barz *et al.*, 1989a; Boal *et al.*, 1989a; Boal *et al.*, 1989b; Barz *et al.*, 1989b; Bauer, 1995].

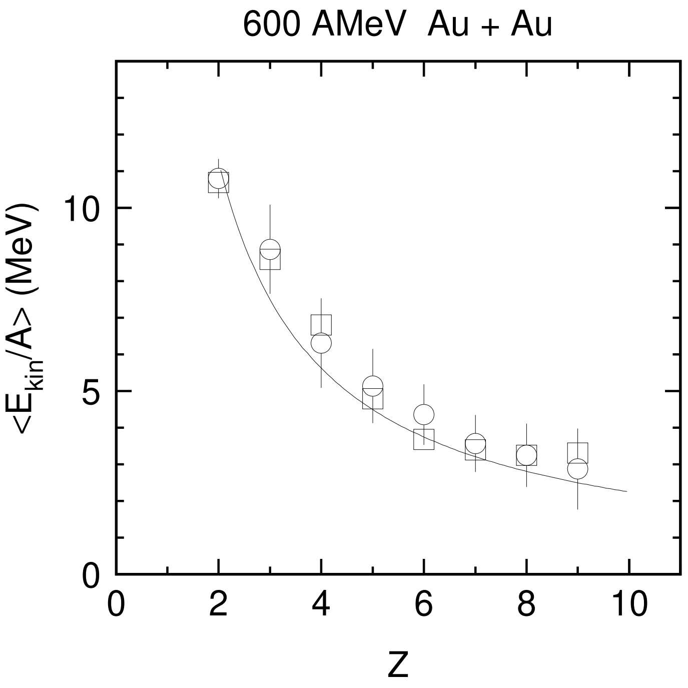

Fig. 9. *Mean kinetic energies per nucleon in the moving frame, deduced from the transverse (circles) and longitudinal (squares) momentum widths as described in the text, for fragments from the reaction* ^{197}Au *on* ^{197}Au *at* $E/A = 600$ *MeV and for* $20 \leq Z_{bound} \leq 60$.

3.2 Universality of the charge partition

In contrast to central collisions, no apparent dependence on the entrance channel is observed in the charge partition of fragmenting spectator nuclei. The decay patterns were found to be mainly governed by the energy transfer to the spectator, as evident from the Z_{bound} scaling of the fragment charges and their correlations [Hubele *et al.*, 1991; Hubele *et al.*, 1992; Kreutz *et al.*, 1993]. The quantity Z_{bound} is defined as the sum of the charges of all product nuclei with $Z \geq 2$. It represents the charge of the original spectator system reduced by the number of hydrogen isotopes emitted during its decay. It follows from the geometric properties of heavy-ion reactions at these energies that the mass (or charge) of the spectator, and therefore also Z_{bound}, is closely related to the impact parameter. When plotted as a function of this quantity the fragment multiplicities and correlations exhibit a universal behaviour.

3.2.1 Target dependence

This universality was first observed as an invariance with respect to the chosen target in the decays of ^{197}Au projectiles at 600 MeV per nucleon [Hubele *et al.*, 1991; Hubele *et al.*, 1992; Ogilvie *et al.*, 1991; Kreutz *et al.*, 1993]. In figure 10 (top) the universal nature of this correlation is demonstrated for ^{238}U projectiles at 1000 MeV per nucleon and for the full set of seven targets. At large Z_{bound}, the number of fragments is small and mainly one heavy residue nucleus (or two fission fragments in case of the Uranium beam) with a (total) charge number close to Z_{bound} is produced. With decreasing Z_{bound} the number of fragments increases. Multi-fragment production dominates for impact parameters corresponding to $Z_{bound} \approx 50$. In central collisions with the heavier targets, the region of small Z_{bound} is strongly populated. Here both M_{IMF} and the maximum fragment charge decrease, reflecting the smaller size of the spectators produced in these collisions. This behavior was termed the *rise and fall* of multi-fragment emission [Ogilvie *et al.*, 1991]. On the side of the rise, at large Z_{bound}, the fragment production is governed by the amount of deposited energy, whereas in the fall region the limit of unconditional partitioning is approached [Hubele *et al.*, 1992]. While, therefore, the general shape of this *rise and fall* is due to these 'trivial' correlations (e.g. $\langle M_{IMF} \rangle \leq int(Z_{bound}/3)$), the height of this

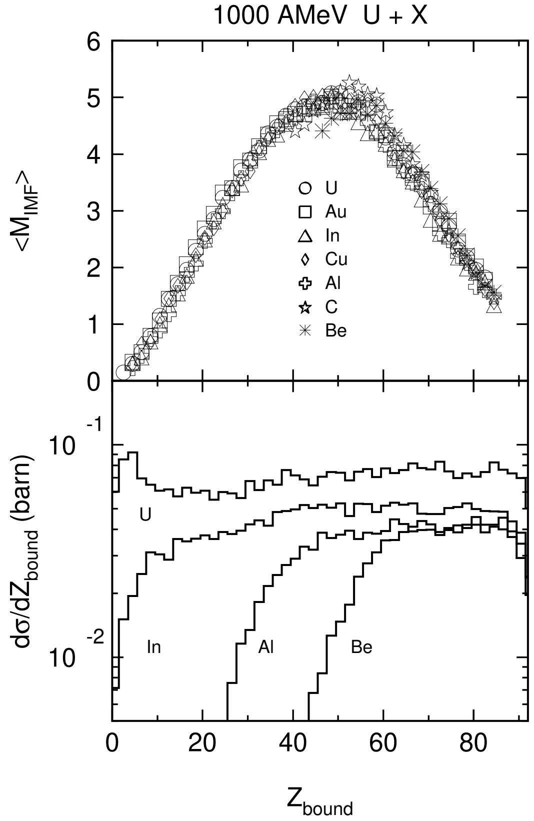

Fig. 10. *Top: Multiplicity of intermediate-mass fragments as a function of Z_{bound} for the reactions of ^{238}U projectiles at E/A = 1000 MeV with the seven targets of Be, C, Al, Cu, In, Au, and U. Bottom: Measured cross sections $d\sigma/dZ_{bound}$ for the reactions of ^{238}U projectiles at E/A = 1000 MeV with the four targets of Be, Al, In, and U [Schüttauf et al., 1996].*

curve and the location of the maximum is not and reflects the physics underlying the fragmentation process [Hubele *et al.*, 1992] (cf. figure 17). With ^{238}U the maximum mean number of fragments ($3 \leq Z \leq 30$) is about five at $Z_{bound} = 50$. The spread over one half unit may not be significant in view of the systematic errors [Schüttauf *et al.*, 1996]. However, a slight tendency towards smaller multiplicities for the heavier targets can be explained by the larger Coulomb deflection that is caused by these targets and its effect on the acceptance for the very light fragments [Lindenstruth, 1993]. Another potential, but not yet explored source for this weak target dependence is the more compact geometry of the primary spectator in reactions with heavy targets.

Generally the influence of dynamical effects due to compression and decompression processes is expected to increase with increasing target mass. Therefore, the observed target independence indicates that such processes are only of minor importance in these reactions.

The reaction cross sections $d\sigma/dZ_{bound}$ are strongly target dependent [Hubele *et al.*, 1991]. For ^{238}U projectiles of 1000 MeV per nucleon this is shown in the lower part of figure 10. Only part of the Z_{bound} range can be covered with the lighter targets. The variation of $d\sigma/dZ_{bound}$ with bombarding energy is insignificant for the collisions with heavy targets. There, the limit above which the spectator excitation is dominated by the collision geometry seems to be already reached. With the lighter targets, on the other hand, the higher bombarding energies allow for considerably larger energy transfers in central collisions [Schüttauf *et al.*, 1996]. This point will be discussed in more detail in section 3.3.

3.2.2 Beam energy invariance

In figure 11 the mean number of intermediate mass fragments is shown as a function of Z_{bound} for the reaction of ^{197}Au on ^{197}Au at four bombarding energies. The correlation between the two quantities is

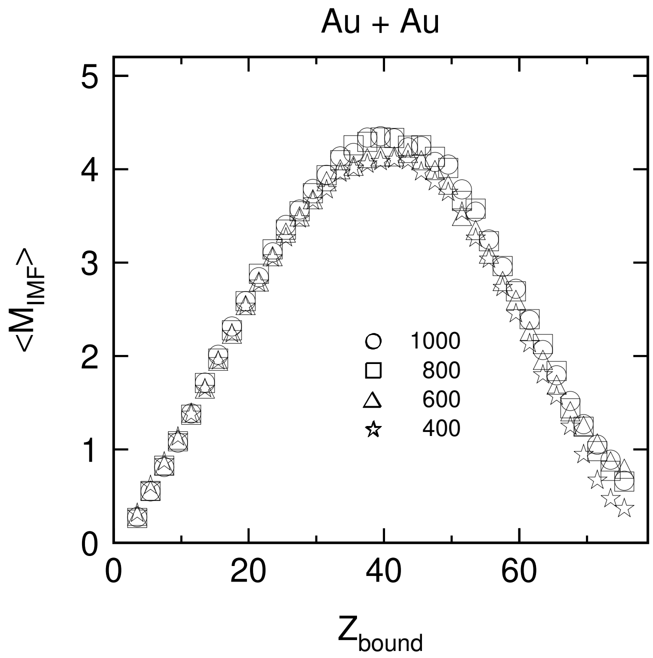

Fig. 11. *Mean intermediate mass fragment (IMF, 3$\leq Z \leq$ 30) multiplicity $\langle M_{IMF} \rangle$ as a function of Z_{bound} for the reaction of ^{197}Au on ^{197}Au at E/A = 400, 600, 800, and 1000 MeV (from [Schüttauf et al., 1996]).*

seen to be independent of the projectile energy within the experimental accuracy. For all energies, the maximum mean multiplicity of 4 to 4.5 fragments is reached at $Z_{bound} \approx 40$.

This universality gives rise to the question as to where its limits may lie. On the high-energy side, there is no limit known at present. Limiting fragmentation, i.e. a saturation of the production cross sections for intermediate mass fragments at bombarding energies in excess of several GeV, has been observed [Kaufmann and Steinberg, 1980; Green and Korteling, 1980]. This suggests that the formation of spectator nuclei with high excitation energies may be common to heavy-ion collisions in the GeV range. A recent study of Jain *et al.* performed with ^{197}Au beams of 10.6 GeV per nucleon, available from the AGS at Brookhaven, and emulsion targets [Jain *et al.*, 1994; Jain and Singh, 1995] reports nearly quantitative agreement with the fragmentation patterns of ^{197}Au on Cu collisions at 600 MeV per nucleon [Hubele *et al.*, 1991; Kreutz *et al.*, 1993]. Note, that the latter data were obtained within the acceptance given by the ALADIN TOF-wall of 1-m width. With respect to the more complete data now available, the maximum number of intermediate-mass fragments of 3.5, reported by Jain *et al.*, is about one unit below the values from the present work, thus signaling an – albeit weak – beam energy dependence.

The fragmentation of ^{197}Au projectiles of 10.6 GeV per nucleon in collisions with emulsion targets was also investigated by the KLMM collaboration [Cherry *et al.*, 1994; Cherry *et al.*, 1995]. The Z_{bound} distributions reported for interactions with light targets (H,C,N, and O) resembles more closely the distribution measured for the ^{197}Au on Al rather than the ^{197}Au on C reaction at 600 MeV per nucleon. This may be considered as another indication for the role of the bombarding energy in reaching large cross sections for the high-multiplicity breakups in asymmetric systems.

3.2.3 Projectile mass scaling

The observed invariance with respect to the entrance channel is not restricted to the multiplicity of intermediate-mass fragments but appears to be a very general feature of the relative asymmetries and other correlations between the abundance and the atomic numbers of the fragmentation products [Kreutz *et al.*, 1993; Schüttauf *et al.*, 1996]. As illustrated in the right part of figure 12, scaled with the size of the decaying system, the multiplicity of produced IMF's (for this analysis only fragments detected

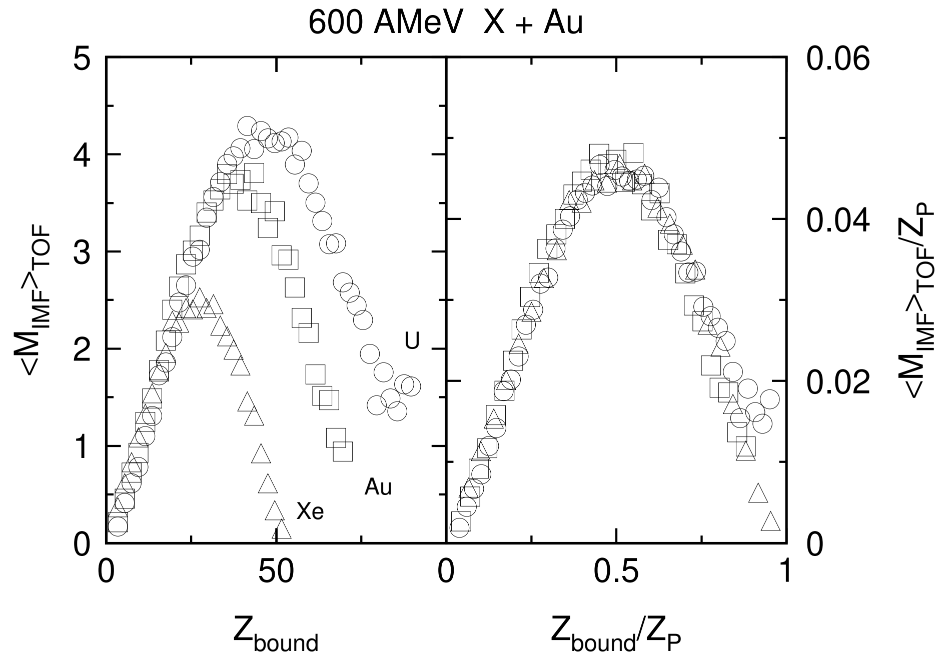

Fig. 12. *Left panel: Mean multiplicity of intermediate-mass fragments $\langle M_{IMF}\rangle_{TOF}$, observed with the TOF wall, as a function of Z_{bound} for the reactions ^{238}U on ^{197}Au (circles), ^{197}Au on ^{197}Au (squares), and ^{129}Xe on ^{197}Au (triangles) at E/A = 600 MeV. Right panel: The same data, as shown in the left panel, after normalizing both quantities with respect to the atomic number Z_P of the projectile. (from [Schüttauf et al., 1996]).*

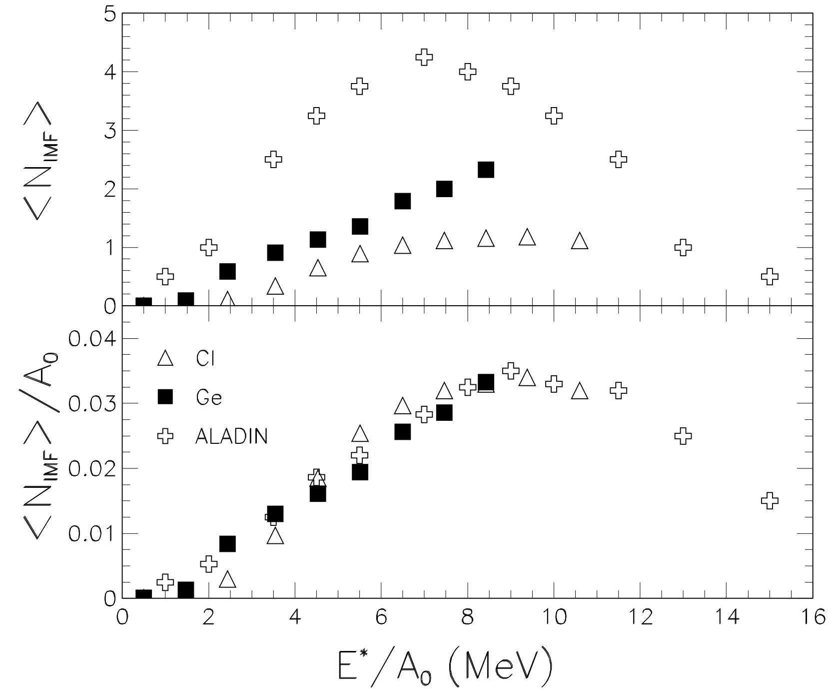

Fig. 13. *Average multiplicity of intermediate mass fragments emitted from the projectile source as a function of it's excitation energy. The data are from 43 MeV per nucleon ^{35}Cl+^{197}Au (open triangles), 35 MeV per nucleon ^{70}Ge+^{nat}Ti (squares) and 600 AMeV ^{197}Au+^{197}Au reactions. In the lower part the fragment multiplicity has been normalized to the system size (from [Beaulieu et al., 1996]).*

with the TOF wall were considered) seems even to be a universal function which is independent of the mass of the decaying system [Schüttauf *et al.*, 1996].

Recently this universal scaling has been verified at much lower incident energies for an even wider range of source sizes down to only 35 nucleons. In figure 13 the Aladin data for 600 AMeV ^{197}Au+^{197}Au

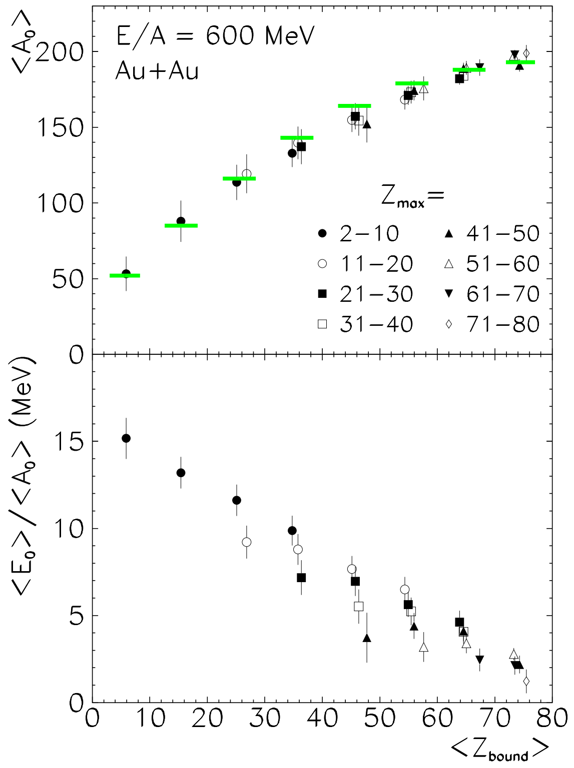

Fig. 14. *Average prefragment size $\langle A_0 \rangle$ and its excitation energy per nucleon $\langle E_0 \rangle / \langle A_0 \rangle$ as a function of Z_{bound} for different bins in Z_{max} [Pochodzalla et al., 1995]. The horizontal bars in the upper part mark the spectator size expected from an ideal participant-spectator geometry.*

collisions are plotted as a function of the excitation energy (see section 3.3) and compared to fragment multiplicities observed in 43 AMeV ^{35}Cl+^{197}Au (open triangles) and 35 AMeV ^{70}Ge+^{nat}Ti (squares) reactions [Beaulieu *et al.*, 1996]). Normalized to the system size again a common relation is found (lower part of figure 13). A comparison of the right part of figure 12 with the lower part of figure 13 suggests that Z_{bound} normalized to the projectile charge is strongly related to the excitation energy. CASCADE simulations supplemented by statistical decay calculations do indeed predict such a relation (see section 3.5.1).

3.3 Excitation energy of the spectator nucleus

The invariant features of the spectator multi-fragment decay and the apparent high kinetic degree of equilibration of the excited systems prior to their decay justifies interpretations in statistical or thermodynamical terms. The necessary baseline for such considerations is a knowledge of the energy transfer to the excited primary nuclear system. Unfortunately, the transient nature of finite nuclear systems makes it difficult to arrive at a unique definition of the decaying system and its associated excitation energy. Depending on the observables we consider, it may characterize different stages of the reaction. In turn, a detailed understanding of the different type of excitation energies might help to understand the temporal evolution of the system.

The procedure used to determine the initial mass and excitation energy of the spectators prior to their decay is very similar to that proposed by Campi *et al.* [Campi *et al.*, 1994]. The basic idea is to determine the invariant mass – and hence the excitation energy with respect to a nucleus in it's groundstate – as well as the total charge and mass numbers of the system by summing up all masses and kinetic energies.

The results for the mass A_0 and the specific excitation energy E_0/A_0 are given in figure 14. The data points represent the results for individual bins in the Z_{max}-versus-Z_{bound} event representation. The

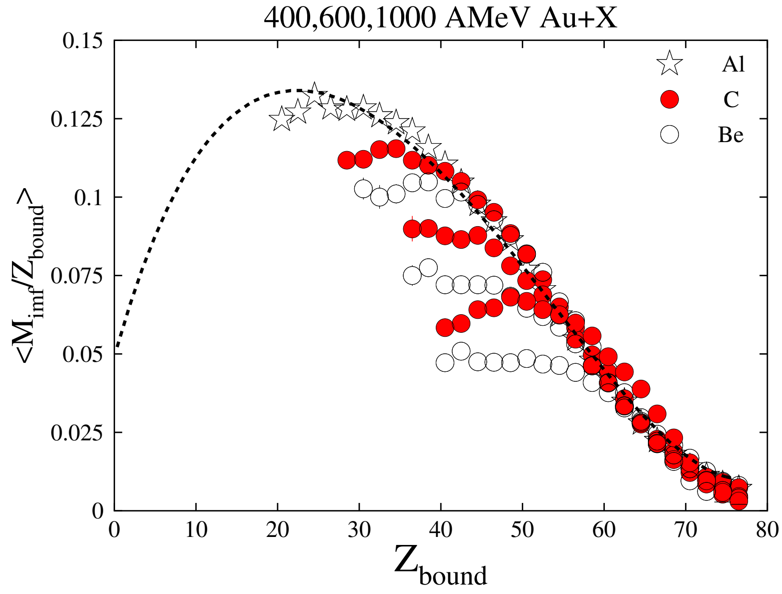

Fig. 15. *Mean fragment multiplicity normalized to* Z_{bound} *for Au induced reactions on light targets. The saturation of the ratio* $\langle M_{IMF}\rangle/Z_{bound}$ *signals a saturation of the average excitation energy once projectile and target overlap completely (from [Kunze, 1996]).*

mass A_0 decreases with decreasing Z_{bound} but is, apparently, independent of Z_{max}. The smallest mean spectator mass in the bin of $Z_{bound} \leq 10$ is $\langle A_0\rangle \approx 50$. Reconstructing the impact parameter from the quantity Z_{bound}, one finds that $\langle A_0\rangle$ is remarkably well described by the simple participant-spectator geometry (see horizontal bars in figure 14).

The excitation energy E_0 appears to be a function of both Z_{bound} and Z_{max}; the higher values correspond to the smaller Z_{max} values, i.e. to more complete disintegration of a system of given mass. The maximum number of fragments, observed at $Z_{bound} \approx 40$, is associated with initial excitation energies of $\langle E_0\rangle/\langle A_0\rangle \approx 8$ MeV. With decreasing Z_{bound} the deduced excitation energies reach up to about two times the nuclear binding energy per nucleon. A still preliminary analysis of Au+Au collisions at 800 and 1000 AMeV indicates that for a given Z_{bound} interval the excitation energy increases with increasing beam energy. Moreover, this analysis – which is based on more complete information on the kinetic energy and isotope distributions of light particles – gives for the 600 AMeV Au+Au reaction excitation energies which are systematically higher by about 10% but which are still within the systematic uncertainties quoted in ref. [Pochodzalla *et al.*, 1995].

For lighter targets such high average excitation energies cannot be reached. Statistical model calculations indicate that the mean fragment multiplicity normalized to the system size (or to the observable Z_{bound}) is strongly related to the excitation energy (cf. right part of figure 12 and lower part of figure 13). Since according to these calculations this relation is rather independent of the system size (see figure 21) it can be used to establish an excitation energy scale. Note, that the *absolute* values for the deduced excitation energies may be somewhat model dependent; in the following we will, therefore, focus on the relative sequence only. Based on this idea, the energy deposition in Au and U induced reactions on several light targets such as ^{9}Be, ^{12}C, and ^{27}Al has been studied [Kunze, 1996]. When going from peripheral to more central collisions the ratio $\langle M_{IMF}\rangle/Z_{bound}$ – and accordingly the excitation energy – is first monotonously increasing in line with the Au+Au reaction (dashed line in figure 15). However, for the most central collisions the quantity $\langle M_{IMF}\rangle/Z_{bound}$ departs from the relation found in Au+Au collisions and saturates at a lower value. In all cases this deviation sets in at impact parameters of about 3 fm, i.e. close to the value corresponding to a complete overlap between target and projectile. For these very central asymmetric collisions fluctuations of the reaction process rather than the impact parameter – here measured via Z_{bound} – seems to determine the energy deposition. Consistent with

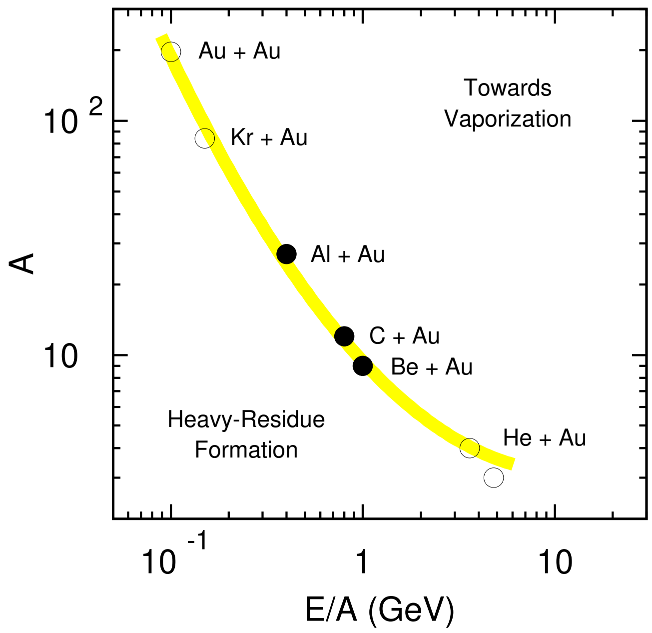

Fig. 16. *Location of reactions for which mean maximum fragment production has been observed in the most violent collisions in a two-dimensional map of projectile mass versus bombarding energy. Full points denote reactions studied by the* ALADIN *collaboration in reverse kinematics, open symbols refer to work reported in [Tsang et al., 1993; Lips et al., 1994; Peaslee et al., 1994; Kwiatkowski et al., 1995b; Pienkowski et al., 1994].*

CASCADE simulations [Barashenkov and Toneev, 1972] the value at which the ratio $\langle M_{IMF}\rangle/Z_{bound}$ saturates, increases with increasing target mass and with rising beam energy. For these light targets excitation energies leading to maximal fragment production – as observed in Au+Au collisions with $\langle M_{IMF}\rangle/Z_{bound} \approx 0.13$ (dashed line in figure 15, cf. also figure 21) – is only reached at beam energies beyond 1000A MeV.

3.4 Borderline between evaporation and vaporization

The systematic set of data now available reveals the universal nature of multi-fragment decays of excited spectator nuclei at relativistic energies. It suggests that the correlation of excitation energy and mass of the produced spectator systems and the statistical nature of their decay are independent of the specific entrance channel. The emulsion data as well as the insight provided by calculations indicate that it should prevail up to very high bombarding energies with virtually unchanged features (see section 3.5.1). There are lower limits of the bombarding energy below which the typical spectator excitation does not suffice to induce a complete disassembly with maximum fragment production. These threshold energies depend on the collision partner, as shown for the case of gold nuclei in figure 16. Besides data measured with the ALADIN spectrometer in inverse kinematics, also data for ^{197}Au on ^{197}Au at lower energies [Tsang *et al.*, 1993], for ^{84}Kr on ^{197}Au [Peaslee *et al.*, 1994], and for ^{4}He on ^{197}Au [Lips *et al.*, 1994] are included. (Note, that for symmetric systems a beam energy of about 50A MeV marks the onset of vaporization [Bacri *et al.*, 1995]. However, these events represent only a very small fraction of the total reaction cross section.) Also in ^{3}He induced reactions on ^{197}Au at 4.8 GeV per nucleon a mean IMF multiplicity of 4.7 has been observed for the largest thermalized energies [Morley *et al.*, 1996]. Furthermore, events with up to 10 IMF's were observed in this reaction [Renshaw Foxford *et al.*, 1996]. However, the average IMF multiplicity in which at least one IMF was detected is significantly lower than previously reported by Lips *et al.* [Lips *et al.*, 1994]. The hatched line indicates these threshold energies as a function of the target mass. If the bombarding energy is raised above the threshold, the maximum fragment production will shift to more peripheral collisions. Below the threshold, the production of

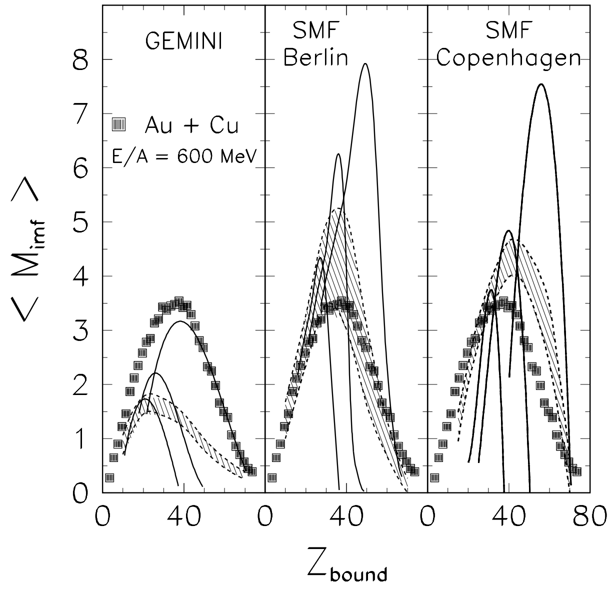

Fig. 17. *Comparison of the $\langle M_{IMF} \rangle$ – Z_{bound} correlation observed for Au + Cu reactions (squares) with predictions of the sequential decay code* GEMINI *(left part) and of the SMF models of Gross and co-workers (center part) and of Bondorf and co-workers (right part). The lines represent excitation functions for a given initial systems (A_1,Z_1) = (100,40), (131,54) and (190,75). The shaded bands are predictions based on initial conditions provided by* BUU *simulations (from [Hubele et al., 1992]).*

heavy residues will be the dominating process.

The maximum of the IMF production marks the borderline between the regime of residue formation and vaporization, or naively speaking between the 'liquid-like' and the 'gaseous' regime. As one moves along the hatched line towards the central collisions of heavy systems, dynamical phenomena become important (section 2). On the other side, large dynamical effects are not expected in light-particle induced reactions with heavy targets, i.e. at the lower end of the hatched line in figure 16. Here the main problem arises from the fact that the cross ' for large energy transfers to the target with maximum fragment production are comparatively small [Lips *et al.*, 1994; Kwiatkowski *et al.*, 1995b; Pienkowski *et al.*, 1994]. New experimental results including exclusive measurements with beams of antiprotons [Goldenbaum *et al.*, 1996] and of protons with energies up to 14 GeV [Viola *et al.*, 1996] have been obtained very recently, and a comprehensive picture of the light-ion reactions should emerge rather soon.

3.5 Statistical fragment production: success and limitations

Before we enter into the interpretation of these observations let us briefly summarize the main features of the projectile spectators:

- The primary projectile spectator emerging from the abrasion phase is a well defined source which can be reconstructed with high accuracy and without thresholds on an event-by-event basis.
- The loss of the memory on the entrance channel signals a high degree of equilibration. During the primary collision the spectators experience no or at most very little compression.
- The excitation energy can be controlled by the impact parameter so that a whole excitation function can be measured simultaneously in a one reaction.

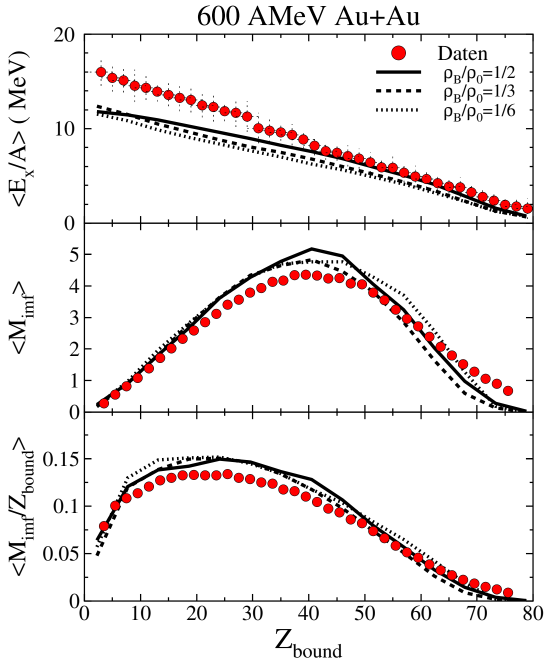

Fig. 18. *Excitation energy per nucleon (top part), mean IMF multiplicity (middle part) and normalized IMF multiplicity (lower part) as a function of Z_{bound}. The lines show results of the Moscow statistical multifragmentation model [Botvina et al., 1995; Kunze, 1996].*

These "compound nucleus–like" properties make an attempt to describe the decay configurations within statistical decay models at least a worthwhile enterprise. First calculations confronting the so called *rise and fall* of multifragmentation [Ogilvie *et al.*, 1991] with such calculations are shown in figure 17 [Hubele *et al.*, 1992]. The shaded areas in this figure mark the results of calculations using as an input to these calculations the excitation energies and masses of primary projectile spectators predicted by microscopic BUU simulations. Qualitatively, all calculations exhibit a rise and fall of the IMF multiplicity. Both, the BERLIN [Li *et al.*, 1993a] and COPENHAGEN [Barz *et al.*, 1993; Bondorf *et al.*, 1995a] multifragmentation codes predict rather similar relations between Z_{bound} and $\langle M_{IMF} \rangle$ which are in reasonable agreement with the data. On the other hand, the decay program GEMINI which assumes a chain of successive binary decays at normal nuclear density [Moretto, 1995] yields fragment multiplicities which are too small by about a factor of 2. Thus these calculations were the first hint that we are not dealing with a system at normal nuclear density but rather with an expanded system.

Soon after these findings, several groups were able to show that not only the multiplicities of intermediate-mass fragments but also the measured charge asymmetries and all higher-order charge correlations [Kreutz *et al.*, 1993] can be reproduced to rather high accuracy with the various statistical multifragmentation model [Botvina and Mishustin, 1992; Botvina *et al.*, 1995; Li *et al.*, 1993a; Barz *et al.*, 1993; Kreutz *et al.*, 1993; Désesquelles, 1995; Désesquelles *et al.*, 1996]. This was achieved by rather freely varying the initial mass or excitation energy or both. Despite several minor differences in the calculations – for example the degree to which the N/Z ratios of the produced fragments can be reproduced [Pochodzalla, 1994; Botvina *et al.*, 1995] depends sensitively on the treatment of the final sequential decay after freeze out – all groups agree that the excitation energy per nucleon needed to describe the data does not exceed 6 to 8 MeV.

Due to the improved acceptance in the more recent experiments [Schüttauf *et al.*, 1996; Schüttauf, 1997] the data exhibit slightly higher mean fragment multiplicities than the earlier ^{197}Au on Cu data at 600 MeV per nucleon [Kreutz *et al.*, 1993]. Applying the same analysis to the more complete data – see for example center and lower parts of figure 18 for the quality of the fit [Schüttauf *et al.*, 1996] – this maximum excitation energy slightly increases up to 12 MeV per nucleon [Kunze, 1996] (see lines in the

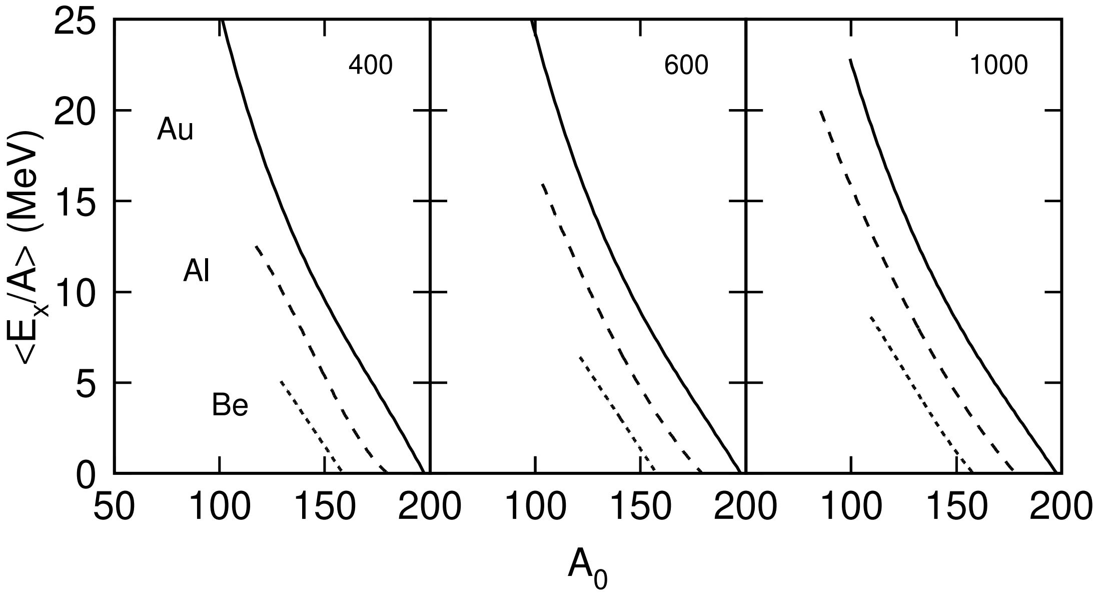

Fig. 19. *Results of the intranuclear-cascade calculations: Mean specific excitation energy $\langle E_x/A \rangle$ as a function of the mass number A_0 of the primary spectator for the reactions ^{197}Au on Be, Al, and Au targets at three bombarding energies of 400 A MeV (left-most panel), 600 A MeV (middle-left), and 1000 A MeV (right). For the purpose of illustration offsets of 20 units of A_0 for each consecutive target were applied.*

upper part of figure 18). Nonetheless, for the range of small Z_{bound} the excitation energies determined from the observed energy and fragment distributions (data points in the upper part of figure 18) still differs significantly from the excitation energies which are required to reproduce the charge correlations within the statistical multifragmentation model. Potentially this difference signals the presence of collective (radial) motion at the time of breakup [Warren *et al.*, 1996; Papp and Nörenberg, 1995] or particle emission prior to the fragment formation [He *et al.*, 1988; Friedman, 1990; Papp and Nörenberg, 1995]. Indeed, as will be discussed in section 3.5.2, the main part of this 'missing energy' is found in the kinetic energies of light particles.

3.5.1 Origin of the Z_{bound}-universality

In order to identify possible reasons for the observed Z_{bound} universality we studied the excitation of the primary spectator nucleus as a function of the number of abraded nucleons with the intranuclear-cascade model. A recent version of the ISABEL code by Yariv and Fraenkel with the slow rearrangement option was used [Sümmerer *et al.*, 1990; Yariv and Fraenkel, 1979]. Less emphasis was given to the absolute values of the excitation energies, which may be overestimated by this model, than to their systematic behavior.

The obtained results, calculated for collisions of ^{197}Au projectiles with different targets, reflect the universality seen in the experiment. The slopes of the correlation of the mean specific excitation energy $\langle E_x/A \rangle$ with the mass A_0 of the primary projectile spectator are found to be independent of the bombarding energy and of the mass of the target (figure 19, note the offsets in A_0). Primary spectators of a given mass seem to always have the same invariant excitation energy. Therefore, if the subsequent decay proceeds statistically, the same universal fragmentation patterns will be observed in the corresponding regions of Z_{bound}. It is further found that the maximum of the specific excitation energy that can be reached with a given target depends strongly on the target mass and, less dramatically, on the bombarding energy (figure 19). Also these features are consistent with the experimental observations (section 3.2).

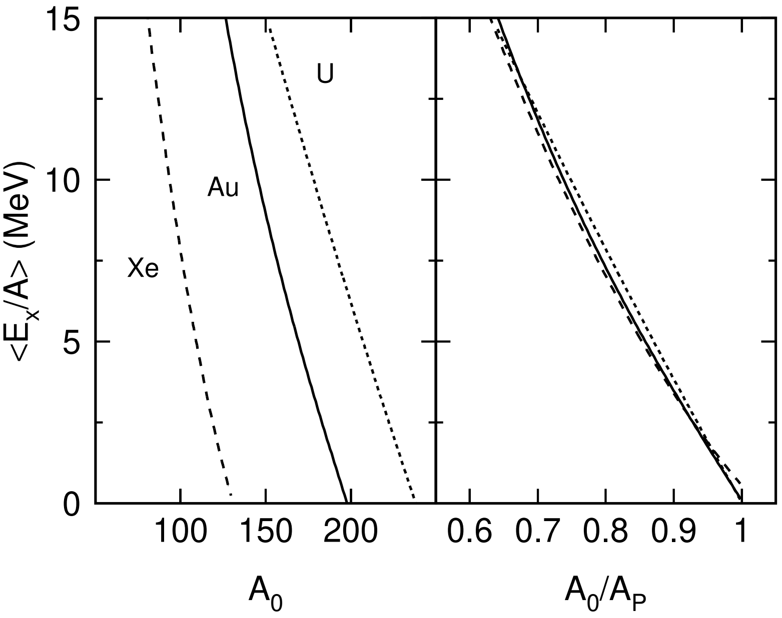

Fig. 20. *Results of intranuclear-cascade calculations:*
Left panel: Mean specific excitation energy $\langle E_x/A \rangle$ as a function of the mass A_0 of the primary spectator for the reactions of ^{238}U, ^{197}Au, and ^{129}Xe on a Au target at E/A = 600 MeV. The calculations were restricted to impact parameters $b \geq$ 8 fm.
Right panel: The same correlations plotted as a function of the reduced mass number A_0/A_P.

In particular for the lightest targets, the heating by Δ excitation may be important on a quantitative level and may determine whether the maximum of fragment production can be observed in a given collision system [Cugnon, 1987; Brown, 1990; Kwiatkowski *et al.*, 1994]. The rate of Δ production grows rapidly with bombarding energy in the range 400 to 1000 MeV per nucleon, as evident from measured pion yields [Harris *et al.*, 1987; Müntz *et al.*, 1995]. Nonetheless, in contrast to $\langle E_x/A \rangle$ versus the impact parameter b, the relation $\langle E_x/A \rangle$ versus A_0 does not depend on whether Δ production is included or suppressed in the calculations [Schüttauf *et al.*, 1996]. It does not respond to this modification of the heating mechanism. As outlined above, it is essentially the invariance of this function which is responsible for the observed Z_{bound} universality. For the case of hadron induced reactions, this invariant feature has been known since the early intranuclear-cascade models were developed [Barashenkov and Toneev, 1972].

The results of the calculations also exhibit the linear scaling with the projectile mass seen in the experiment (section 3.2). The slopes of $\langle E_x/A \rangle$ versus A_0 grow steeper with decreasing mass of the projectile but are the same when plotted versus A_0/A_P (figure 20). This behavior is expected for the purely geometric abrasion. The intranuclear-cascade calculations demonstrate that this feature is not altered by the additional mechanisms of spectator excitation.

It is not a priori obvious why the linear scaling with the projectile mass should be preserved during the statistical decay. The surface energies play an important role in the multi-fragment decays, and the ratio of surface to volume of the decaying system may not be unimportant. Calculations within the statistical multifragmentation model show, however, that effects of this origin are not significant in the range of projectile masses from krypton to uranium (figure 21). Here, the Berlin model in the version implemented in the code McFRAG code [Gross, 1990; DeAngelis and Gross, 1993] was used; similar results are obtained [Kunze, 1996] with the Moscow statistical multifragmentation model [Botvina *et al.*, 1995]. In these calculations the mass A_0 and charge Z_0 were kept fixed while E_x/A was varied. This ignores the correlation between excitation energy and mass of the primary spectator, caused by the primary reaction stage, and results in much larger peak multiplicities than experimentally observed. The figure, nevertheless, demonstrates that both scaled functions $\langle Z_{bound} \rangle / Z_0$ and $\langle M_{IMF} \rangle / Z_0$ follow universal curves

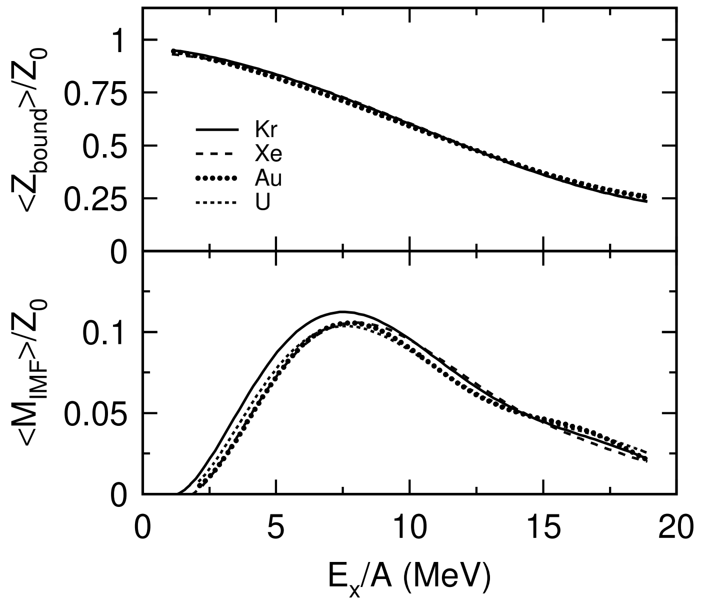

Fig. 21. *Results of calculations with the statistical multifragmentation model McFRAG [Gross, 1990; DeAngelis and Gross, 1993]: Reduced variables $\langle Z_{bound} \rangle / Z_0$ (top) and $\langle M_{IMF} \rangle / Z_0$ (bottom) as a function of the specific excitation energy E_x/A for excited Kr, Xe, Au, and U nuclei.*

as a function of the specific excitation energy E_x/A. Combined with the intranuclear-cascade relation between $\langle E_x/A \rangle$ and A_0/A_P (figure 20), the model result is compatible with the observed dependence on the projectile mass. The top part of figure 21, furthermore, illustrates how Z_{bound}, according to the model, increasingly deviates from the charge Z_0 of the produced spectator system as its excitation energy increases.

The link between the first and the later reaction stages is a subject of high current activity (see, e.g., [Botvina and Mishustin, 1992; Friedman, 1990; Papp and Nörenberg, 1995]). This concerns the expansion and equilibration which are thought to have occurred prior to the fragment decay described by the statistical multifragmentation models. Intuitively, one may suspect that the random knockout of nucleons from and the injection of nucleons into the primary spectator produce a highly disordered system capable of rapidly evolving towards equilibrium. The origin of the Z_{bound} universality may thus be primarily seen in the stochastic nature of the initial cascade process.

3.5.2 Testing kinematic probes

Kinetic energy spectra of light particles emitted from the target spectator in symmetric Au+Au collisions at 1 GeV per nucleon incident energy and integrated over finite ranges of Z_{bound}, are shown in figure 22 [Xi *et al.*, 1996b]. One overall normalization factor is used to relate the experimental and model spectra. The inverse slope parameters T_{slope} characterizing the kinetic-energy spectra of hydrogen and helium isotopes are much larger than the chemical temperatures derived from the isotope yields. They are in the range of 15 to about 25 MeV for the lower range of Z_{bound}, and slightly decrease with increasing Z_{bound}. T_{slope} also seems to be inversely correlated with the particle mass.

The spectra obtained from the statistical model calculations are represented by the open dots in figure 22. For the range of $Z_{bound} < 40$ the corresponding inverse slope parameters are in the vicinity of 10 MeV and nearly the same for the five particle species. Equal slopes would be expected for a simple thermal source with little additional effects such as Coulomb repulsion or secondary decays after breakup. However, the value of $T_{slope} = 10$ MeV is considerably higher than the internal temperatures at breakup which reflects the additional fluctuations due to these effects as they are incorporated in the

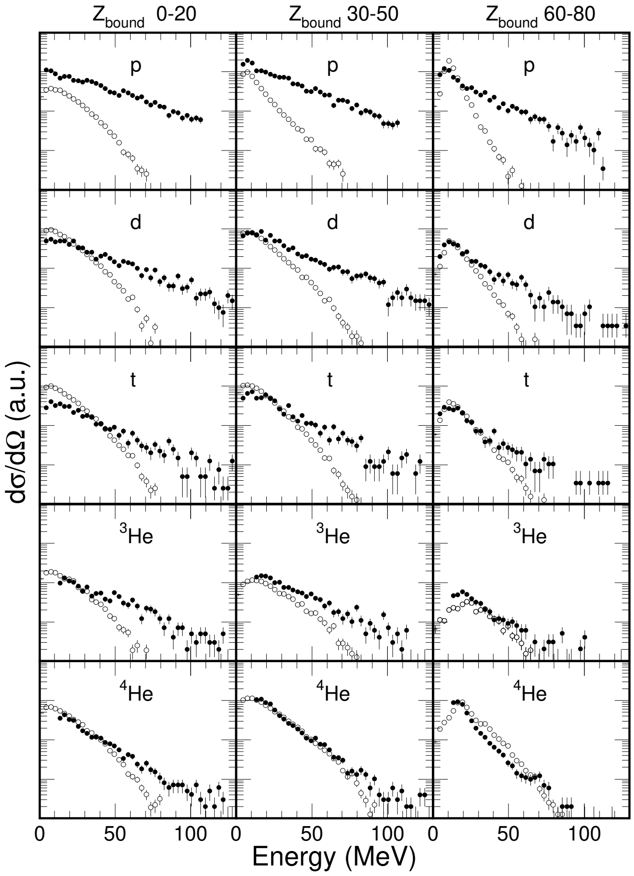

Fig. 22. *Energy spectra of light charged particles p, d, t, ^3He, and ^4He observed in 1AGeV Au+Au collisions for three intervals of Z_{bound} as indicated. The closed circles represent the measured spectra, the open circles are the results of the calculations with the* Moscow *statistical multifragmentation model (from [Xi et al., 1996b]) which has been adjusted to describe the IMF charge distributions.*

model. Apparently, they account for only part of the difference to the experimental spectra. Among the effects not included in the model are multibody Coulomb interactions during the multifragmentation process and the associated large fluctuations of the Coulomb potential at breakup. This interpretation is consistent with the systematically smaller slope parameters of tritons, as compared to ^{3}He which also has mass 3, but not necessarily with the behavior of the deuterons which have a smaller charge and a smaller charge-to-mass ratio than ^{3}He. Emission during the expansion of the system but prior to the breakup [He *et al.*, 1988; Friedman, 1990; Papp and Nörenberg, 1995] and/or collective (radial) flow phenomena [Papp and Nörenberg, 1995; Barz *et al.*, 1996; Warren *et al.*, 1996] can also contribute to this temperature mismatch. Alternatively, or in addition, the difference may be caused by the Fermi momenta of the nucleons forming these fragments [Goldhaber, 1974; Bauer, 1995]. In this case, the fluctuations should be inversely correlated with the mass which, qualitatively, is observed.

Towards larger values of Z_{bound}, the direct comparison of the spectra for large Z_{bound} (right column of figure 22) shows that, over a wide range of energies, good agreement is observed in the case of the helium isotopes. In particular, the spectra of the α particles which, among the five species, have the smallest slopes are well reproduced. In this range of Z_{bound}, where large fragments and excited residue-like heavy nuclei are produced, a major contribution to the observed α yield is expected from secondary evaporation which, apparently, is modelled well. On the other hand, in peripheral collisions the protons and – at a smaller level – also the deuterons show a significantly harder spectrum as expected from the model calculations. In these rather peripheral collisions flow effects are expected to be small [Papp and Nörenberg, 1995; Barz *et al.*, 1996; Warren *et al.*, 1996]. Therefore, this deviation may indeed signal particle emission prior to the fragmentation process.

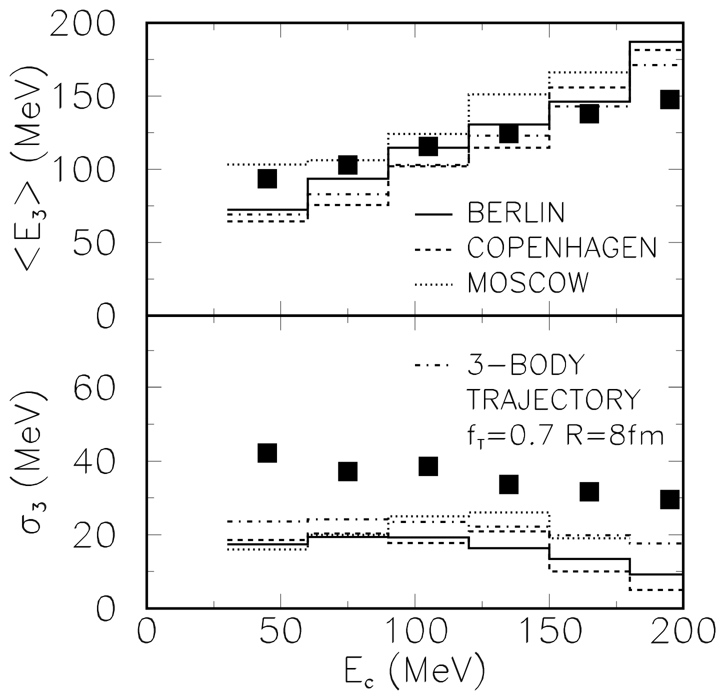

Fig. 23. *Mean center-of-mass kinetic energy and its standard deviation of three heavy fragments produced in Au induced reactions at 600A MeV. The dotted, dashed and solid histograms present predictions of the* COPENHAGEN, BERLIN, *and* MOSCOW *statistical multifragmentation models, respectively. The dashed-dotted line shows the result of a classical trajectory calculation (from [Begemann-Blaich et al., 1997]).*

Not only for light fragments but also for more heavy nuclear remnants the kinetic energy distributions are not yet fully understood within the statistical decay picture. To illustrate this point, momentum correlations between three heavy fragments (Z $\geq$8) produced in Au induced reactions at 600A MeV were studied in detail [Lindenstruth, 1993; Begemann-Blaich *et al.*, 1997]. In figure 23 the mean kinetic energy $\langle E_3 \rangle$ of these simultaneously produced fragments in their center-of-momentum frame (top part) and the width of this distribution σ_3 are plotted versus the nominal Coulomb energy E_c. The nominal Coulomb energy is determined event-by-event from the measured charges and masses according to the relation

$$E_c = e^2 \cdot \sum_{i<j} Z_i Z_j / (1.4 \cdot (A_i^{1/3} + A_j^{1/3})). \tag{1}$$

Within a purely thermal scenario the increase of $\langle E_3 \rangle$ with increasing E_c reflects the mutual Coulomb repulsion between the fragments and is, therefore, sensitive to their initial spatial distribution. On the other hand, the offset at E_c=0 and the width σ_3 depend mainly on the temperature of the system, i.e. $\langle E_3 \rangle (E_c = 0) \sim 4T$ and $\sigma_3(E_c = 0) \sim 2T$.

Whereas the mean kinetic energies are in general quite well described by the model calculations (histograms in figure 23) the calculations underestimate the width of the energy distribution by almost a factor of two. This deficiency is obviously a problem common to all multifragmentation models. In more schematic three-body Coulomb trajectory calculations with parameters corresponding to those of the statistical models a very similar underprediction of σ_3 is seen. Since in the latter case no additional light fragments are considered, the agreement between these calculations suggests that multi-body (n > 3) Coulomb effects are of minor importance for these three-fragment correlations. In a series of calculations it was also verified that the underprediction of σ_3 can not be compensated by allowing fluctuations of the initial excitation energy.

Formally, the schematic three-body calculations can be reconciled with the observed kinetic energy distributions by assuming a large radius (R $\geq$ 12 fm) and – at the same time – a high temperature (T $\approx$ 13 MeV) [Lindenstruth, 1993; Pochodzalla, 1994]. This, however, may not only be counter-intuitive,

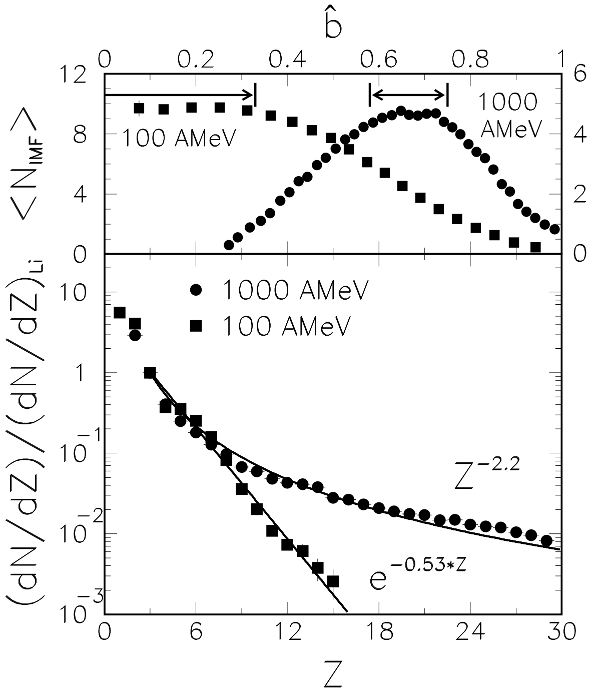

Fig. 24. *Top: Mean observed multiplicity of nuclear fragments of intermediate mass measured in Au + Au collisions at E/A = 100 and 1000 MeV as a function of the reconstructed relative impact parameter $\hat{b}$. Bottom: Charge distributions of the observed fragments for the impact parameter regions of maximum multiplicity indicated by the arrows in the top part of the figure (from [Kunde et al., 1995]).*

but adopting such input parameters in the statistical multifragmentation calculations resulted in charge distributions which are in contradiction with the observations.

Recently [Botvina *et al.*, 1995] angular momentum was suggested as a further source of kinetic energy fluctuations. Indeed, by allowing an angular momentum of about $0.75\hbar$, the width σ_3 of the kinetic energy distribution is significantly enhanced and comes closer to the data [Begemann-Blaich *et al.*, 1997]. However, most of the observed charge correlations [Kreutz *et al.*, 1993] turn out to be inconsistent with such angular momenta. One, therefore, comes to the conclusion that the presently available implementations of statistical multifragmentation models are not able to describe simultaneously the charge partition and the momentum distributions of neither light nor heavy fragments. One has to keep in mind though that the origin for this inconsistancy may be different for different fragment sizes.

3.5.3 Interplay between radial flow and the charge partition

The decay statistical decay models discussed above model a quasi-static freeze-out situation. Unfortunately, a consistant description of a statistical decay in the presence of collective internal (radial) flow does not exist hitherto. On the other hand, it is well known that velocity gradients in a system may alter its phase behaviour significantly [Dhont, 1994; Dhont, 1996] In the following a simple coalescence picture will be employed to illustrate that the partition space for heavy fragments may indeed be sensitive the the underlying collective motion.

Experimentally it is found that the relative element yields are systematically correlated with the magnitude of the observed radial flow [Reisdorf, 1994; Kunde *et al.*, 1995]. In order to compare multifragmentation in central (=large flow) and multifragmentation in peripheral collisions (=small flow) we consider the system ^{197}Au + ^{197}Au at incident energies of E/A = 100 and 1000 MeV. The choice of the bombarding energy for the peripheral collisions is not critical since – as was shown before – the energy dependence is rather weak over a wide range of incident energies. The mean IMF multiplicity is shown in the upper part of figure 24 as a function of the reconstructed and normalized impact parameter $\hat{b}$. The impact parameter scale was derived from the multiplicity of light particles at E/A=100 MeV

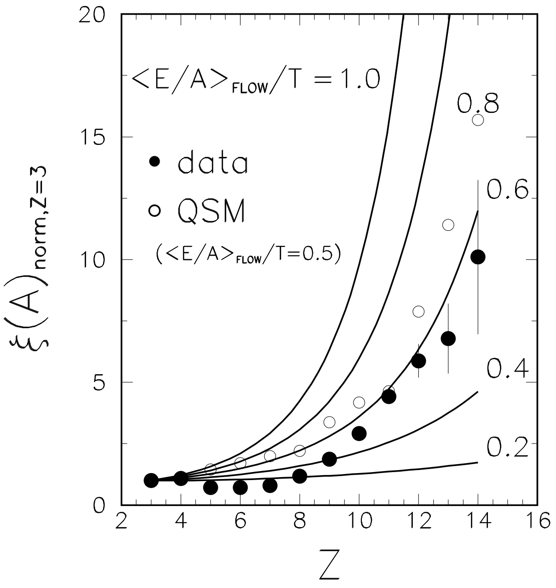

Fig. 25. *Suppression factor $\xi(A)$ as a function of the fragment atomic number Z. The dots represent the IMF yield ratios measured for ^{197}Au + ^{197}Au at E/A = 100 MeV and 1000 MeV at selected impact parameters (cf. figure 24) and normalized at Z = 3. The lines are the results of a coalescence model for the indicated values of the parameter $\langle E/A\rangle_{flow}/T$ [Kunde et al., 1995]. Predictions within a quantum statistical model for $\langle E/A\rangle_{flow}/T$=0.5 are given by the circles [Pal et al., 1996].*

[Tsang *et al.*, 1993] and Z_{bound} at E/A=1000 MeV [Hubele *et al.*, 1991]. The maximum $\hat{b}$ = 1 corresponds to an impact parameter of about 15 fm. At E/A = 100 MeV a maximum value $\langle N_{IMF}\rangle \approx 10$ is recorded in central collisions and the majority of fragments originate from the interaction region. At E/A = 1000 MeV the maximum of the fragment multiplicity $\langle N_{IMF}\rangle \approx 5$ is found near $\hat{b} \approx 0.7$, corresponding to an impact parameter of about 10 fm, and the dominant source is the projectile spectator. However, if the multiplicities are corrected for the detection efficiency and normalized to the average size of the decaying system (2×160 participating nucleons in central and approximately 2×150 spectator nucleons in peripheral collisions) nearly the same probability of one IMF per about 30 nucleons is obtained in both cases.

As explored in detail by the FOPI collaboration the element distributions are significantly different in central and peripheral collisions [Kuhn *et al.*, 1993]. This is illustrated in the lower part of the figure 24. The yields were normalized at Z = 3 and the used ranges of impact parameters are indicated by the boxes in the top panel of the figure. In peripheral collisions the familiar power-law behavior with an exponent $\tau \approx 2.2$ is observed; in central collisions the yield of heavier fragments is strongly reduced and an exponential charge distribution is found. The ratio between these two distributions is shown in figure 25 as a function of the fragment charge.

As mentioned at the beginning the observation of element distributions with a power law or with a more exponential behavior has been associated with the two possibilities that the reaction path of the decaying nuclear system hits the critical point or region or that it never comes close to it [Siemens, 1983]. Compared to the excitation energies of 6 to 8 MeV per nucleon deduced for the equilibrized spectators in peripheral collisions [Botvina and Mishustin, 1992; Li *et al.*, 1993a; Barz *et al.*, 1993] the total center-of-mass energy of 25 MeV per nucleon, available in central collisions at E/A = 100 MeV, is indeed very different. However, a large fraction of this energy is not thermalized during the collision and survives as collective energy of the expansion. Thus the observation that the normalized probabilities of fragment formation are nearly equal represents a first hint that the thermalized excitation energies are not too different in both types of reaction. As will be shown in section 5.1.2 temperatures measured via isotope ratios support this conclusion.

Since the two processes of fragment formation differ considerably in the quantity of the observed radial flow it is tempting to relate the observed difference of the charge distribution to this collective motion. For the peripheral collisions an upper limit of 1 MeV per nucleon has been established in the relevant impact parameter range [Lindenstruth, 1993; Pochodzalla *et al.*, 1994]. The corresponding quantity for the central collisions, i.e. $\langle E_r/A \rangle$ minus the Coulomb energy, is of the order of 7 to 10 MeV per nucleon. (Compare for example figures 9 and 3.) One may, therefore, try to relate the suppression of fragment formation in central collisions to the reduction of the nucleon density in momentum space caused by the radial flow [Kunde *et al.*, 1995]. Within a coalescence picture and under the assumption of a common freeze-out temperature, the probability that a fragment of mass A is formed in central collisions is reduced by the factor

$$f_A = \left[\frac{p_{rms}^{thermal}}{\sqrt{(p_{rms}^{thermal})^2 + (p_{rms}^{flow})^2}} \right]^{3 \cdot A} . \tag{2}$$

The thermal width may be expressed in terms of the break-up temperature T as

$$p_{rms}^{thermal} = \sqrt{3 m_0 T}, \tag{3}$$

where m_0 denotes the nucleon mass. The additional flow contribution across the coalescence volume of a fragment is given by

$$p_{rms}^{flow} = \sqrt{(\langle E/A \rangle_{flow}) \cdot \left(\frac{R_f}{R_s} \right)^2 \cdot 2 m_0}. \tag{4}$$

Here, $\langle E/A \rangle_{flow}$ is the mean flow energy per nucleon, R_s is the radius of the source and R_f denotes the spherical coalescence volume of the fragment. For a homogeneous system the ratio R_f/R_s is given by $(A/A_s)^{1/3}$ where A and A_s are the mass numbers of the fragment and of the total system, respectively.

The lines in figure 25 show the ratio

$$\xi(A) = \frac{f_A(A_S = 150, 0)}{f_A(A_S = 320, \langle E/A \rangle_{flow}/T)} \tag{5}$$

which compares a system of 150 nucleons having no initial flow (representative for the situation at E/A = 1000 MeV) and a system composed of 320 nucleons with a non-zero flow $\langle E/A \rangle_{flow}$ and temperature T (representing central Au + Au collisions at E/A = 100 MeV). In order to compare the calculations with the data shown in figure 25 the ratio $\xi(A)$ has been normalized at $A = 6$. The calculations indicate that, in particular, the formation probability of heavy fragments is sensitive to the underlying flow dynamics. A satisfactory description of the measured intensity ratios is obtained for a value $\langle E/A \rangle_{flow}/T \approx 0.6$ which is in qualitative agreement with flow energies extracted for light fragments with Z$\leq$6 from the analysis of the kinetic energy spectra for the same reaction [Hsi *et al.*, 1994] (see figure 4).

In the mean time similar results have been obtained [Pal *et al.*, 1996] in the framework of a quantum statistical model (QSM) which takes the effect of a fragment mass dependent collective radial flow into account. Also within these calculations, the fragment yields are shifted towards smaller charges. As an example, the open points in figure 25 represent the QSM-results for a ratio $\langle E/A \rangle_{flow}/T$ = 0.5 and a temperature T = 6 MeV.

Considered for themselves both, the chemical composition of the fragments as well as the various kinetic degrees of freedom exhibit no rememberance on the entrance channel and show a high degree of equilibration. Nonetheless, the phase space occupancy of the dynamical and chemical degrees of freedom

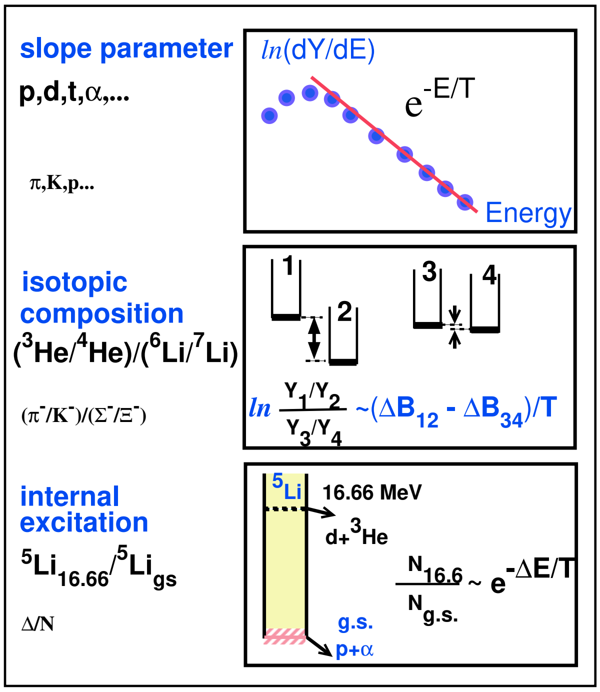

Fig. 26. *Illustration of different thermometers for hadronic systems: inverse slope parameter (top part), isotope ratios (center part), and relative population of states (lower part).*

can not be described by the same parameters. In section 5.3 this point will be taken up again. We will see that also the *internal* degrees of freedom of the individual fragment do not support a picture of a quasi-static system in global equilibrium.

4 Hadronic Thermometer

Less straightforward than the determination of an excitation energy is the determination of a nuclear temperature. Nuclei are closed systems without an external heat bath. Consequently, the temperature of the system cannot be pre-determined but has to be reconstructed from observable quantities. For a microcanonical ensemble, the thermodynamic temperature of a system may be defined in terms of the total-energy state density. An experimental determination of the state density and its energy dependence is, however, hitherto impossible. Therefore, nuclear temperature determinations take recourse to 'simple' observables of specific degrees-of-freedom which constitute – at least for some ideal situations and generally within a canonical treatment – a good approximation to the true thermodynamic temperature.

Figure 26 illustrates three different methods to extract a temperature of a hadronic system. At low excitation energies, the inverse slope parameters describing the kinetic energies or transverse mass distributions of the emitted particles are a good measure of the temperature. In intermediate energy and relativistic nucleus-nucleus interactions, however, these distributions suffer from possible collective flow effects [Brockmann *et al.*, 1984; Bass *et al.*, 1994; Müntz *et al.*, 1995], secondary decay processes [Pochodzalla *et al.*, 1987], multiple Coulomb interaction and Fermi motion [Bauer, 1995]. While the spectral distributions are indispensable to disentangle thermal and collective phenomena, a more direct way to test whether locally thermal equilibrium is achieved and to determine a temperature is to study in detail the particle abundance [Hoyle, 1946; Albergo *et al.*, 1985; Hahn and Stöcker, 1988; Braun-Munzinger *et al.*, 1995; Panagiotou *et al.*, 1996]. Finally, from the relative population of two states of a given fragment, the so called emission temperature can be deduced. Whereas the latter analysis requires a more demanding coincidence measurement of the decay products, isotope temperatures can be extracted from single particle yields.

For the following considerations we will assume a nuclear system at low density and in chemical and

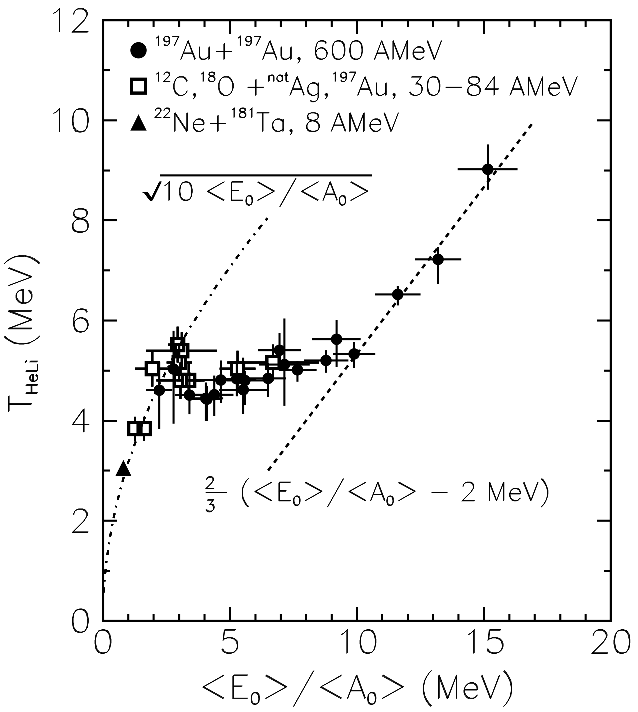

Fig. 27. *Caloric curve of nuclei determined by the dependence of the isotope temperature T_{HeLi} on the excitation energy per nucleon [Pochodzalla et al., 1995].*

thermal equilibrium. For such a system a measure of the temperature T may be obtained via the double yield ratio of two isotope pairs, (Y_1/Y_2) and (Y_3/Y_4), differing by the same number of neutrons and/or protons [Albergo *et al.*, 1985]:

$$R = \frac{Y_1/Y_2}{Y_3/Y_4} = a \cdot e^{[(B_1-B_2)-(B_3-B_4)]/T} = a \cdot e^{\Delta B/T}. \tag{6}$$

Here, B_i denotes the binding energy of particle species i and the constant a contains known spins and mass numbers of the fragments. Recently, Kolomiets and co-workers have shown [Kolomiets *et al.*, 1997] that by adopting Maxwell-Boltzmann statistics and the Wigner-Seitz approximation for the Coulomb interaction between the fragments eq. 6 can also be derived without imposing the condition of chemical equilibrium.

Of course, a meaningful temperature scale can only be derived if the ratio R is sufficiently sensitive to the temperature of the system and if the yields of the considered fragments are measurable over a large range of excitation energy. By differentiating equation 6 we see that a relative error (or modification due to sequential decay) of the isotope yield ratio of $\Delta R/R$ results in a relative modification of the temperature by

$$\frac{\Delta T}{T} = -\frac{T}{\Delta B} \cdot \frac{\Delta R}{R}. \tag{7}$$

Thus, a large sensitivity of this thermometer can be achieved if the binding energy difference $\Delta B = (B_1 - B_2) - (B_3 - B_4)$ is larger than the typical temperature to be measured. The analysis of more than 1000 possible 'thermometer' defined via equation 6 by Tsang *et al* [Tsang *et al.*, 1996b] supports this rule of thumb.

Particularly large values for b are obtained if a $^3He/^4He$ ratio is involved. Indeed, the large cross section of He fragments as an abundant constituent in both the 'liquid' and the 'vapor' regime of nuclear systems *and* the strong binding energy of the α-particle is the lucky coincidence which is the basis of the temperature determination presented hereafter. In order to acquire for the second yield ratio also a sufficient production yield we define in the following a temperature $T_{HeLi,0}$ in terms of the yield ratios ^{3}He/^{4}He and ^{6}Li/^{7}Li

$$T_{HeLi,0} := 13.33/ln(2.18 \cdot \frac{Y_{6Li}/Y_{7Li}}{Y_{3He}/Y_{4He}}). \quad (8)$$

Using the d/t ratio rather than the ^{6}Li/^{7}Li ratio, a similar temperature scale, $T_{HHe,0}$, may be derived [Albergo *et al.*, 1985]. Whereas the d/t ratio was not accessible in the first experiment, $T_{HHe,0}$ may be more appropriate for central collisions. In general, by employing four nuclei species which all differ only little in proton and neutron numbers, emission from a similar stage of the reaction becomes more likely.

Up to this point we considered nuclei in their ground state only and we ignored the effect of sequential decays during the final stage of the disassembly process. In particular, the yield of α-particles may be modified by secondary decays. (Note, however, that the effect of the α-feeding is partially neutralized by the feeding of ^3He. Similarly, contributions from γ-unstable states in ^{6}Li and ^{7}Li partially cancel each other [Campi *et al.*, 1996].) In order to test the model dependence of the temperature definition via Eq. (8) and to investigate the influence of sequential decays and low lying γ-unstable states we analyzed the fragment distributions predicted by several decay models [Hahn and Stöcker, 1988; Konopka *et al.*, 1994; Charity *et al.*, 1988; Gross *et al.*, 1986]. Despite the strong feeding of the light particle yields through secondary decays these first calculations predict an almost linear dependence of $T_{HeLi,0}$ on the actual temperature T of the system. However, in order to account pragmatically for a systematic underestimation of the temperature by the quantity $T_{HeLi,0}$, we define the final isotope temperature via

$$T_{HeLi} = 1.2 \cdot T_{HeLi,0}. \quad (9)$$

For consistency reasons all values of T_{HeLi} presented hereafter include the factor $f_T = 1.2$. It is important to realize, though, that this calibration is model dependent and other decay models might predict different corrections (compare for example [Pochodzalla *et al.*, 1985] and [Tsang *et al.*, 1996b]). Also each isotope thermometer will require an individual calibration [Tsang *et al.*, 1996b; Kolomiets *et al.*, 1996; Möhlenkamp, 1996]. This model dependence may only be reduced if more data on the population of excited states and the fragment distribution become available. First attempts to overcome this difficulty will be discussed in section 5.3.

5 Nuclear Calorimetry

5.1 Caloric curves of nuclei – present experimental situation

5.1.1 Calorimetry of spectator nuclei

Figure 27 shows the isotope temperature as a function of the total excitation energy per nucleon [Pochodzalla *et al.*, 1995]. This caloric curve can be divided into three distinctly different sections. In line with previous studies in the fusion evaporation regime [Fabris *et al.*, 1987] the rise of T_{HeLi} for excitation energies below 2 MeV per nucleon is compatible with the low-temperature approximation of a fermionic system. Within the range of $\langle E_0\rangle/\langle A_0\rangle$ from 3 MeV to 10 MeV an almost constant value for T_{HeLi} of about 4.5-5 MeV is observed. This plateau may be related to the finding of rather constant emission temperatures over a broad range of incident energies which were deduced from the population of particle unstable levels in He and Li fragments [Kunde *et al.*, 1991]. We also note that the mean

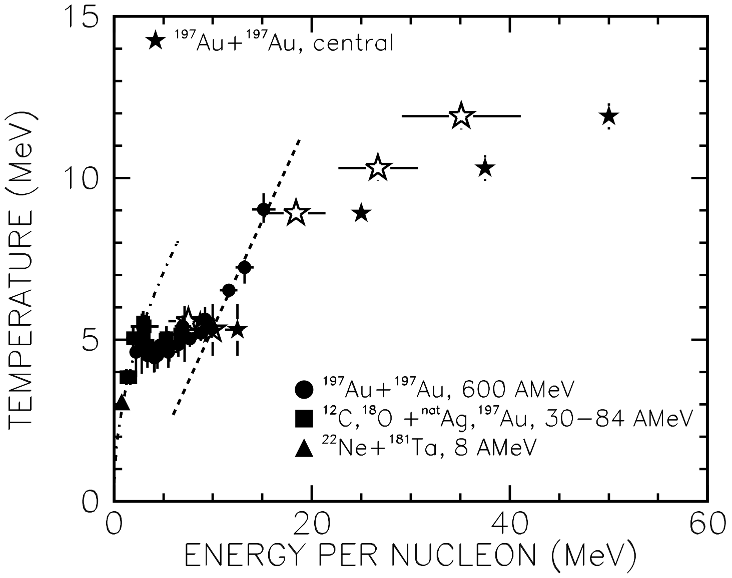

Fig. 28. *Caloric curve of nuclei determined by the dependence of the isotope temperature* T_{HeLi} *on the excitation energy per nucleon. The stars indicate results for central Au+Au collisions at 35 (from [Huang et al., 1996]), 50, 100, 150 and 200 MeV per nucleon incident beam energy [Serfling, 1996]. For the filled stars the energy scale is given by the center-of-mass energy whereas in case of the open stars the radial flow energies (dashed line in figure 4) have been subtracted. For orientation the lines given in figure 27 are also shown.*

excitation energy of the plateau coincides with the limiting excitation energy of about 4.5-6.4 MeV per nucleon for the observation of a fusion-evaporation process [Bohne *et al.*, 1990; Bohne *et al.*, 1993; Figuera *et al.*, 1995]. Finally, beyond a total excitation energy of 10 MeV per nucleon, a steady rise of T_{HeLi} with increasing $\langle E_0\rangle/\langle A_0\rangle$ is seen.

5.1.2 *Caloric curve of the nuclear fireball*

While in central collisions between equally heavy nuclei the slope parameters and the collective radial motion are strongly interlaced, the chemical temperatures deduced from the isotopic composition reflect a local property and are expected to be less affected by a radial flow. Indeed, within the simple coalescence picture outlined in section 3.5.3 the double ratio entering into the evaluation of T_{HeLi} will be modified by not more than 5% for a typical ratio between flow and thermal energy of one.

The filled stars in figure 28 show preliminary values for T_{HeLi} for central Au+Au collisions at beam energies of 50, 100, 150 and 200 MeV per nucleon [Serfling, 1996; Immé *et al.*, 1996] together with a point measured at 35 MeV per nucleon by the MINIBALL Collaboration. Central reactions were selected by the number of light particles detected in the forward hemisphere in the center-of-mass. Isotope ratios measured close to 90^o in the cm-system were used to evaluate the isotope temperatures. For these data points, the *total* available center-of-mass energy per nucleon has been chosen as the horizontal axis. However, as discussed in section 2, only part of this energy is available for heating. For a proper comparison with the caloric curve determined by the spectator nuclei, one had to determine the thermal excitation energy *at normal density.* A lower limit for this energy can be obtained by subtracting the measured flow energies (figure 4) from the available center-of-mass energy. The corresponding data points are indicated by the open stars in figure 28. Even considering the fact that the flow energy generated during the expansion from normal nuclear density towards the freeze-out density should – for

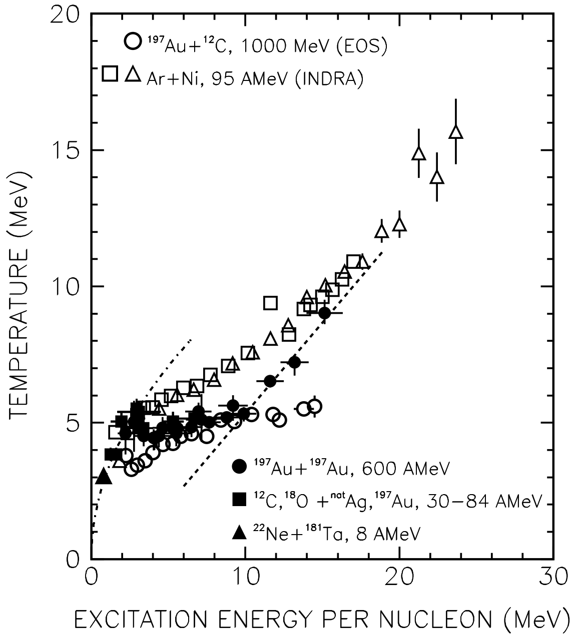

Fig. 29. *Comparison of* ALADIN*'s caloric curve (solid points) to results obtained by the EOS collaboration for spectators produced in Au+C reactions at 1000 AMeV [Hauger et al., 1996] (open circles) and by the INDRA collaboration for quasi-projectiles produced in 95 AMeV Ar+Ni reactions [Ma et al., 1996] (open triangles and squares).*

consistency – be included in the energy scale, the similarity between the caloric curves in central and peripheral collisions is quite impressive and may be viewed as a signal of common underlying physics in both types of reactions. Of course, a more quantitative understanding of the expansion dynamics will be required before the question can be answered whether and to what extent radial flow modifies the properties of the caloric curve.

5.1.3 Caloric curves in other reactions

Figure 29 summarizes the presently available caloric curves measured via T_{HeLi} as defined in Eq. 9. A recent result of the EOS collaboration for ^{197}Au+^{12}C reactions at 1000 AMeV beam energy is shown by the open circles [Hauger *et al.*, 1996]. These data nicely confirm the plateau-like behaviour at intermediate excitation energies between 5 and 10 MeV per nucleon, though the rise at high excitation energies is not observed in that experiment. This is in line with a similar observation by the ALADIN collaboration at 600 MeV per nucleon Au induced reactions on light targets [Möhlenkamp, 1996] (lower part of figure 30). Though it is important to note that for the light carbon target the cross section strongly drops for Z_{bound} values below about 40 (see circles in the upper part of figure 30). At small Z_{bound}, fluctuations in the decay as well as in the detection process might diminish the sensitivity of the event characterizing observable (here Z_{bound}) to the actual initial excitation energy for the central reactions in asymmetric systems. As a consequence, no reliable temperature values can be extracted from the ALADIN data for Z_{bound} values less than 30. If also for the excitation energy the Z_{bound} universality holds this means that only the 'plateau' region can be probed by C+Au reactions.

The different reaction geometry represents a further possible source for the deviation between Au+Au and Au+C reactions: in Au+C reactions the participant and spectator regions have a larger overlap in momentum space. In addition, spectator nuclei produced in Au+Au reactions might be more compact compared to more rarified spectators in the most central Au+C collisions.

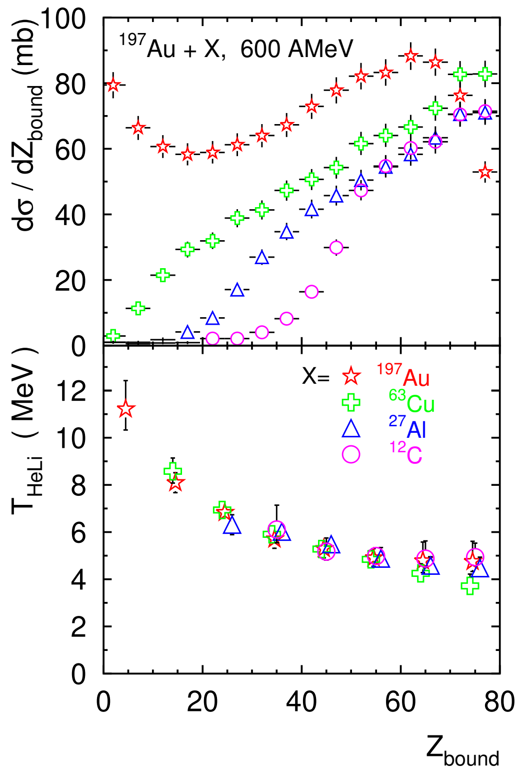

Fig. 30. *Lower part: Isotope temperatures as a function of Z_{bound} for Au+C,Al,Cu and Au reactions at 600 MeV per nucleon (from [Möhlenkamp, 1996]). Upper part: Differential cross section as a function of Z_{bound}.*

A recent result of the INDRA collaboration for the Ar+Ni system at 95 AMeV [Ma *et al.*, 1996] is indicated by the open triangles and squares in figure 29. In this reaction, charged particles emitted into the forward hemisphere of the projectile-like source supplemented by information on the heaviest detected fragment have been used to reconstruct the quasi-projectile [Péter *et al.*, 1995]. Thus, this analysis is based on experimental information covering slightly more than half of the original projectile mass. At low excitation energies the temperature increases steadily. However, also these data show an upswing at an excitation energy of about 10 MeV per nucleon. Compared to the ALADIN data the temperatures appear to be systematically higher by about 1-2 MeV.

Clearly, more systematic studies are needed in order to clarify whether this discrepancy is for example due to the definition of the decaying source (which in the Fermi-energy regime is not well separated from the fireball), the small size of the system in the Ar+Ni reaction ($\approx$ 34 nucleons [Ma *et al.*, 1996]) or the different neutron-to-proton contents of the source.

5.2 The caloric curve of nuclei – present understanding

The qualitative similarity of the caloric curve of water and that of nuclei is striking. Although it is clear, that *this analogy should not be overemphasized*, it was surely this resemblance which triggered a widespread activity, both experimental [Tsang *et al.*, 1996a; Tsang *et al.*, 1996b; Hauger *et al.*, 1996; Huang *et al.*, 1996] and theoretical concerning the interpretation of a caloric curve [Natowitz *et al.*, 1995; Papp and Nörenberg, 1995; Karnaukhov, 1996; Moretto *et al.*, 1996; Campi *et al.*, 1996] as well as the more technical aspect of the temperature determination from isotope yield-ratios [Campi *et al.*, 1996; Kolomiets *et al.*, 1996; Xi *et al.*, 1996a; Majka *et al.*, 1996]. We will first turn to the latter point.

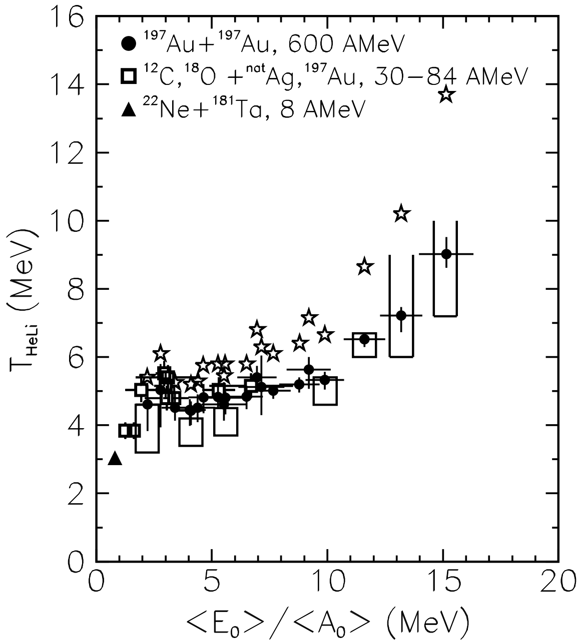

Fig. 31. *Same as in figure 27 but including the emission temperatures extracted by Xi et al. (open rectangles [Xi et al., 1996a]) and by Majka et al. (open stars [Majka et al., 1996]) by reanalysing the* ALADIN *data shown in figure 27.*

5.2.1 *Isotope thermometer and sequential decay*

While the determination of the excitation energy is well defined, any nuclear thermometer is in practise model dependent and may, therefore, suffer from large systematic uncertainties. For example, temperatures deduced from kinetic energy distributions as well as the so called emission temperatures extracted from the relative population of internal states, are altered by sequential decays from excited fragments [Pochodzalla *et al.*, 1985; Pochodzalla *et al.*, 1987; Hahn and Stöcker, 1988]. Similarly, the formulas given by Albergo [Albergo *et al.*, 1985] which are the basis for the isotope thermometers can only be used as a guidance to define a temperature scale. As mentioned before, side-feeding from particle unstable resonances as well as contributions from γ-unstable states are neglected in the definition of T$_{HeLi}$ by equation 8. In order to provide a simple, model-independent prescription to evaluate T$_{HeLi}$ from the measured yield-ratios we, therefore, adopted a single correction factor in equation 9.

In order to avoid this simple scaling the formalism of Albergo *et al.* has been modified to take the effect of feeding from γ decays [Campi *et al.*, 1996] and also 1-step particle emission [Kolomiets *et al.*, 1996] self-consistently in the definition of the isotope temperature into account. Applying these recipes, the qualitative shape of the caloric curve does not change. It is, however, important to realize that even though these analytical relations may help to elucidate the role of e.g. the γ unstable states in the lithium isotopes [Campi *et al.*, 1996], the validity of these relations – which neglect multi-step particle emission [Kolomiets *et al.*, 1996] or even all particle decays [Campi *et al.*, 1996] – may be limited to rather low temperatures. For high temperatures corrections due to additional sequential processes will be required, making again more complete calculations indispensable.

As a first attempt to go beyond the feeding calculations presented in ref. [Pochodzalla *et al.*, 1995], Xi and collaborators included also feeding from high lying continuum states in their sequential decay calculations [Xi *et al.*, 1996a]. While according to these calculations the 'plateau' at excitation energies below about 10 MeV per nucleon should be shifted to slightly smaller temperatures (corresponding to a correction factor of about f_T = 1.0 rather than 1.2 in equation 9) only lower limits for the temperature in the rising, 'gaseous' part could be extracted from this re-analysis of the ALADIN data (figure 31). Concerning the underlying decay-model it may be important to realize that observed 'apparent'

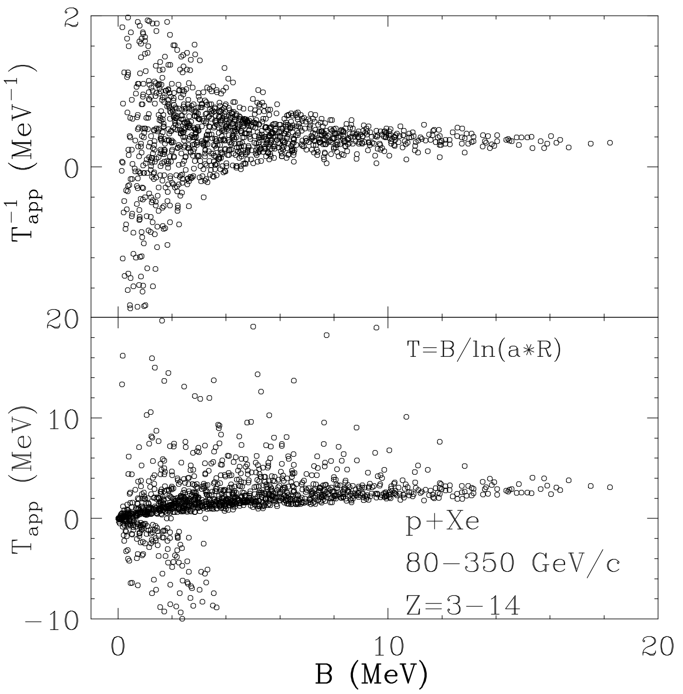

Fig. 32. *Lower panel: apparent temperatures from 1326 isotope quartets as a function of the binding energy difference (see equation 7) for p+Xe collisions. The upper panel shows the same data plotted as inverse apparent temperature (from [Tsang et al., 1996b]).*

T_{HeLi} values exceeding about 10 MeV can not be described by these calculations. The fact that larger temperatures are indeed observed in central collisions (figure 28) points to important physics which is beyond of the scope of these equilibrium calculations.

The role of the excluded volume assigned to the fragments in quantum statistical decay and the effect on the amount of sequential decays has been addressed in ref. [Gulminelli and Durand, 1996]. By assuming non-spherical shapes for the effective excluded volume for particle unstable resonances the production of more loosely bound fragments like excited states is strongly suppressed with respect to e.g. protons, neutrons or alpha particles. As a consequence, the apparent (measured) isotope temperatures are significantly reduced thus suggesting correction factors $f_T \approx 2$ in equation 9 which are significantly larger than f_T=1.2.

Finally, quantum statistical decay calculations presented by Majka and co-workers [Majka *et al.*, 1996] predicted correction factors which for break-up densities below $0.5\rho_0$ and temperatures below 15 MeV varies between about 1.4 and 2. The net effect is that in particular for excitation energies beyond 10 MeV per nucleon the caloric curve is shifted towards even higher temperatures. The result of this re-analysis is indicated by the open stars in figure 31.

In summary, the different decay calculations clearly demonstrate the importance of feeding corrections for the determination of a thermodynamic temperature from apparent isotope temperatures. At present there exists, however, no consensus on the amount of sequential decay. Although the originally proposed [Pochodzalla *et al.*, 1995] correction factor of f_T=1.2 to $T_{HeLi,0}$ marks the 'mean' value of the various calculations, it is clear that more experimental information on the decay of particle unstable resonances is required in order to solve this dilemma.

5.2.2 Different thermometer = different temperatures?

The validity of a hadronic thermometer generally rests on model assumptions. Only an experimental cross comparison with alternative thermometers can lend additional credibility to a temperature scale. As was shown before, apparent temperatures deduced from kinetic energy distributions are in

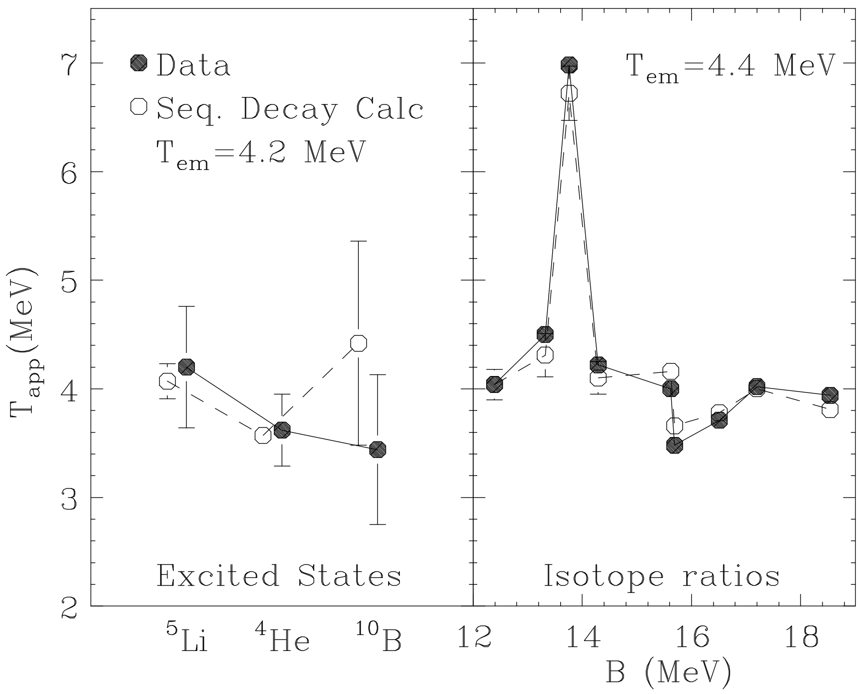

Fig. 33. *Apparent temperatures obtained from relative populations of excited states (left) and from isotope ratios (right) in central Au+Au collisions at 35A MeV. The closed points are the data and the open points are predictions of sequential decay calculations assuming freeze-out temperatures of 4.2 and 4.4 MeV, respectively (from [Huang et al., 1996]).*

clear disagreement with the isotope temperatures. Because of the many effects which influence the kinetic energies in these reactions – e.g. sequential decay, collective motion, Coulomb interaction, pre-fragmentation emission and Fermi motion – we will in the following focus on a comparison of different chemical temperatures. We will then turn to a first cross check between isotope temperatures and so called emission temperatures.

As a first check for internal consistency Tsang *et al.* [Tsang *et al.*, 1996b] compared in total 1326 different thermometers based on all available isotope ratios measured previously in 80-350 GeV p+Xe interactions [Hirsch *et al.*, 1984] as well as in 35A MeV ^{14}N+Ag and 22A MeV ^{32}S+Ag heavy ion induced reactions [Nayak *et al.*, 1992; Xu *et al.*, 1989]. (Note, however, that not all apparent temperatures are independent of each other since the same isotope yields are used several times.) Different apparent isotope temperatures were found for different isotope quartets (figure 32). As already mentioned in section 4 large variations due to distortions from sequential decay were seen for those pairs for which the temperature exceeds the binding energy difference [Pochodzalla *et al.*, 1985]. For pairs with large binding energy differences – as is also the case for the HeLi-Thermometer – reasonably small correction factors could be provided which allow to extract consistent isotope temperatures.

In a further step, isotope temperatures were compared to temperatures deduced from the relative population of excited states. A first cross comparison of the T_{HeLi} thermometer with emission temperatures gave compatible results for the ^{36}Ar+^{197}Au reaction at 35A MeV [Tsang *et al.*, 1996a]. A similar agreement was also found in central Au+Au collisions at 35A MeV [Huang *et al.*, 1996]. The quality of the agreement between the different thermometers investigated in the latter reaction is shown in figure 33. Both, the temperatures deduced from the relative population of states (left part) and the isotopic yield ratios (right part; the T_{HeLi} thermometer corresponds to the data point at B=13.3 MeV) are well described by rather similar temperatures, once the effect of sequential decay is taken into account.

5.2.3 *Caloric curve as an image of the finite size*

Calculations of the limiting temperature T_{lim}, at which a nucleus enters into the region of Coulomb instability [Bonche *et al.*, 1984; Bonche *et al.*, 1985] are expected to increase with decreasing system size [Jaqaman, 1989; Song and Su, 1991; Haddad and Weigel, 1994; Zhang *et al.*, 1996]. As has been stressed already in section 2, the physics of spectator nuclei produced in peripheral collisions suffers from a strong correlation between the excitation energy and the size of system (see figure 14). It was, therefore, proposed that – rather than the transition from a liquid to a nuclear gas phase – the caloric curves marks only this limiting temperature and that the increase of the temperature with increasing excitation energy is mainly due to the decreasing system size [Natowitz *et al.*, 1995]. One has to keep in mind, however, that T_{lim} gives the maximum temperature for a nuclear system which still remains self-bound. It does, of course, not exclude the existence of nuclear systems with higher temperatures. Indeed, while in a later more detailed analysis an interpretation of the caloric curve in terms of limiting temperatures was still possible for the excitation energies below approximately 12 MeV per nucleon, it was also recognized that the highest energy point lies above the expected value of T_{lim} for the corresponding nucleus [Majka *et al.*, 1996]. Similarly, the T_{HeLi} values measured in central Au+Au collisions reach far beyond the limiting temperatures (figure 28). Although the role of the limiting temperature for the plateau regime of the caloric curves clearly deserves further attention, the rise of the isotope temperature T_{HeLi} far beyond the highest possible T_{lim} values may indicate that indeed the vaporization phase has been reached.

5.2.4 *Shape of the caloric curves as a signal for a phase transition?*

Treating a first order phase transition of a one-component system in the framework of standard equilibrium thermodynamics, Moretto *et al.* stressed [Moretto *et al.*, 1996] that in general the path of a system in the coexistence region and hence its caloric curve depends on the external fields and boundary conditions. This well known fact [Reichl, 1980; Pochodzalla *et al.*, 1995] shows that the unequivocal interpretation of a caloric curve requires the knowledge of the external conditions. Although one might suspect, that for nuclear systems the assumed phase equilibrium might be realized very well for example in neutron stars, a treatment of the liquid-gas phase transition of nuclei in terms of equilibrium thermodynamics will not do justice to the complex nature of such finite, self-bound objects. Since nuclei are transient systems without external field (e.g. pressure), any consideration based on equilibrium thermodynamics assuming constant external fields (pressure) or boundary conditions (volume) may, therefore, only be used as a guideline and – in the absence of a complete dynamical theory for this non-equilibrium process – as a well-defined points of reference. In turn, conclusions drawn on the basis of equilibrium thermodynamics of macroscopic systems, may not be the whole truth for nuclei. For example, inspecting the nuclear caloric curve shown in figure 27, it is evident that a weak rise of the plateau with $(dT/d(E_0/A0))_{coex} \leq 0.1$ can not be excluded. Such a rise may indeed signal a non-isobaric process. While this conclusion may be justified and satisfactory for a macroscopic PVT-system, a finite system undergoing a self-driven expansion and break-up process clearly calls for a more profound explanation.

One point that should be made though is that the crossing from the liquid-vapor regime to the superheated vapor is – irrespective of the detailed path of the system in the coexistence region – marked by a significant increase of the specific heat, giving rise to a kink in the caloric curve. Therefore, a "plateau" – even if it is slightly ascending – followed by an upward sweep seems to be a robust signal of a transition into the vapor phase. Again, one has to keep in mind that also this argument is based on equilibrium thermodynamics of an infinite system and it remains to be seen whether these features will be recovered in more microscopic formulations.

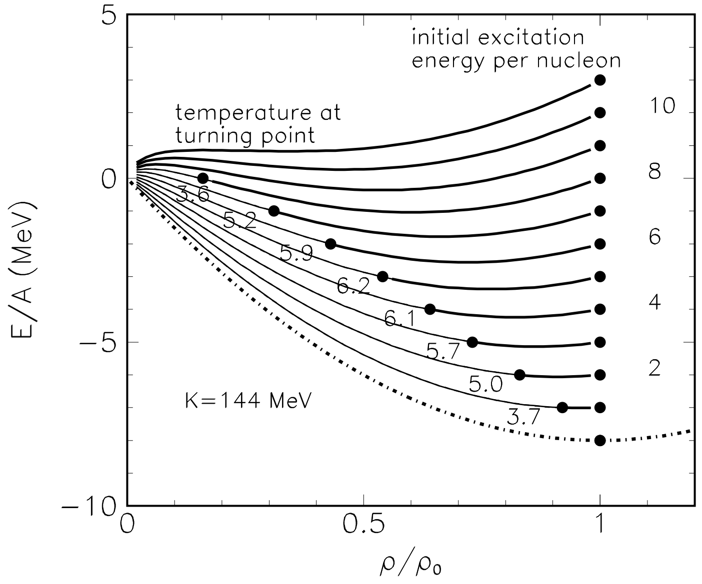

Fig. 34. *Evolution of an isentropically expanding Fermi gas in the energy per nucleon vs. density plane.*

5.2.5 Caloric curves as an image of the expanded system

First hints (figures 4 and 18 top) and further experimental evidence [Warren *et al.*, 1996] for the build-up of flow during a thermal driven decay of spectator nuclei have been found. This calls for a dynamical treatment of the fragmentation process. The temporal evolution of the heated spectator nucleus will depend on its initial excitation energy and will, therefore, influence or even dominate the shape of the caloric curve. To explore the role of the expansion dynamics we will consider as an illustrative example the temporal evolution of an isentropically expanding Fermi system. The lines in figure 34 show the evolution of the summed thermal and potential energy as a function of its density. The total excitation energy of the system at normal density is indicated by the numbers on the right hand side. The energy stored (momentarily) in the collective expansive motion is then given by the difference between these two energies. For the low density equation-of-state of the finite nuclear system, a parabolic density dependence

$$(E/A)_{T=0} = K_c/18 \cdot (1 - \rho/\rho_0)^2 - 8MeV \tag{10}$$

with a compressibility $K_c = 144$ MeV was used [Stöcker *et al.*, 1979; Friedman, 1992]. Furthermore, we ignore any dissipative processes during the expansion.

For initial excitation energies below 8 MeV per nucleon the system is not able to expand freely to zero density but will stop at a finite density before it collapses again. Since at the turning point of this monopole vibration the Coulomb barrier reaches its minimum value and since the system spends most of its time in this region, it is probably reasonable to assume that the fragmentation happens at this point. Indeed, the temperatures at the turning point lie, rather independent of the initial excitation energy, in the region of about 5 - 6 MeV. For excitation energies beyond 8 MeV per nucleon, the system may energetically expand to zero density prior to its freeze-out. In such a case, the initial energy would be subdivided in a potential energy of 8 MeV per nucleon and a collective flow energy. In our experiment, we do, however, observe high temperatures in the 'gas' regime of the caloric curve. These high values signal a freeze out at a finite density, which is not too surprising considering the finite range of the strong interaction and considering the fact that the expansion velocity is still moderate.

Calculations which take into account nucleon emission during the expansion and a more sophisticated equation-of-state were performed by Papp and Nörenberg [Papp and Nörenberg, 1995]. Within this

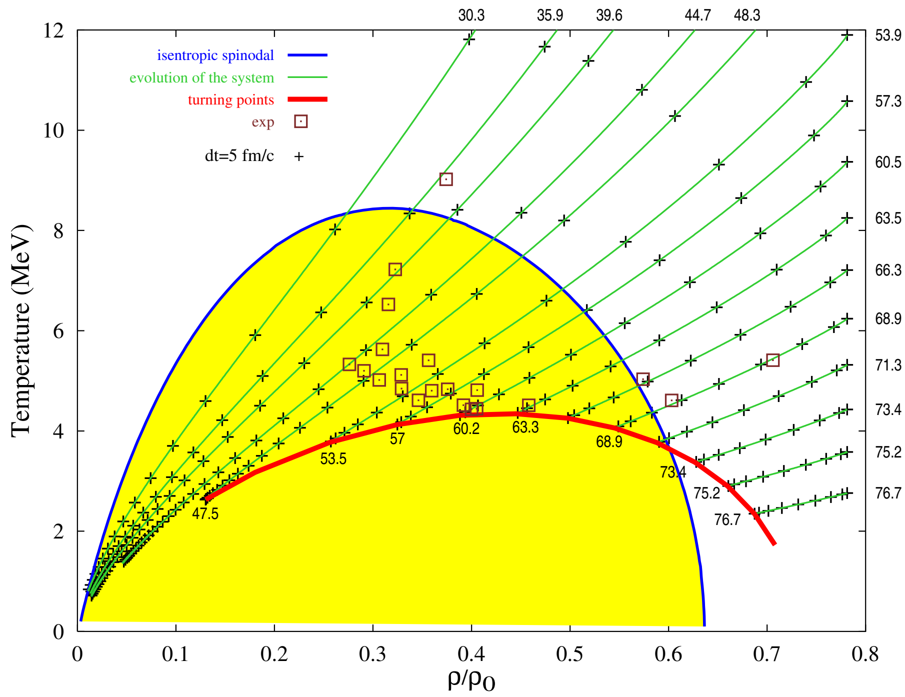

Fig. 35. *Path of hot nuclei in the temperature-density plane. The squares mark the T-ρ values which are determined by the caloric curve shown in figure 27 (from [Papp and Nörenberg, 1995]).*

model the temperature of the 'gas branch' of the caloric curve can be explained with a nearly constant freeze-out density of about 1/3 of normal nuclear matter density (figure 35). It may be interesting to note that a quite similar relation between the temperature and density at break-up was also predicted by the COPENHAGEN statistical multifragmentation model more than a decade ago (see for example figure 9 in [Bondorf *et al.*, 1985]).

Note that the picture outlined in this paragraph is also of quasi-static nature. This may be sufficient considering the chemical degree only. As we will in the subsequent section, other degrees of freedom might provide different snapshots of the expansion process.

5.3 Emission temperatures: the breakdown of equilibrium?

For a cross calibration of the isotope thermometer with so called emission temperatures over a large excitation energy region and in order to quantify the amount of sequential decay, the relative population of excited states in light fragments produced in Au+Au reactions at various beam energies was determined [Serfling, 1996; Immé *et al.*, 1996]. For this purpose the ALADIN spectrometer was supplemented by three hodoscopes consisting of 216 Si-CsI(Tl) telescopes. Their angular resolution and granularity were optimized in order to permit the identification of excited particle unstable resonances in light fragments from the correlated detection of their decay products. For the measurements at beam energies below 200 MeV per nucleon, the hodoscopes were placed in the forward hemisphere in order to cover the angular region close to 90^o in the center-of-mass system. At 1 GeV per nucleon incident energy, the hodoscopes were moved to the backward hemisphere in order to select mainly target spectator products. In addition, a set of seven high resolution Si-telescopes were placed at selected angles in order to measure simultaneously the yields of isotopically resolved light fragments.

Initially the analysis of this experiment focused on fragments with two widely separated states as e.g. ^{4}He, ^{5}Li, and ^{8}He. For these states modifications of the apparent emission temperatures due to feeding from higher lying states are expected to be small [Fields *et al.*, 1987; Chen and Gelbke, 1988]. In figure 36 we compare the isotope temperature T_{HeLi} (closed symbols) with apparent emission temperatures deduced from the relative population of states in ^{5}Li (open symbols). Here, the estimated random part

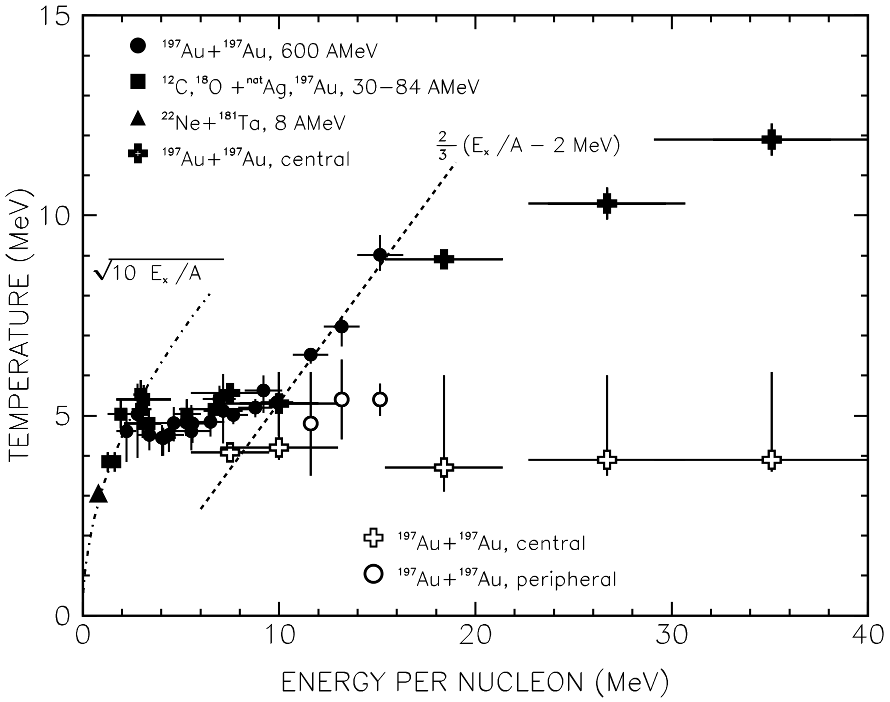

Fig. 36. *Comparison of the caloric curve measured via the isotope temperature T_{HeLi} (closed symbols) with apparent emission temperatures deduced from the relative population of states in ^5Li (open symbols; the data point at $E/A \approx 7$ MeV is from ref. [Huang et al., 1996]; all other data from [Serfling, 1996]).*

of the available excitation energy is used as the horizontal axis. Note, however, that the energy scale is not of prime relevance for this comparison. In central collisions at beam energies between 50 and 200 MeV we observe a clear discrepancy between the isotope temperature (closed crosses) and the emission temperature (open crosses) which is increasing with rising beam energy. Besides the very low value for the emission temperatures of only 4 MeV, their constancy – despite an increase of the beam energy by a factor of four – is particularly striking. A similar divergence of the two thermometers is seen for the three uppermost central bins in spectator fragmentation at 600 resp. 1000 MeV per nucleon incident beam energy. Also there the emission temperatures (open circles) show a rather constant value, even though at a slightly higher level of about 5 MeV.

If the population of excited states is indeed as small and constant as the emission temperatures suggest, sequential decays will only moderately disturb the isotope temperatures and, moreover, the relative correction will not change significantly with increasing excitation or beam energy. Surely this corroborates the isotope ratios as a robust thermometer. But it also implies that - although sequential decays undoubtfully affect the difference between the emission and isotope temperatures – sequential feeding alone can probably not account for the observed discrepancy between the two thermometers. Calculations within an extended quantum statistical model [Gulminelli and Durand, 1996] support this conclusion.

5.3.1 Production of quantum clusters in exploding nuclei

Lacking at the moment a quantitative explanation of this surprising observation, it might be instructive to recall a similar phenomenon during the cosmic big-bang. Also there different degrees-of-freedom freeze out at various stages of the big-bang evolution, hence signaling different temperatures. Of course, this cooling is intimately related to the existence of collective radial flow. It may, therefore, not be to surprising that the discrepancy between the two thermometer emerges as soon as collective flow starts

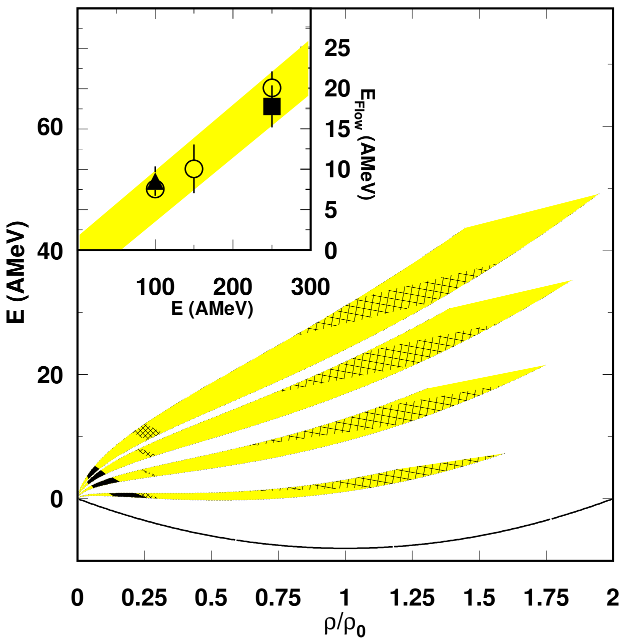

Fig. 37. *Isentropic expansion of a hot Fermi gas. The cross-hatched, fine hatched and black areas mark the regions for the freeze-out of flow, of chemical reactions and of the internal excitation, respectively (from [Schwarz et al., 1997b]).*

to represent a significant part of the available energy.

On first sight such a scenario appears to be rather disappointing since we would have to give up the idea of equilibrium between chemical and internal degrees of freedom at freeze-out. However, this complication may turn into an advantage since the various thermometers – supplemented by detailed analyses of fragment-fragment momentum correlations [Cornell *et al.*, 1996; Wang *et al.*, 1997] – might enable us to sample the thermodynamic evolution of the system [Barz *et al.*, 1989b].

For illustration, we will again turn to an isentropical expanding Fermi gas. Figure 37 shows the evolution of the internal and potential energy as a function of density (cf. figure 34). The four shaded areas correspond to initial excitation energies given by the center-of-mass energies in symmetric nucleus-nucleus collisions at 50, 100, 150, and 200 AMeV. The width of these bands reflects a variation of the initial density between 0.75 and 1.0 times the predicted maximum density in central collisions [Danielewicz and Pan, 1992].

The values of excitation energy–density pairs which are consistent with the measured temperatures or flow energies are marked by the cross-hatched resp. filled areas. Taking the values of T_{HeLi} (figure 36) at it's face value, the temporal evolution of the temperature indicates – independent of the beam energy – a chemical freeze-out density close to 1/4 of normal nuclear density (small cross-hatched; see also figure 35). Accordingly, the emission temperatures are fixed at significantly lower densities which also decrease with increasing beam energy. On the other hand, the slope parameters of the emitted particles suggest that the decoupling of the translational motion happens rather early. However, as stressed before, these slope parameters can not be directly interpreted as temperatures at freeze-out of the kinetic degrees of freedom. Alternatively, the fraction of the available energy stored in radial flow (see insert in figure 37) may serve as a measure of the freeze-out density. Though the uncertainties are rather large, one observes for all four reactions a kinematic freeze-out density which is larger than 3/4 times the normal nuclear density, suggesting that the chemical freeze-out and the decoupling of flow does not happen simultaneously.

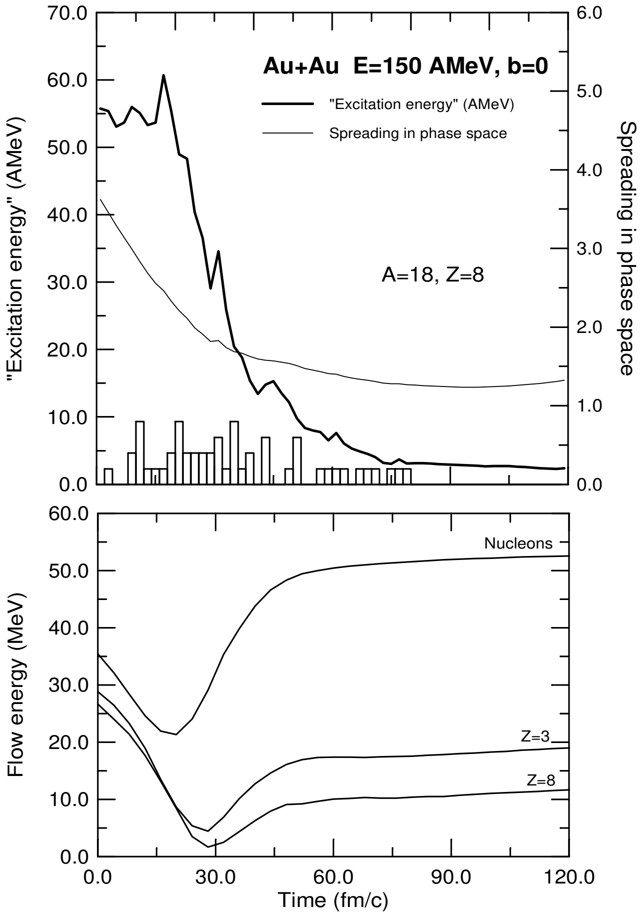

Fig. 38. *Prediction of a molecular dynamics model for the temporal evolution of the excitation energy (upper part, left scale) and the spreading in phase space (upper part, right scale) within an ^{18}O cluster. The environmental collision rate is shown by the histogram. The lower part shows the evolution of the flow energy for nucleons, lithium, and oxygen clusters (from [Barz et al., 1996]).*

Qualitatively, features supporting a sequential freeze-out of various degrees of freedom can be observed in quantum molecular simulations. Figure 38 shows the temporal evolution of the properties of a ^{18}O cluster which is produced in Au+Au collisions at 150A MeV[Barz *et al.*, 1996]. For this cluster, the spreading in phase space approaches it's final value already rather early at about 30 - 40 fm/c. Thus, as it has been noted already earlier [Boal *et al.*, 1989a; Boal *et al.*, 1989b; Kunde *et al.*, 1991], clusters are formed chemically in a rather early stage of the collision [Dorso and Balonga, 1994; Dorso and Aichelin, 1995]. But even after this self-organisation [Bondorf *et al.*, 1995b] of the nucleons, a fragment will still suffer collisions with surrounding nucleons. The histogram in the upper part of figure 38 displays the corresponding collision rate. These collisions may cause a depletion of excited states, thus lowering the internal fragment temperatures [Boal, 1984]. Although such a scenario may qualitatively explain the low values for the emission temperatures, it does not account for their surprising constancy. Moreover, figure 38 suggests a nearly simultaneous kinetic and chemical freeze-out which is not in line with the analysis depicted in figure 37. It is important to realize, however, that within this rather schematic expansion picture any energy leakage via particle emission prior to break-up will give rise to a smaller freeze-out density for the flow and at the same time a larger chemical freeze-out density.

Especially in view of the not yet understood constancy of the emission temperatures, a word of caution should be added. Microscopic calculations suggest, that the internal excitation of produced fragments may not only be influenced by the local momentum distribution of the surrounding nucleons but may also reflect correlations within the initial projectile [Knoll and Wu, 1988; Kunde *et al.*, 1991; Dorso and Balonga, 1994; Puri *et al.*, 1996; Barz *et al.*, 1996] Furthermore, a detailed treatment of the quantum nature of the produced fragments warrants more attention in future studies (see for example [Pratt *et al.*, 1989; Ohnishi and Randrup, 1996; Feldmeier and Schnack, 1997]). Finally, it remains to be seen whether an equilibrium approach is justified at all in an fast expanding nucleus. [Cugnon, 1983].

6 Summary and Concluding Remarks

Disentangling collective and thermal motion in fireballs generated in central collisions, one observes a similar caloric behaviour as in spectator fragmentation at high excitation energies. This concordance suggests that, despite the very different underlying kinematics, the multifragment decays in both reaction types may be governed by common physics. Although various entrance channels lead to different caloric curves for quasi-projectiles, the qualitative agreement between these curves signaling a change of the decay mechanism at an excitation energy of about 10 MeV per nucleon is encouraging. Clearly, a better knowledge of secondary processes and of the different experimental constraints is mandatory for a further interpretation of the observed differences.

The shape of the caloric curve as observed by the ALADIN collaboration is suggestive of a first-order phase transition with a substantial latent heat. It also seems to exclude - on first sight - the occurrence of a second-order phase transition which is the *sine qua non* for the determination of critical-point exponents [Gilkes *et al.*, 1994; Elliott *et al.*, 1994]. For a finite system with N constituents a transition is, on the other hand, no longer characterized by a singular point but acquires a finite width over a temperature range ΔT_c around the transition temperature T_c. In case of a second order phase transition, $\Delta T_c/T_c$ is approximately given by $\Delta T_c/T_c \sim 1/\sqrt{N}$ [Imry, 1980]. For typical nuclear sizes of N≈100, the influence of a second order phase transition may, therefore, be perceptible at temperatures deviating by as much as 10% from the critical value. Furthermore, for a classical van der Waals gas the latent heat increases close to the critical point with $\sqrt{1 - T/T_c}$ and reaches already at $T/T_c = 0.95$ values larger than $k_B T_c$. Thus, in finite systems typical features of a first-order phase transition - like a latent heat - and signals indicating the proximity of the critical point - like diverging moments - are not necessarily inconsistent, making the attempt to extract critical-point exponents – at least – a worthwhile and interesting venture. Time must show, whether the hope to apply the concept of criticality to such small systems like nuclei is really justified.

The ideal scenario of a system in global equilibrium is not realized in nuclear collisions. The interplay between the expansion dynamics and the density dependent properties of a Fermi gas might perhaps help to elucidate the gross features of the caloric curves and the different temperature measurements via the chemical and kinetic degrees of freedom. However, one has to keep in mind that we are not dealing with a homogeneous system. An internally consistent equation-of-state taking into account the clusterisation [Peilert *et al.*, 1991], the particle loss during the expansion prior to the breakup [Friedman, 1990; Papp and Nörenberg, 1995], the viscosity of nuclear matter, and the systematic variation of the source size in peripheral collisions as well as the explosive initial flow in central collisions is required before more definite conclusions can be drawn. Nonetheless, if this scenario holds, the amount of energy which is transferred during the expansion into collective radial motion, will reflect both, the freeze-out density and the degree of dissipation during the expansion. Particle interferometry for light particles as well as fragments might provide another, independent determination of the density evolution. Thus a combination of all these experimental informations will allow a closer look at the expansion dynamics in near future. Indeed first attempts along this line have already been started [Kotte *et al.*, 1995; Wang *et al.*, 1997; Schwarz *et al.*, 1997a; Fritz *et al.*, 1997].

Last but not least, a new, intriguing question resulted from the latest ALADIN experiment: Why are the emission temperatures so low and – perhaps even more puzzling – why are they constant in central collisions despite a variation of the beam energy by a factor of four? Clearly, new experiments exploring for example the dependence of emission temperatures on the system size and extending this work to very low excitation energies are mandatory. While the associated small feeding contributions may be viewed as good news for the validity of the isotope thermometer, it clearly exemplifies that we are still far away from a detailed understanding of the thermodynamics of a finite, decaying nucleus and it's decay into quantum clusters.

All these open questions – and probably many more – will find their analogy in atomic cluster physics, cosmology and high energy particle/nuclear physics, where the concept of *phase-transition* is equally important. In this respect, a deeper understanding of the liquid-gas phase transition of nuclei might also shed some light on the past history of our universe as well as the world around us. While it is safe to say that nuclei do (un)fortunately *not* behave just like ordinary water, we are rewarded by the experience of a rich variety of phenomena which originate – to a large extent though not exclusively – from the finite size of nuclei or, as expressed by Lucretius [Lucretius, 50BC] from the vicinage of bodies and void: *" nam corpora sunt et inane"*.

Acknowledgments

The present review could not have been written without the help of many collaborators. Particularly I would like to thank all present and temporary members of the ALADIN group: J.C. Adloff, S. Aiello, H.W. Barz, R. Bassini, M. Begemann-Blaich, Th. Blaich, A. Botvina, P. Bouissou, D.R. Bowman, R.J. Charity, A. Cosmo, A.R. DeAngelis, A. Ferrero, W.A. Friedman, S. Fritz, S. Gaff, C.K. Gelbke, C. Groß , D.H.E. Gross, R. Heck, W.C. Hsi, J. Hubele, G. Immé, I. Iori, H.R. Jaqaman, J. Kempter, U. Kleinevoß , P. Kreutz, G.J. Kunde, W.D. Kunze, S. Leray, V. Lindenstruth, M.A. Lisa, Z. Liu, W.G. Lynch, U. Lynen, V. Maddalena, M. Mahi, M. Mang, R.J. Meijer, U. Milkau, T. Möhlenkamp, L.G. Moretto, A. Moroni, W.F.J. Müller, M. Neumann, C. Ngô, C. Nociforo, B. Ocker, T. Odeh, C.A. Ogilvie, V. Pappalardo, G.F. Peaslee, F. Petruzzelli, G. Raciti, G. Riccobene, F.P. Romano, F. Rosenberger, T. Rubehn, G. Rudolf, A. Saija, H. Sann, R. Scardaoni, M. Schnittker, A. Schüttauf, C. Schwarz, W. Seidel, V. Serfling, C. Sfienti, L.G. Sobotka, J. Stroth, L. Stuttge, W. Trautmann, A. Trzcinski, M.B. Tsang, A. Tucholski, C.W. Williams, A. Wörner, H. Xi, E. Zude, and B. Zwieglinski. Numerous and enlightning discussions are gratefully acknowledged with J. Aichelin, J.P. Bondorf, H. Feldmeier, J. Konopka, W. Nörenberg, G. Papp, J. Péter, and E. Plagnol. The work was supported in part by the Deutsche Forschungsgemeinschaft under the Contract No. Po256/2-2.

References

[Acicastello, 1996] *Proceedings of the 1st Catania Relativistic Ion Studies: Critical Phenomena and Collective Observables*, Acicastello, Italy, 1996, edts. S. Costa, S. Albergo, A. Insolia, C. Tuvè, World Scientific (1996).

[Aguiar *et al.*, 1992] C.E. Aguiar, R. Donangelo, C.O. Dorso, R.S. Gomes, and N. Goncalves. *Emission of the outer layer by an expanding hot nucleus. Phys. Rev.* C **46**, 1069 (1992)

[Aichelin, 1994] J. Aichelin. *Apparent temperature of medium mass fragments. Phys. Rev.* C **30**, 718 (1984)

[Aichelin *et al.*, 1988] J. Aichelin, G. Peilert, A. Bohnet, A. Rosenhauer, H. Stöcker, and W. Greiner. *Quantum molecular dynamics approach to heavy ion collisions: description of the model, comparison with fragmentation data, and the mechanism of fragment formation. Phys. Rev.* C **37**, 2451 (1988).

[Albergo *et al.*, 1985] S. Albergo, S. Costa, E. Costanzo, and A. Rubbino. *Temperature and free-nucleon densities of nuclear matter exploding into light clusters in heavy-ion collisions. Nuovo Cimento A* **89**, 1 (1985); the underlying ideas can already be found in [Hoyle, 1946].

[Bacri *et al.*, 1995] Ch.O. Bacri, B. Borderie, J.L. Charvet, D. Cussol, R. Dayras, O. Lopez, A. Ouatizerga, M.F. Rivet, G. Auger, A. Benkerane, J. Benlliure, B. Berthier, R. Bougault, R. Brou, P. Box, Y. Cassagnou, A. Chbihi, J. Colin, E. De Filippo, A. Demeyer, D. Durand, P. Ecomard, P. Eudes, A. Genoux-Lubain, D. Gourio, D. Guinet, L. Lakehal-Ayat, P. Lautesse, J.L. Laville, L. Lebreton, C. Lebrun, J.F. Lecolley, A. Le Fèvre, R. Legrain, M. Louvel, M. Mahi, N. Marie, V. Mitivier, L. Nalpas, T. Nakagawa, M. Parlog, J. Péter, E. Plagnol, E. Pollacco, A. Rahmani, R. Regimbart, T. Reposeur, E. Rosato, F. Saint-Laurent, M. Squalli, J.C. Steckmeyer, B. Tamain, L. Tassan-Got, E. Vient, C. Volant, J.P. Wieleczko, A. Wieloch, K. Yuasa-Nakagawa. *Onset of vvaporization for the Ar+Ni system. Phys. Lett.* B **353**, 27 (1995).

[Barashenkov and Toneev, 1972] V.S. Barashenkov and V.D. Toneev. *Interactions of high-energy particles and atomic nuclei with nuclei.* Moscow, Atomizdat, 1972 (in Russian); V.D. Toneev, private communication (1994).

[Barz *et al.*, 1989a] H.W. Barz, H. Schulz, and G.F. Bertsch. *Temperatures from intermediate energy heavy ion collisions. Phys. Lett.* B **217**, 397 (1989).

[Barz *et al.*, 1989b] H.W. Barz, J.P. Bondorf, R. Donangelo, H. Schulz, and K. Sneppen. *Kinetic and internal fragment temperatures of a highly excited nucleus. Phys. Lett.* B **228**, 453 (1989).

[Barz *et al.*, 1993] H.W. Barz, W. Bauer, J.P. Bondorf, A.S. Botvina, R. Donangelo, H. Schulz, and K. Sneppen. *Charged-particle correlations in 600 AMeV gold induced disasembly reactions – a statistical multifragmentation analysis. Nucl. Phys.* A **561**, 466 (1993).

[Barz *et al.*, 1996] H.W. Barz, J.P Bondorf, D. Idier, and I.N. Mishustin. *Cluster production and correlations in nuclear molecular dynamics. Phys. Lett.* B **382**, 343 (1996).

[Bass *et al.*, 1994] S.A. Bass, M. Hofmann, C. Hartnack, H. Stöcker, and W. Greiner. *Probing Δ resonance production in Au+Au collisions at 1 GeV/nucleon. Phys. Lett.* B **335**, 289 (1994).

[Bauer *et al.*, 1993] W. Bauer, J.P. Bondorf, R. Donangelo, R. Elmér, B. Jakobson, H. Schulz, F. Schussler, and K. Sneppen. *Large radial flow in nucleus-nucleus collisions. Phys. Rev.* C **47**, R1383 (1993).

[Bauer, 1995] W. Bauer. *Temperatures of fragment kinetic energy spectra. Phys. Rev.* C **51**, 803 (1995)

[Bauer and Botvina, 1995] W. Bauer and A. Botvina. *Pre-equilibrium particle emission and critical exponent analysis. Phys. Rev.* C **52**, R1760 (1995).

[Bauer and Friedmann, 1995] W. Bauer and W.A. Friedman. *Comment on "Determination of critical exponents from multifragmentation of gold nuclei". Phys. Rev. Lett.* **75**, 767 (1995) and M.L. Gilkes, Y. Choi, J.B. Elliott, J.A. Hauger, A.S. Hirsch, E.L. Hjort, N.T. Porile, R. Scharenberg, B.K. Srivastava, M. Tincknell, and P. Warren. *Reply for the EOS collaboration. Phys. Rev. Lett.* **75**, 768 (1995).

[Beaulieu *et al.*, 1996] L. Beaulieu, D.R. Bowman, D. Fox, S. Das Gupta, J. Pan, G.C. Ball, B. Djerroud, D. Dore, A. Galindo-Uribarri, D. Guinet, E. Hagberg, D. Horn, R. Laforest, Y. Larochelle, P. Lautesse, M. Samri, R. Roy, and C. St-Pierre. *Source size scaling of fragment production in projectile breakup. Phys. Rev. Lett.* **75**, 768 (1995).

[Begemann-Blaich *et al.*, 1997] M.L. Begemann-Blaich, V. Lindenstruth, J. Pochodzalla, J.C. Adloff, A. Botvina, P. Bouissou, D.H.E. Gross, J. Hubele, G. Imme, I. Iori, P. Kreutz, G.J. Kunde, S. Leray, Z. Liu, U. Lynen, R.J. Meijer, U. Milkau, A. Moroni, W.F.J. Müller, C. Ngô, C.A. Ogilvie, G. Raciti, G. Rudolf, H. Sann, A. Schüttauf, W. Seidel, L. Stuttge, W. Trautmann, and A. Tucholski. *Breakup configurations in multiple disintegration of projectile fragments.* (in preparation).

[Bertsch and Siemens, 1983] G. Bertsch and P.J. Siemens. *Nuclear fragmentation. Phys. Lett.* B **126**, 9 (1983).

[Blaich *et al.*, 1992] Th. Blaich, Th.W. Elze, H. Emling, H. Freiesleben, K. Grimm, W. Henning, R. Holzmmann, G. Ickert, J,G. Keller, H. Klingler, W. Kneissl, R. König, R. Kulessa, J.V. Kratz, D. Lambrecht, J.S. Lange, Y. Leifels, E. Lubkiewicz, M. Proft, W. Prokopowicz, C. Schütter, R. Schmidt, H. Spies, K. Stelzer, J. Stroth, W. Walus, E. Wajda, H.J. Wollersheim, M. Zinser, and E. Zude. *A large area detector for high-energy neutrons. Nucl. Instrum. Methods* A **A314**, 136 (1992).

[Blink and Hoover, 1985] J.A. Blink and W.G. Hoover. *Fragmentation of suddenly heated liquids. Phys. Rev.* A **32**, 1027 (1985).

[Blümel *et al.*, 1988] R. Blümel, J.M. Chen, E. Peik, W. Quint, W. Schleich, Y.R. Shen, and H. Walther. *Phase transitions of stored laser-cooled ions. Nature* **334**, 309 (1988).

[Boal, 1984] D.H. Boal. *Hadronic thermometry and final state interactions. Phys. Rev.* C **30**, 749 (1984).

[Boal *et al.*, 1989a] D.H. Boal, J.N. Glosli, and C. Wicentowich. *Computer simulations of temperature measurements in heavy-ion collisions. Phys. Rev. Lett.* **62**, 737 (1989).

[Boal *et al.*, 1989b] D.H. Boal, J.N. Glosli, and C. Wicentowich. *Temperatures in heavy ion reactions: simulations via quasiparticle dynamics. Phys. Rev.* C **40**, 601 (1989).

[Bohne *et al.*, 1990] W. Bohne, H. Morgenstern, K. Grabisch, T. Nakagawa, and S. Proschitzki. *Critical excitation energy in fusion-evaporatio reactions. Phys. Rev.* C **41**, R5 (1990).

[Bohne *et al.*, 1993] W. Bohne, P. Figuera, H. Morgenstern, and S. Proschitzki. *Limiting excitation energies in fusion evaporation reactions. Z. Phys.* A **347**, 135 (1993).

[Bonche *et al.*, 1984] P. Bonche, S. Levit, and D. Vautherin. *Properties of highly excited nuclei. Nucl. Phys.* A **427**, 278 (1984).

[Bonche *et al.*, 1985] P. Bonche, S. Levit, and D. Vautherin. *Statistical properties and stability of hot nuclei. Nucl. Phys.* A **436**, 265 (1985).

[Bondorf *et al.*, 1978] J.P. Bondorf, S.I.A. Garpman, and J. Zimanyi. *A simple analytic hydrodynamic model for expanding fireballs. Nucl. Phys.* A **296**, 320 (1978).

[Bondorf, 1981] J.P. Bondorf. *Chaotic fragmentation of nuclei.*, Proc. Nucl. Phys. Workshop I.C.T.P. Trieste, Oct. 5-30, 1981; ed. C.H. Dasso, North Holland (1982) 765; *Nucl. Phys.* A **387**, 25c (1982).

[Bondorf *et al.*, 1985] J.P. Bondorf, R. Donangelo, I.N. Mishustin, and H. Schulz. *Statistical multifragmentation of nuclei (II). Application of the model to finite nuclei disassembly. Nucl. Phys.* A **444**, 460 (1985).

[Bondorf *et al.*, 1994] J.P. Bondorf, A.S. Botvina, I.N. Mishustin, and S.R. Souza. *Formation and breakup of extra-large composite system in central Au+Au collisions. Phys. Rev. Lett.* **73**, 628 (1994).

[Bondorf *et al.*, 1995a] J.P. Bondorf, A.S. Botvina, A.S. Iljinov, I.N. Mishustin, and K. Sneppen. *Statistical multifragmentation of nuclei. Phys. Rep.* **257**, 133 (1995).

[Bondorf *et al.*, 1995b] J.P. Bondorf, D. Idier, I.N. Mishustin. *Self-organization in expanding nuclear matter. Phys. Lett.* B **359**, 261 (1995).

[Botvina and Mishustin, 1992] A.S. Botvina and I.N. Mishustin. *Multifragmentation of thermalized residual nuclei in intermediate-energy heavy ion collisions. Phys. Lett.* B **294**, 23 (1992).

[Botvina *et al.*, 1995] A.S. Botvina, I.N. Mishustin, M. Begemann–Blaich, J. Hubele, G. Imme, I. Iori, P. Kreutz, G.J. Kunde, W.D. Kunze, V. Lindenstruth, U. Lynen, A. Moroni, W.F.J. Müller, C.A. Ogilvie, J. Pochodzalla, G. Raciti, Th. Rubehn, H. Sann, A. Schüttauf, W. Seidel, W. Trautmann, and A. Wörner. *Multifragmentation of spectators in relativistic heavy-ion reactions. Nucl. Phys.* A **584**, 737 (1995).

[Braun-Munzinger *et al.*, 1995] P. Braun-Munzinger, J. Stachel, J.P. Wessels, and N. Xu. *Thermal and hadrochemical equilibration in nucleus-nucleus collisions at the SPS. Phys. Lett.* B **344**, 43 (1995); and P. Braun-Munzinger, J. Stachel, J.P. Wessels, and N. Xu. *Thermal equilibration and expansion in nucleus-nucleus collisions at the AGS. Phys. Lett.* B **365**, 1 (1996).

[Bravina and Zabrodin, 1996] L.V. Bravina and E.E. Zabrodin. *From criticality to supercooling in expanding hot nuclear matter: possible solution of low-τ puzzle. Phys. Rev.* C **54**, R464 (1996).

[Brockmann *et al.*, 1984] R. Brockmann, J.W. Harris, A. Sandoval, R. Stock, H. Ströbele, G. Odyniec, H.G. Pugh, L.S. Schroeder, R.E. Renfordt, D. Schall, D. Bangert, W. rauch, and K.L. Wolf. *Pion and proton "temperatures" in relativistic heavy-ion reactions. Phys. Rev. Lett.* **53**, 2012 (1984).

[Brown, 1990] G.E. Brown. *Heavy ion collisions at Bevalac energies. Comments Nucl. Part. Phys.* **19**, 185 (1990).

[Campi, 1986] X. Campi. *Multifragmentation: nuclei break up like percolation clusters. J. Phys.*A **19**, L917 (1986).

[Campi, 1988] X. Campi. *Signals of a phase transition in nuclear multifragmentation. Phys. Lett.* B **208**, 351 (1988).

[Campi *et al.*, 1994] X. Campi, H. Krivine, and E. Plagnol. *Size and excitation energy distributions of projectile spectators in multifragmentation data. Phys. Rev.* C **50**, R2680 (1994).

[Campi *et al.*, 1996] X. Campi, H. Krivine, and E. Plagnol. *Examining some aspects of the nuclear caloric curve. Phys. Lett.* B **385**, 1 (1996).

[Charity *et al.*, 1988] R.J. Charity, M.A. McMahan, G.J. Wozniak, R.J. McDonald, L.G. Moretto, D.G. Sarantites, L.G. Sobotka, G. Guarino, A. Pantaleo, L. Fiore, A. Gobbi, and K.D. Hildenbrand. *Systematics of complex fragment emission in niobium-induced reactions. Nucl. Phys.* A **483**, 371 (1988).

[Chen and Gelbke, 1988] Z. Chen and C.K. Gelbke. *Sequential feeding and temperature determinations from the relative populations of widely separated states in ^{4}He, ^{5}Li, and ^{8}Be nuclei. Phys. Rev.* C **38**, 2630 (1988).

[Cheng *et al.*, 1992] Hai-Ping Cheng, Xiuling Li, R.L. Whetten, and R.S. Berry. *Complete statistical thermodynamics of the cluster solid-liquid transition. Phys. Rev.* A **46**, 791 (1992).

[Cherry *et al.*, 1994] M.L. Cherry, A. Dabrowska, P. Deines-Jones, A.J. Dubinina, R. Holynski, W.V. Jones, E.D. Kolganova, A. Olszewski, E.A. Pozharova, K. Sengupta, T.Yu. Skorodko, V.A. Smirnitski, M. Szarska, C.J. Waddington, J.P. Wefel, B. Wilczynska, and W. Wolter. *Interactions of 10.6 GeV/n gold nuclei with light and heavy target nuclei in nuclear emulsion. Z. Phys.* C **63**, 549 (1994).

[Cherry *et al.*, 1995] M.L. Cherry, A. Dabrowska, P. Deines-Jones, R. Holynski, W.V. Jones, E.D. Kolganova, A. Olszewski, K. Sengupta, T.Yu. Skorodko, M. Szarska, C.J. Waddington, J.P. Wefel, B. Wilczynska, B. Wosiek, and W. Wolter. *Fragmentation and multifragmentation of 10.6 A GeV gold nuclei. Phys. Rev.* C **52**, 2652 (1995).

[Cornell *et al.*, 1996] E.W. Cornell, T.M. Hamilton, D. Fox, Y. Lou, R.T. de Souza, M.J. Huang, W.C. Hsi, C. Schwarz, C. Williams, D.R. Bowman, J. Dinius, C.K. Gelbke, D.O. Handzy, M.A. Lisa, W.G. Lynch, G.F. Peaslee, L. Phair, M.B. Tsang, G. VanBuren, R.J. Charity, L.G. Sobotka, W.A. Friedman. *Investigating the evolution of multifragmenting systems with fragment emission order. Phys. Rev. Lett.* **77**, 4508 (1996).

[Cugnon, 1983] J. Cugnon. *Chemical reactions in an expanding fireball. Phys. Lett.* B **123**, 155 (1983).

[Cugnon, 1984] J. Cugnon. *Possible fragmentation instability in a nuclear expanding fireball. Phys. Lett.* B **135**, 374 (1984).

[Cugnon, 1987] J. Cugnon. *Proton-nucleus interaction at high energy. Nucl. Phys.* A **462**, 751 (1987).

[D'Agostino *et al.*, 1995] M. D'Agostino, G.J. Kunde, P.M. Milazzo, J.D. Dinius, M. Bruno, N. Colonna, M.L. Fiandri, C.K. Gelbke, T. Glasmacher, F. Gramegna, D.O. Handzy, W.C. Hsi, M. Huang, M.A. Lisa, W.G. Lynch, P.F. Mastinu, C.P. Montoya, A. Moroni, D.F. Peaslee, L. Phair, R. Rui, C. SChwarz, M.B. Tsang, G. Vannini, and C. Williams. *Multifragmentation in $E/A = 35$ MeV collisions: evidence for a Coulomb driven breakup?. Phys. Rev. Lett.* **75**, 4373 (1995).

[Danielewicz and Pan, 1992] P. Danielewicz and Q. Pan. *Blast of light fragments from central heavy-ion collisions. Phys. Rev.* C **46**, 2002 (1992).

[DeAngelis and Gross, 1993] A.R. DeAngelis and D.H.E. Gross. *A microcanonical model of hot nuclei.* Comput. Phys. Commun. 76 (1993) 113.

[Désesquelles, 1995] P. Désesquelles. *Multivariate analysis in nuclear physics. Ann. Phys. Fr.* **20**, 1, (1995).

[Désesquelles *et al.*, 1996] P. Désesquelles, J.P. Bondorf, I.N. Mishustin, and A.S. Botvina. *Global protocol for comparison of simulated data with experimental data. Nucl. Phys.* A **604**, 183 (1996).

[de Souza *et al.*, 1990] R.T. de Souza, N. Carlin, Y.D. Kim, J. Ottarson, L. Phair, D.R. Bowman, C.K. Gelbke, W.G. Gong, W.G. Lynch, R.A. Pelak, T. Peterson, G. Poggi, M.B. Tsang, and H.M. Xu. *The MSU Miniball 4π fragment detection array. Nucl. Instrum. Methods* A **295**, 109 (1990).

[Dhont, 1994] J.K.G. Dhont. *Effects of shear flow on long ranged correlations, on spinodal decomposition kinetics and on the location of the critical point and cloud point. Physica Scripta* **T55**, 127 (1994).

[Dhont, 1996] J.K.G. Dhont. *Shear induced displacement of the spinodal of Brownian systems. Phys. Rev. Lett.* **76**, 4269 (1996).

[Dorso and Balonga, 1994] C.O. Dorso and P.E. Balonga. *Fluctuation dynamics of fragmenting spherical nuclei. Phys. Rev.* C **50**, 991 (1994).

[Dorso and Aichelin, 1995] C.O. Dorso and J. Aichelin. *When and how are fragments formed in heavy ion collisions? Phys. Lett.* B **345**, 197 (1995).

[Dreute *et al.*, 1991] J. Dreute, W. Heinrich, G. Rusch, and B. Wiegel. *Fragmentation of gold projectiles with energies of 200-980 MeV/nucleon. I. Experimental method, charge yields, and transverse momenta. Phys. Rev.* C **44**, 1057 (1991)

[Elliott *et al.*, 1994] J.B. Elliott, M.L. Gilkes, J.A. Hauger, A.S. Hirsch, E. Hjort, N.T. Porile, R. P. Scharenberg, B.K. Srivastava, M.L. Tincknell, and P.G. Warren. *Extraction of critical exponents from very small percolation lattices. Phys. Rev.* C **49**, 3185 (1994).

[Elliott *et al.*, 1996] J.B. Elliott, S. Albergo, F. Bieser, F.P. Brady, Z. Caccia, D.A. Cebra, A.D. Chacon, J.L. Chance, Y. Choi, S. Costa, M.L. Gilkes, J.A. Hauger, A.S. Hirsch, E.L. Hjort, A. Insolia, M. Justice, D. Keane, J.C. Kintner, V. Lindenstruth, M.A. Lisa, U. Lynen, H.S. Matis, M. McMahan, C. McParland, W.F.J. Müller, D.L. Olson, M.D. Partlan, N.T. Porile, R. Potenza, G. Rai, J. Rasmussen, H.G. Ritter, J. Romanski, J.L. Romero, G.V. Russo, H. Sann, R. Scharenberg, A. Scott, Y. Shao, B.K. Srivastava, T.J.M. Symons, M. Tincknell, C. Tuvé, S. Wang, P. Warren, H.H. Wieman, and K. Wolf. *Individual fragment yields and determination of the critical exponent σ. Phys. Lett.* B **381**, 35 (1996).

[Empedocles, 440BC] Empedocles. *Fragment 12/6 and 17/109.* ($\approx$ 440BC), in Brad Inwood, *The Poem of Empedocles*, University of Toronto Press (1991).

[Fabris *et al.*, 1987] D. Fabris, K. Hagel, J.B. Natowitz, G. Nebbia, R. Wada, R. Billerey, B. Cheynis, A. Demeyer, D. Drain, D. Guinet, C. Pastor, J. Alarja, A. Giorni, D. Heuer, C. Morond, B. Viano, C. Mazur, C. Ngo, S. Leray, R. Lucas, M. Ribrag, and E. Tomasi. *α-emission temperatures, Coulomb instabilities and nuclear cracking. Phys. Lett.* B **196**, 429 (1987) and references therein.

[Feldmeier and Schnack, 1997] H. feldmeier and J. Schnack. *Fermionic molecular dynamics.* nucl-th/9703014 (1997).

[Fields *et al.*, 1987] D.J. Fields, C.K. Gelbke, W.G. Lynch, and J. Pochodzalla. *Nuclear fragmentation and sequential decay. Phys. Lett.* B **187**, 257 (1987).

[Figuera *et al.*, 1995] P. Figuera, W. Bohne, B. Drescher, F. Goldenbaum, D. Hilscher, U. Jahnke, B. Lott, L. Pienkowski, P. Ziem. *Maximum excitation energy in fusion-evaporation reactions from light particle multiplicity measurements in $^{32}S+^{58}Ni$ at 25 MeV/A. Z. Phys.* A **352**, 315 (1995).

[Finn *et al.*, 1982] J.E. Finn, S. Agarwal, A. Bujak, J. Chuang, L.J. Gutay, A.S. Hirsch, R.W. Minich, N.T. Porile, R.P. Scharenberg, B.C. Stringfellow, and F. Turkot. *Nuclear fragment mass yields from high-energy proton-nucleus interactions. Phys. Rev. Lett.* **49**, 1321 (1982).

[Fisher, 1967] M.E. Fisher. *The theory of equilibrium critical phenomena. Rep. Prog. Phys.* **30**, 615 (1967); *The theory of critical point singularities*, *Critical Phenomena*, Proceedings of the International School of Physics "Enrico Fermi", Course LI, edited by M.S. Green (Academic, New York, 1971); *Physics (N.Y.)* **3**, 255 (1967).

[Friedlander and Heckmann, 1985] E.M. Friedlander and H.H. Heckmann. *Treatise on Heavy-Ion Science.* Edt. D.A. Bromley, Plenum Press, New York 1985, Vol. 4, p. 403.

[Friedman, 1990] W.A. Friedman. *Rapid massive cluster formation. Phys. Rev.* C **42**, 667 (1990).

[Friedman, 1992] W.A. Friedman. 8-th Winter Workshop on Nuclear Dynamics, Jackson Hole, Wyoming, (1992).

[Fritz *et al.*, 1997] S. Fritz, R. Bassini, M. Begemann-Blaich, A.S. Botvina, S.J. Gaff, C. Groß, G. Immé, I. Iori, U. Kleinevoß, G.J. Kunde, W.D. Kunze, U. Lynen, V. Maddalena, M. Mahi, T. Möhlenkamp, A. Moroni, W.F.J. Müller, C. Nociforo, B. Ocker, T. Odeh, F. Petruzzelli, J. Pochodzalla, G. Raciti, G. Riccobene, F.P. Romano, Th. Rubehn, A. Saija, M. Schnittker, A. Schüttauf, C. Schwarz, W. Seidel, V. Serfling, C. Sfienti, W. Trautmann, A. Trzcinski, G. Verde, A. Wörner, Hongfei Xi, B. Zwieglinski. *Emission temperatures and freeze out densities from light particle correlation functions in Au+Au collisions at 1 AGeV.* 35th International Winter Meeting on Nuclear Physics, Bormio, Italy, 26. Januar - 1. Februar, 1997, nucl-ex/9704002.

[Gilkes *et al.*, 1994] M.L. Gilkes, S. Albergo, F. Bieser, F.P. Brady, Z. Caccia, D.A. Cebra, A.D. Chacon, J.L. Chance, Y. Choi, S. Costa, J.B. Elliott, J.A. Hauger, A.S. Hirsch, E.L. Hjort, A. Insolia, M. Justice, D. Keane, J.C. Kintner, V. Lindenstruth, M.A. Lisa, U. Lynen, H.S. Matis, M. McMahan, C. McParland, W.F.J. Müller, D.L. Olson, M.D. Partlan, N.T. Porile, R. Potenza, G. Rai, J. Rasmussen, H.G. Ritter, J. Romanski, J.L. Romero, G.V. Russo, H. Sann, R. Scharenberg, A. Scott, Y. Shao, B.K. Srivastava, T.J.M. Symons, M. Tincknell, C. Tuvé, S. Wang, P. Warren, H.H. Wieman, and K. Wolf. *Determination of critical exponents from multifragmentation of gold nuclei. Phys. Rev. Lett.* **73**, 1590 (1994).

[Glendenning, 1992] N.K. Glendenning. *First-order phase transitions with more than one conserved charge: consequences for neutron stars. Phys. Rev.* D **46**, 1274 (1992).

[Goldhaber, 1974] A.S. Goldhaber. *Statistical models of fragmentation processes. Phys. Lett.* B **53**, 306 (1974).

[Goldenbaum *et al.*, 1996] F. Goldenbaum, W. Bohne, J. Eades, T. v.Egidy, P. Figuera, H. Fuchs, J. Galin, Ye.S. Golubeva, K. Gulda, D. Hilscher, A.S. Iljinov, U. Jahnke, J. Jastrzebski, W. Kurcewicz, B. Lott, M. Morjean, G. Pausch, A. Peghaire, L. Pienkowski, D. Polster, S. Proschitzki, B. Quednau, H. Rossner, S. Schmid, W. Schmid, and P. Ziem. *Heating of nuclei with energetic antiprotons. Phys. Rev. Lett.* **77**, 1230 (1996).

[Goodman *et al.*, 1984] A.L. Goodman, J.I. Kapusta, and A.Z. Mekjian. *Liquid-gas phase instabilities and droplet formation in nuclear reactions. Phys. Rev.* C **30**, 851 (1984).

[Green and Korteling, 1980] R.E.L. Green and R.G. Korteling. *Fragment production from p+Ag interactions at intermediate energies. Phys. Rev.* C **22**, 1594 (1980).

[Gross and Meng Ta-chung, 1981] D.H.E. Gross and Meng Ta-chung. *4th Nordic Meeting on Intermediate and High Energy Physics*, page 29, Geilo Sportell, Norway, 1981.

[Gross *et al.*, 1982] D.H.E. Gross, L. Satpathy, Meng Ta-chung, and M. Satpathy. *Mass-yield distribution in proton and heavy ion induced target fragmentation processes. Z. Phys.* A **309**, 41 (1982).

[Gross *et al.*, 1986] D.H.E. Gross, Zhang Xiao-ze, and Xu Shu-yan. *Decay of very hot nuclei. Phys. Rev. Lett.* **56**, 1544 (1986); D.H.E. Gross. *Multifragmentatio, link between fission and the liquid-gas phase-transition. Prog. Part. Nucl. Phys.* **30**, 155 (1993).

[Gross, 1990] D.H.E. Gross. *Statistical decay of very hot nuclei - the production of large clusters. Rep. Prog. Phys.***53**, 605 (1990).

[Gulminelli and Durand, 1996] F. Gulminelli and D. Durand. *Theoretical comparison of different thermometers for the determination of the nuclear caloric curve. Nucl. Phys.* A **615**, 117 (1997).

[Haddad and Weigel, 1994] S. Haddad and M.K. Weidel. *Thermostatic properties and Coulomb instability of highly excited nuclei. Phys. Rev.* C **49**, 3228 (1994).

[Hahn and Stöcker, 1988] D. Hahn and H. Stöcker. *The quantum statistical model of fragment formation. Nucl. Phys.* A **476**, 718 (1988).

[Harris *et al.*, 1987] J.W. Harris, G. Odyniec, H.G. Pugh, L.S. Schroeder, M.L. Tincknell, W. Rauch, R. Stock, R. Bock, R. Brockmann, A. Sandoval, H. Ströbele, R.E. Renfordt, D. Schall, D. Bangert, J.P. Sullivan, K.L. Wolf, A. Dacal, C. Guerra, and M.E. Ortiz. *Pion production in high-energy nucleus-nucleus collisions. Phys. Rev. Lett.* **58**, 463 (1987).

[Harris and Müller, 1996] J.W. Harris and B. Müller. *Annu. Rev. Nucl. Part. Sci.*. **46**, 71 (1996).

[Hauger *et al.*, 1996] J.A. Hauger, S. Albergo, F. Bieser, F.P. Brady, Z. Caccia, D.A. Cebra, A.D. Chacon, J.L. Chance, Y. Choi, S. Costa, J.B. Elliott, M.L. Gilkes, A.S. Hirsch, E.L. Hjort, A. Insolia, M. Justice, D. Keane, J.C. Kintner, V. Lindenstruth, M.A. Lisa, U. Lynen, H.S. Matis, M. McMahan, C. McParland, W.F.J. Müller, D.L. Olsen, M.D. Partlan, N.T. Porile, R. Potenza, G. Rai, J. Rasmussen, H.G. Ritter, J. Romanski, J.L. Romero, G.V. Russo, H. Sann, R. Scharenberg, A. Scott, Y. Shao, B.K. Srivastava, T.J.M. Symons, M. Tincknell, C. Tuvé, S. Wang, P. Warren, H.H. Wieman, T. Wienold, and K. Wolf. *Dynamics of the multifragmentation of 1 AGeV Gold on Carbon. Phys. Rev. Lett.* **77**, 235 (1996).

[He *et al.*, 1988] Z. He, J. Wu, and W. Nörenberg. *Evaporation of particles from hot nuclei. Nucl. Phys.* A **489**, 421 (1988).

[Heckmann *et al.*, 1978] H.H. Heckmann, H.J. Crawford, D.E. Greiner, P.J. Lindstrom, and L.W. Wilson. *Central collisions produced by relativistic heavy ions in nuclear emulsion. Phys. Rev.* C **17**, 1651 (1978).

[Heckmann *et al.*, 1986] H.H. Heckmann, Y.J. Karant, and E.M. Friedlander. *Angular correlations between projectile and target fragments emitted from nuclear collisions of ^{238}U at 0.85 A GeV. Phys. Rev.* C **34**, 1333 (1986).

[Hervieux and Gross, 1995] P.A. Hervieux and D.H.E. Gross. *Evaporation of hot mesoscopic atomic metal clusters. Z. Phys.* D **33**, 295 (1995); D.H.E. Gross and P.A. Hervieux. *Statistical fragmentation of hot atomic clusters. Z. Phys.* D **35**, 27 (1995).

[Heuer *et al.*, 1994] D. Heuer, A. Chabane, M.E. Brandan, M. Charvet, A.J. Cole, P. Désesquelles, A. Giorni, A. Lleres, A. Menchaca-Rocha, J.B. Viano, D. Benchekroun, B. Cheynis, A. Demeyer, E. Gerlic, D. Guinet, M. Stern, and L. Vagneron. *Explosive multifragmentation in the $^{32}S+^{27}Al$ reaction at 37.5 MeV/nucleon. Phys. Rev.* C **50**, 1943 (1994).

[Hirsch *et al.*, 1984] A.S. Hirsch, A. Bujak, J.E. Finn, L.J. Gutay, R.W. Minich, N.T. Porile, R.P. Scharenberg, B.C. Stringfellow, and F. Turkot. *Experimental results from high energy proton-nucleus interactions, critical phenomena, and the thermal liquid drop model of fragment production. Phys. Rev.* C **29**, 508 (1984).

[Hoyle, 1946] F. Hoyle. *The synthesis of the elements from hydrogen. Monthly Notices of the Royal Astronom. Soc.* **106**, 343 (1946).

[Hsi *et al.*, 1994] W.C. Hsi, G.J. Kunde, J. Pochodzalla, W.G. Lynch, M.B. Tsang, M.L. Begemann-Blaich, D.R. Bowman, R.J. Charity, A. Cosmo, A. Ferrero, C.K. Gelbke, T. Glasmacher, T. Hoffmann, J. Hubele, G. Imme, I. Iori, J. Kempter, P. Kreutz, W.D. Kunze, V. Lindenstruth, M.A. Lisa, U. Lynen, M. Mang, A. Moroni, W.F.J. Müller, M. Neumann, B. Ocker, C.A. Ogilvie, G.F. Peaslee, G. Raciti, F. Rosenberger, H. Sann, R. Scardoni, A, Schüttauf, C. Schwarz, W. Seidel, V. Serfling, L.G. Sobotka, L. Stuttge, W. Trautmann, A. Tucholski, C. Williams, A. Wörner, B. Zwieglinski. *Collective expansion in central Au+Au collisions. Phys. Rev. Lett.* **73**, 3367 (1994).

[Huang *et al.*, 1996] M.J. Huang, H. Xi, W.G. Lynch, M.B. Tsang, J.D. Dinius, S.J. Gaff, C.K. Gelbke, T. Glasmacher, G.J. Kunde, L. Martin, C.P. Montoya, E. Scannapieco, P.M. Milazzo, M. Azzano, G.V. Margagliotti, R. Rui, G. Vannini, N. Colonna, L. Celano, G. Tagliente, M.D'Agostino, M. Bruno, M.L. Fiandri, F. Gramegna, A. Ferrero, I. Iori, A. Moroni, F. Petruzzelli, and P.F. Mastuni. *Temperature measurements for central Au+Au collisions at 35A MeV. Phys. Rev. Lett.* **78**, 1648 (1997).

[Hubele *et al.*, 1991] J. Hubele, P. Kreutz, J.C. Adloff, M. Begemann–Blaich, P. Bouissou, G. Imme, I. Iori, G.J. Kunde, S. Leray, V. Lindenstruth, Z. Liu, U. Lynen, R.J. Meijer, U. Milkau, A. Moroni, W.F.J. Müller, C. Ngô, C.A. Ogilvie, J. Pochodzalla, G. Raciti, G. Rudolf, H. Sann, A. Schüttauf, W. Seidel, L. Stuttge, W. Trautmann, and A. Tucholski. *Fragmentation of gold projectiles: from evaporation to total disassembly. Z. Phys.* A **340**, 263 (1991).

[Hubele *et al.*, 1992] J. Hubele, P. Kreutz, V. Lindenstruth, J.C. Adloff, M. Begemann–Blaich, P. Bouissou, G. Imme, I. Iori, G.J. Kunde, S. Leray, Z. Liu, U. Lynen, R.J. Meijer, U. Milkau, A. Moroni, W.F.J. Müller, C. Ngô, C.A. Ogilvie, J. Pochodzalla, G. Raciti, G. Rudolf, H. Sann, A. Schüttauf, W. Seidel, L. Stuttge, W. Trautmann, A. Tucholski, R. Heck, A.R. DeAngelis, D.H.E. Gross, H.R. Jaqaman, H.W. Barz, H. Schulz, W.A. Friedman, and R.J. Charity. *Statistical fragmentation of Au projectiles at E/A=600 MeV. Phys. Rev.* C **46**, R1577 (1992).

[Hüfner, 1985] J. Hüfner. *Heavy fragments produced in proton-nucleus and nucleus-nucleus collisions at relativistic energies. Phys. Rep.* **125**, 129 (1985).

[Hüller, 1992] A. Hüller. *First order phase transition in the canonical and the microcanonical ensemble. Z. Phys.* B **93**, 401 (1994).

[Hüller and Promberger, 1996] A. Hüller and M. Promberger. *Proceedings of the 1st Catania Relativistic Ion Studies: Critical Phenomena and Collective Observables*, edts. S. Costa, S. Albergo, A. Insolia, C. Tuvè, World Scientific, p. 287 (1996).

[Immé *et al.*, 1996] G. Immé, V. Maddalena, C. Nociforo, G. Raciti, G. Riccobene, F.P. Romano, A. Saija, C. Sfienti, G. Verde, M. Begemann-Blaich, S. Fritz, C. Gross, U. Kleinevoß , U. Lynen, M. Mahi, W.F.J. Müller, B. Ocker, T. Odeh, M. Schnittker, C. Schwarz, V. Serfling, W. Trautmann, A. Wörner, H. Xi, T. Möhlenkamp, W. Seidel, W.D. Kunze, A. Schüttauf, J. Pochodzalla, G.J. Kunde, S. Gaff, R. Bassini, I. Iori, A. Moroni, F. Petruzzelli, A. Trzcinski, and B. Zwieglinski. *Last minute from ALADIN: Temperature Measurements in Au+Au Reactions at Relativistic Energies. Proceedings of the 1st Catania Relativistic Ion Studies: Critical Phenomena and Collective Observables*, edts. S. Costa, S. Albergo, A. Insolia, C. Tuvè, World Scientific, p. 143 (1996).

[Imry, 1980] Y. Imry. *Finite-size rounding of a first-order phase transition. Phys. Rev.* B **21**, 2042 (1980).

[Jain and Singh, 1992] P.L. Jain, G. Singh. *Rise and fall of multifragment emission at relativistic energy. Phys. Rev.* C **46**, R10 (1992).

[Jain *et al.*, 1994] P.L. Jain, G. Singh, and A. Mukhopadhyay. *Intermediate mass fragment emission by ^{197}Au projectiles at relativistic energy in nuclear emulsion. Phys. Rev.* C **50**, 1085 (1994).

[Jain and Singh, 1995] P.L. Jain and G. Singh. *Fluctuations and clustering in relativistic heavy ion interactions. Nucl. Phys.* A **591**, 711 (1995).

[Jain and Singh, 1996] P.L. Jain and G. Singh. *Liquid-gas coexistence in ^{208}Pb-emulsion interactions at 160A GeV. Phys. Lett.* B **382**, 289 (1996).

[Jaqaman *et al.*, 1983] H. Jaqaman, A.Z. Mekjian, and L. Zamick. *Nuclear condensation. Phys. Rev.* C **27**, 2782 (1983) and H. Jaqaman, A.Z. Mekjian, and L. Zamick. *Liquid-gas phase transitions in finite nuclear matter. Phys. Rev.* C **29**, 2067 (1984).

[Jaqaman, 1989] H.R. Jaqaman. *Coulomb instability of hot nuclei. Phys. Rev.* C **39**, 169 (1989).

[Jeong *et al.*, 1994] S.C. Jeong, N. Herrmann, J. Randrup, J.P. Alard, Z. Basrak, N. Bastid, I.M. Belayev, M. Bini, T. Blaich, A. Buta, R. Caplar, C. Cerruti, N. Cindro, J.P. Coffin, R. Dona, P. Dupieux, J. Ero, Z.G. Fan, P. Fintz, Z. Fodor, R. Freifelder, L. Fraysse, S. Frolov, A. Gobbi, Y. Grigorian, G. Guillaume, K.D. Hildenbrand, S. Hölbling, A. Houari, M. Jorio, F. Jundt, J. Kecskemeti, P. Koncz, Y. Korchagin, R. Kotte, M. Kramer, C. Kuhn, I. Legrand, A. Lebedev, C. Maguire, V. Manko, T. Matulewicz, G. Mgebrishvili, J. Mosner, D. Moisa, G. Montarou, P. Morel, W. Neuberg, A. Olmi, G. Pasquali, D. Pelte, Petrovici, M., G. Poggi, F. Rami, W. Reisdorf, A. Sadchikov, D. Schull, Z. Seres, B. Sikora, V. Simion, S. Smolyankin, U. Sodan, K. Teh, R. Tezkratt, M. Trzaska, M.A. Vasilev, P. Wagner, J.P. Wessels, T. Wienold, Z. Wilhelmi, D. Wohlfarth, A.V. Zhilin. *Collective motion in selected central collisions of Au on Au et 150A MeV. Phys. Rev. Lett.* **72**, 3468 (1994).

[Jeong *et al.*, 1996] S.C. Jeong, D. Cussol, D. Durand, R. Laforest, J. Péter, J.C. Angélique, G. Auger, G. Bizard, R. Brou, A. Buta, C. Cabot, Y. Cassagnou, E. Crema, Y. El Masri, P. Eudes, Z.Y. He, A. Kerambrun, C. Lebrun, R. Legrain, J.P. Patry, A. Péghaire, R. Régimbart, E. Rosato, F. Saint-Laurent, J.C. Steckmeyer, B. Tamain, E. Vient. *Onset of collective expansion in nucleus-nucleus collisions below 100 MeV/u. Nucl. Phys.* A **604**, 208 (1996).

[Karnaukhov, 1996] V.A. Karnaukhov. *On nuclear liquid-gas phase transition via multifragmentation and fission.* JINR pre-print E7-96-182 (1996).

[Kaufmann and Steinberg, 1980] S.B. Kaufman and E.P. Steinberg. *Cross-section measurements of nuclides formed by the reaction 0.20-6.0 GeV protons with Au. Phys. Rev.* C **22**, 167 (1980)

[Knoll and Wu, 1988] J. Knoll and J. Wu. *Expansion dynamics and multifragmentation of a saturating system of fermions. Nucl. Phys.* A **481**, 173 (1988).

[Kolomiets *et al.*, 1996] A. Kolomiets, E. Ramakrishnan, H. Johnston, F. Gimeno-Nogues, B. Hurst, D. O'Kelly, D.J. Rowland, S. Shlomo, T. White, J. Winger, and S. J. Yennello. *Nuclear temperature of the disassembling source in central heavy-ion collisions from isotope yields. Phys. Rev.* C **54**, R472 (1996).

[Kolomiets *et al.*, 1997] A. Kolomiets, V.M. Kolomietz, and S. Shlomo. *Determination of the temperature of a disassembling nucleus from fragment yields. Phys. Rev.* C **55**, 1376 (1997).

[Konopka *et al.*, 1994] J. Konopka, H. Graf, H. Stöcker, and W. Greiner. *Observable consequences of chemical equilibration in energetic heavy ion collisions. Phys. Rev.* C **50**, 2085 (1994).

[Kotte *et al.*, 1995] R. Kotte, B. Kämpfer, J. Mössner, W. Neubert, D. Wohlfarth, J.P. Alard, V. Amouroux, Z. Basrak, N. Bastid, I.M. Belayev, L. Berger, Th. Blaich, S. Boussange, A. Buta, R. Čaplar, C. Cerruti, N. Cindro, J.P. Coffin, R. Doná, P. Dupieux, J. Erö, Z.G. Fan, P. Fintz, Z. Fodor, L. Fraysse, R. Freifelder, S. Frolov, A. Gobbi, Y. Grigorian, G. Guillaume, N. Herrmann, K.D. Hildenbrand, S. Hölbling, O. Houari, M. Ibnouzahir, S.C. Jeong, F. Jundt, J. Kecskemeti, P. Koncz, Y. Korchagin, M. Krämer, C. Kuhn, I. Legrand, A. Lebedev, V. Manko, T. Matulewicz, G. Mgebrishvili, D. Moisa, G. Montarou, I. Montbel, D. Pelte, M. Petrovici, P. Pras, F. Rami, V. Ramillien, W. Reisdorf, A. Sadchikov, D. Schüll, Z. Seres, B. Sikora, V. Simion, S. Smolyankin, U. Sodan, K. Teh, R. Tezkratt, M. Trzaska, M.A. Vasiliev, P. Wagner, J.P. Wessels, T. Wienold, Z. Wilhelmi, and A.V. Zhilin. *Interplay of collective flow phenomena and velocity correlations of intermediate-mass fragments in collisions of AU+Au at E=(100-400)A MeV. Phys. Rev.* C **51**, 2686 (1995).

[Kreutz *et al.*, 1993] P. Kreutz, J.C. Adloff, M. Begemann–Blaich, P. Bouissou, J. Hubele, G. Imme, I. Iori, G.J. Kunde, S. Leray, V. Lindenstruth, Z. Liu, U. Lynen, R.J. Meijer, U. Milkau, A. Moroni, W.F.J. Müller, C. Ngô, C.A. Ogilvie, J. Pochodzalla, G. Raciti, G. Rudolf, H. Sann, A. Schüttauf, W. Seidel, L. Stuttge, W. Trautmann, and A. Tucholski. *Charge correlations as a probe of nuclear disassembly. Nucl. Phys.* A **556**, 672 (1993).

[Kuhn *et al.*, 1993] C. Kuhn, J. Konopka, J.P. Coffin, C. Cerruti, P. Fintz, G. Guillaume, A. Houari, F. Jundt, C. Maguire, F. Rami, R. Tezkratt, P. Wagner, Z. Basrak, R. Caplar, N. Cindro, S. Hölbling, J.P. Alard, N. Bastid, L. Berger, S. Boussange, I.M. Belayev, T. Blaich, A. Buta, R. Donà, P. Dupieux, J. Erö, Z.G. Fan, Z. Fodor, R. Freifelder, L. Fraysse, S. Frolov, A. Gobbi, Y. Grigorian, N. Herrmann, K.D. Hildenbrand, S.C. Jeong, M. Jorio, J. Kecskemeti, P. Koncz, Y. Korchagin, R. Kotte, M. Krämer, I. Legrand, A. Lebedev, V. Manko, T. Matulewicz, G. Mgebrishvili, J. Mösner, D. Moisa, G. Montarou, I. Montbel, W. Neubert, D. Pelte, M. Ptrovici, S. Ramillien, W. Reisdorf, A. Sadchikov, D. Schüll, Z. Seres, B. Sikora, V. Simion, S. Smolyankin, U. Sodan, K.M. Teh, M. Trzaska, M.A. Vasiliev, J.P. Wessels, T. Wienold, Z. Wilhelmi, D. Wohlfarth, and A.V. Zhilin. *Entropy production in the Au+Au reaction between 150A and 800A MeV. Phys. Rev.* C **48**, 1232 (1993).

[Kunde *et al.*, 1991] G.J. Kunde, J. Pochodzalla, J. Aichelin, E. Berdermann, B. Berthier, C. Cerruti, C.K. Gelbke, J. Hubele, P. Kreutz, S. Leray, R. Lucas, U. Lynen, U. Milkau, W.F.J. Müller, C. Ngo, C.H. Pinkenburg, G. Raciti, H. Sann, and W. Trautmann. *Emission temperatures in ^{40}Ar + ^{197}Au reactions in the limiting fragmentation regime. Phys. Lett.* B **272**, 202 (1991).

[Kunde *et al.*, 1995] G.J. Kunde, W.C. Hsi, W.D. Kunze, A. Schüttauf, A. Wörner, M. Begemann–Blaich, Th. Blaich, D.R. Bowman, R.J. Charity, A. Cosmo, A. Ferrero, C.K. Gelbke, J. Hubele, G. Imme, I. Iori, P. Kreutz, V. Lindenstruth, M.A. Lisa, W.G. Lynch, U. Lynen, M. Mang, T. Möhlenkamp, A. Moroni, W.F.J. Müller, M. Neumann, B. Ocker, C.A. Ogilvie, G.F. Peaslee, J. Pochodzalla, G. Raciti, T. Rubehn, H. Sann, W. Seidel, V. Serfling, L.G. Sobotka, J. Stroth, L. Stuttge, S. Tomasevic, W. Trautmann, M.B. Tsang, A. Tucholski, G. Verde, C.W. Williams, E. Zude, and B. Zwieglinski. *Fragment flow and the multifragmentation phase space. Phys. Rev. Lett.* **74**, 38 (1995).

[Kunze, 1996] W.D. Kunze. *Energie- und Targetabhängigkeit der Projektilfragmentation in asymmetrischen Schwerionenstößen.* PhD-thesis, Universität Frankfurt a.M. (1996).

[Kwiatkowski *et al.*, 1994] K. Kwiatkowski, W.A. Friedman, L.W. Woo, V.E. Viola, E.C. Pollacco, C. Volant, and S.J. Yennello. *Energy dissipation and multifragment decay in the ^{3}He+^{nat}Ag system. Phys. Rev.* C **49**, 1516 (1994).

[Kwiatkowski *et al.*, 1995a] K. Kwiatkowski, D.S. Bracken, K.B. Morley, J. Brzychczyk, E. Renshaw Foxford, K. Komisarcik, V.E. Viola, N.R. Yoder, J. Dorsett, J. Poehlman, N. Madden, J. Ottarson. *The Indiana silicon sphere 4π charged-particle detector array. Nucl. Instrum. Methods* A **360**, 571 (1995).

[Kwiatkowski *et al.*, 1995b] K. Kwiatkowski, K.B. Morley, E. Renshaw Foxford, D.S. Bracken, V.E. Viola, N.R. Yoder, R. Legrain, E.C. Pollaco, C. Volant, W.A. Friedman, R.G. Korteling, J. Brzychczyk, and H. Breuer. *Multifragmentation in the 4.8 GeV ^{3}He+^{nat}Ag, ^{197}Au reactions. Phys. Rev. Lett.* **74**, 3756 (1995).

[Labastie and Whetten, 1990] P. Labastie and R.L. Whetten. *Statistical thermodynamics of the cluster solid-liquid transition. Phys. Rev. Lett.* **65**, 1567 (1990).

[Lamb *et al.*, 1978] D.Q. Lamb, J.M. Lattimer, C.J. Pethick, and D.G. Ravenhall. *Hot dense matter and stellar collapse. Phys. Rev. Lett.* **41**, 1623 (1978).

[Levit and Bonche, 1985] S. Levit and P. Bonche. *Coulomb instability in hot compound nuclei approaching liquid-gas transition. Nucl. Phys.* A **437**, 426 (1985).

[Lewenkopf *et al.*, 1991] C. Lewenkopf, J. Dreute, A. Abul-Magd, J. Aichelin W. Heinrich, J. Hüfner, G. Rusch, and B. Wiegel. *Fragmentation of gold projectiles with energies of 200-980 MeV/nucleon. II. Multiplicity distributions and correlations. Phys. Rev.* C **44**, 1065 (1991).

[Li *et al.*, 1993a] Bao-An Li, A.R. DeAngelis, and D.H.E. Gross. *Statistical model analysis of* ALADIN *multifragmentation data. Phys. Lett.* B **303**, 225 (1993).

[Li *et al.*, 1993b] T. Li, W. Bauer, D. Craig, M. Cronqvist, E. Gualtieri, S. Hannuschke, R. Lacey, W.J. Llope, T. Reposeur, A.M. Vander Molen, G.D. Westfall, W.K. Wilson, J.S. Winfield, J. Yee, S.J. Yenello, A. Nadasen, R.S. Tickle, E. Norbeck. *Intermediate mass fragment production in central collisions of intermediate energy heavy ions. Phys. Rev. Lett.* **70**, 1924 (1993).

[Li *et al.*, 1994] T. Li, W. Bauer, D. Craig, E. Gualtieri, S. Hannuschke, R. Pak, A.M. Vander Molen, G.D. Westfall, J.S. Winfield, J. Yee, S.J. Yenello, R. Lacey, A. Nadasen, R.S. Tickle, E. Norbeck. *Mass dependence of critical behaviour in nucleus-nucleus collisions., Phys. Rev.* C **49**, 1630 (1994).

[Lindenstruth, 1993] V. Lindenstruth. *Dynamik der Multifragmentation.* PhD-thesis, Universität Frankfurt a.M., 1993, report GSI-93-18.

[Lips *et al.*, 1994] V. Lips, R. Barth, H. Oeschler, S.P. Avdeyev, V.A. Karnaukhov, W.D. Kuznetsov, L.A. Petrov, O.V. Bochkarev, L.V. Chulkov, E.A. Kuzmin, W. Karcz, W. Neubert, E. Norbeck. *Multifragmentation induced by relativistic α projectiles. Phys. Rev. Lett.* **72**, 1604 (1994).

[Lisa *et al.*, 1995] M.A. Lisa, M.A. Lisa, S. Albergo, F. Bieser, F.P. Brady, Z. Caccia, D.A. Cebra, D.A. Chacon, J.L. Chance, Y. Choi, S. Costa, J.B. Elliott, M.L. Gilkes, J.A. Hauger, A.S. Hirsch, E.L. Hjort, A. Insolia, M. Justice, D. Keane, J.C. Kintner, H.S. Matis, M. McMahan, C. McParland, D.L. Olson, M.D. Partland, N.T. Porile, R. Potenza, G. Rai, J. Rasmussen, H.G. Ritter, J. Romanski, J.L. Romero, G.V. Russo, R. Scharenberg, A. Scott, Y. Shao, B.K. Srivastava, T.J.M. Symons, M. Tincknell, C. Tuve, S. Wang, P. Warren, G.D. Westfall, H.H. Wieman, and K. Wolf. *Radial flow in Au+Au collisions at E=(0.25-1.15)A GeV. Phys. Rev. Lett.* **75**, 2662 (1995).

[Lopez and Siemens, 1984] J.A. Lopez and P.J. Siemens. *Nuclear fragmentation. Nucl. Phys.* A **431**, 728 (1984).

[Lucretius, 50BC] Titus Lucretius Carus. *De rerum natura.* 1. book, verse 716*ff* (50BC).

[Ma *et al.*, 1996] Y.G. Ma, A. Siwek, J. Péter, F. Gulminelli, R. Dayras, L. Nalpas, B. Tamein, E. Vient, G. Auger, Ch.O. Bacri, J. Benlliure, E. Bisquer, B. Borderie, R. Bougault, R. Brou, J.L. Charvet, A. Chbihi, J. Colin, D. Cussol, E. De Filippo, A. Demeyer, D. Doré, D. Durand, P. Ecomard, P. Eudes, E. Gerlic, D. Gourio, D. Guinet, R. Laforest, P. Lautesse, J.L. Laville, L. Lebreton, J.F. Lecolley, A. Le Fèvre, T. Lefort, R. Legrain, O. Lopez, M. Louvel, J. Lukasik, N. Marie, V. Métivier, A. Ouatizerga, M. Parlog, E. Plagnol, A. Rahmani, T. Reposeur, M.F. Rivet, E. Rosato, F. Saint-Laurent, M. Squalli, J.C. Steckmeyer, M. Stern, L. Tassan-Got, C. Volant, and J.P. Wieleczko. *Surveying the nuclear caloric curve.* LPC pre-print LPCC 96-10 (1996).

[Majka *et al.*, 1996] Z. Majka, P. Staszel, J. Cibor, J.B. Natowitz, K. Hagel, J. Li, N. Mdeiwayeh, R. Wada, and Y. Zhao. *Quantum statistical thermodynamics of hot nuclear systems: temperatures and isotopic yield ratios.* Texas A&M preprint 96-03 (1996).

[Marie *et al.*, 1997] N. Marie, R. Laforest, R. Bougault, J.P. Wieleczko, D. Durand, Ch.O. Bacri, J.F. Lecolley, F. Saint-Laurent, G. Auger, J. Benlliure, E. Bisquer, B. Borderie, R. Brou, J.L. Charvet, A. Chbihi, J. Colin, D. Cussol, R. Dayras, E. De Filippo, A. Demeyer, D. Doré, P. Ecomard, P. Eudes, D. Gourio, D. Guinet, P. Lautesse, J.L. Laville, A. Le Fèvre, T. Lefort, R. Legrain, O. Lopez, M. Louvel, V. Métivier, L. Nalpas, A. Ouatizerga, M. Parlog, J. Péter, E. Plagnol, A. Rahmani, T. Reposeur, M.F. Rivet, E. Rosato, S. Salou, M. Squalli, J.C. Steckmeyer, B. Tamain, L. Tassan-Got, E. Vient, C. Volant. *A hot expanding source in 50A MeV Xe+Sn central reactions. Phys. Lett.* B **391**, 15 (1997).

[Milkau *et al.*, 1993] U. Milkau, M.L. Begemann-Blaich, E.M. Eckert, G. Imme, P. Kreutz, A. Kühmichel, M. Lattuada, U. Lynen, C. Mazur, W.F.J. Müller, J.B. Natowitz, C. Ngo, J. Pochodzalla, G. Raciti, M. Ribrag, H. Sann, W. Trautmann, R. Trockel. *Inclusive fragment production in $^{84}Kr+^{197}Au$ at E/A = 35 MeV. Z. Phys.* A **346**, 227 (1993).

[Möhlenkamp, 1996] T. Möhlenkamp. *Bestimmung der Aufbruchtemperatur hochangeregter Kerne aus Isotopenverhältnissen leichter Fragmente.* PhD-thesis, Universität Dresden (1996).

[Moretto, 1995] L.G. Moretto. *Statistical emission of large fragments: a general theoretical approach. Nucl. Phys.* A **247**, 211 (1975).

[Moretto *et al.*, 1996] L.G. Moretto, R. Ghetti, L. Phair, K. Tso, and G.J. Wozniak. *Comment on "Probing the Nuclear Liquid-Gas Phase Transition" . Phys. Rev. Lett.* **76**, 2822 (1996).

[Morley *et al.*, 1996] K.B. Morley, K. Kwiatkowski, D.S. Bracken, E. Renshaw Foxford, V.E. Viola, N.R. Yoder, C. Volant, E.C. Pollaco, R. Legrain, R.G. Korteling, J. Brzychczyk, and H. Breuer. *4 π studies of the 1.8-4.8 GeV $^{3}He+^{nat}Ag$, ^{197}Au reactions. I. Energy deposition. Phys. Rev.* C **54**, 737 (1996).

[Müller *et al.*, 1996] W.F.J. Müller, R. Bassini, M. Begemann-Blaich, Th. Blaich, H. Emling, A. Ferrero, S. Fritz, C. Groß , G. Immé, I. Iori, U. Kleinevoß , G.J. Kunde, W.D. Kunze, V. Lindenstruth, U. Lynen, M. Mahi, A. Moroni, T. Möhlenkamp, B. Ocker, T. Odeh, J. Pochodzalla, G. Raciti, Th. Rubehn, H. Sann, M. Schnittker, A. Schüttauf, C. Schwarz, W. Seidel, V. Serfling, J. Stroth, W. Trautmann, A. Trzcinski, G. Verde, A. Wörner, E. Zude, B. Zwieglinski. *Determination of Critical Exponents in Nuclear Systems. Proceedings of the 1st Catania Relativistic Ion Studies: Critical Phenomena and Collective Observables*, edts. S. Costa, S. Albergo, A. Insolia, C. Tuvè, World Scientific, p. 107 (1996).

[Müntz *et al.*, 1995] C. Müntz, P. Baltes, H. Oeschler, A. Sartorius, A. Wagner, W. Ahner, R. Barth, M. Cieślak, M. Debowski, E. Grosse, W. Henning, P. Koczoń, D. Miśkowiec, R. Schicker, P. Senger, C. Bormann, D. Brill, Y. Shin, J. Stein, R. Stock, H. Ströbele, B. Kohlmeyer, H. Pöppl, F. Pühlhofer, J. Speer, K. Völkel, and W. Walus. *Properties of high-energy pions emitted from heavy-ion collisions at 1 GeV/nucleon. Z. Phys.* A **352**, 175 (1995), and references therein.

[Natowitz *et al.*, 1995] J.B. Natowitz, K. Hagel, R. Wada, Z. Majka, P. Gonthier, J. Li, N. Mdeiwayeh, B. Xiao, and Y. Zhao. *Limiting temperature of neutron rich nuclei: a possible interpretation of data from isotope yield ratios. Phys. Rev.* C **52**, R2322 (1995).

[Nayak *et al.*, 1992] T.K. Nayak, T. Murakami, W.G. Lynch, K. Swartz, D.J. Fields, C.K. Gelbke, Y.D. Kim, J. Pochodzalla, M.B. Tsang, H.M. Xu, F. Zhu, K. Kwiatkowski. *Emission temperatures from the decay of particle unstable complex nuclei. Phys. Rev.* C **45**, 132 (1992).

[Ogilvie *et al.*, 1991] C.A. Ogilvie, J.C. Adloff, M. Begemann–Blaich, P. Bouissou, J. Hubele, G. Imme, I. Iori, P. Kreutz, G.J. Kunde, S. Leray, V. Lindenstruth, Z. Liu, U. Lynen, R.J. Meijer, U. Milkau, W.F.J. Müller, C. Ngô, J. Pochodzalla, G. Raciti, G. Rudolf, H. Sann, A. Schüttauf, W. Seidel, L. Stuttge, W. Trautmann, and A. Tucholski. *Rise and fall of multifragment emission. Phys. Rev. Lett.* **67**, 1214 (1991).

[Ohnishi and Randrup, 1996] A. Ohnishi and J. Randrup. *Inclusion of quantum fluctuations in wave packet-dynamics.*, Ann. Phys. (in press), nucl-th/9604040; A. Ohnishi and J. Randrup. *Quantum fluctuation effects on nuclear fragment formation. Phys. Lett.* B **394**, 260 (1997).

[Pak *et al.*, 1996] R. Pak, D. Craig, E.E. Gualtieri, S.A. Hannuschke, R.A. Lacey, J. Lauret, W.J. Llope, N.T.B. Stone, A.M. Vander Molen, G.D. Westfall, and J. Yee. *Radial flow in $^{40}Ar+^{45}Sc$ reactions at E=35-115 MeV/nucleon. Phys. Rev.* C **54**, 1681 (1996).

[Pal *et al.*, 1996] S. Pal, S.K. Samaddar, and J.N. De. *The effect of flow on nuclear multifragmentation in a quantum statistical model. Nucl. Phys.* A **608**, 49 (1996).

[Panagiotou *et al.*, 1984] A.D. Panagiotou, M.W. Curtin, H. Toki, D.K. Scott, and P.J. Siemens. *Experimental evidence for a liquid-gas phase transition in nuclear systems. Phys. Rev. Lett.* **52**, 496 (1984).

[Panagiotou *et al.*, 1996] A.D. Panagiotou, G. Mavromanolakis, and J. Tzoulis. *Determination of temperature and transverse flow velocity at chemical freeze-out in relativistic nuclear interactions. Phys. Rev.* C **53**, 1353 (1996).

[Papp and Nörenberg, 1995] G. Papp and W. Nörenberg. *The path of hot nuclei towards multifragmentation.* International Workshop XXII on Gross Properties of Nuclei and Nuclear Excitations, Hirschegg 1994, p. 87, GSI-preprint GSI-95-30 (1995) and nucl-th/9506012.

[Peaslee *et al.*, 1994] G.F. Peaslee, M.B. Tsang, C. Schwarz, M.J. Huang, W.S. Huang, W.C. Hsi, C. Williams, W. Bauer, D.R. Bowman, M. Chartier, J. Dinius, C.K. Gelbke, T. Glasmacher, D.O. Handzy, M.A. Lisa, W.G. Lynch, C.M. Mader, L. Phair, M-C. Lemaire, S.R. Souza, G. Van Buren, R.J. Charity, L.G. Sobotka, G.J. Kunde, U. Lynen, J. Pochodzalla, H. Sann, W. Trautmann, D. Fox, R.T. de Souza, G. Peilert, W.A. Friedman, and N. Carlin. *Energy dependence of multifragmentation in* $^{84}Kr+^{197}Au$ *collisions. Phys. Rev.* C **49**, R2271 (1994).

[Peilert *et al.*, 1991] G. Peilert, J. Randrup, H. Stöcker, and W. Greiner. *Clustering in nuclear matter at saturation densities. Phys. Lett.* B **260**, 271 (1991).

[Péter *et al.*, 1995] J. Péter, S.C. Jeong, J.C. Angélique, G. Auger, G. Bizard, R. Brou, A. Buta, C. Cabot, Y. Cassagnou, E. Crema, D. Cussol, D. Durand, Y. El Masri, P. Eudes, Z.Y. He, A. Kerambrun, C. Lebrun, R. Legrain, J.P. Patry, A. Péghaire, R. Régimbart, E. Rosato, F. Saint-Laurent, J.C. Steckmeyer, B. Tamain, E. Vient. *Binary dissipative processes and formation of hot nuclei in* $^{36}Ar+^{27}Al$ *reactions from 55 to 95 MeV/u. Nucl. Phys.* A **593**, 95 (1995).

[Phair *et al.*, 1993] L. Phair, W. Bauer and C.K. Gelbke. *Percolation withg bubbles and toroids. Phys. Lett.* B **314**, 271 (1993).

[Pienkowski *et al.*, 1994] L. Pienkowski, H.G. Bohlen, J. Cugnon, H. Fuchs, J. Galin, B. Gatty, B. Gebauer, D. Guerreau, D. Hilscher, D. Jacquet, U. Jahnke, M. Josset, X. Ledoux, S. Leray, B. Lott, M. Morjean, A. Péghaire, G. Röschert, H. Rossner, R.H. Siemssen, C. Stéphan. *Hot nuclei in reactions induced by 475 MeV, 2 GeV* ^{1}H *and 2 GeV* ^{3}He*. Phys. Lett.* B **336**, 147 (1994).

[Pochodzalla *et al.*, 1985] J. Pochodzalla, W.A. Friedman, C.K. Gelbke, W.G. Lynch, M. Maier, D. Ardouin, H. Delagrange, H. Doubre, C. Gregóire, A. Kyanowski, W. Mittig, A. Péghaire, J. P eter, F. Saint-Laurent, Y.P. Viyogi, B. Zwieglinski, G. Bizard, F. Lefèbvres, B. Tamain, and J. Quebert. *Nuclear temperature and the population of particle- unstable states of* ^{6}Li *in* ^{40}Ar*-induced reactions on* ^{197}Au *at E/A = 60 MeV. Phys. Rev. Lett.* **55**, 177 (1985).

[Pochodzalla *et al.*, 1987] J. Pochodzalla, C.K. Gelbke, W.G. Lynch, M. Maier, D. Ardouin, H. Delagrange, H. Doubre, C. Greghóire, A. Kyanowski, W. Mittig, A. Péghaire, J. P eter, F. Saint-Laurent, B. Zwieglinski, G. Bizard, F. Lefèbvres, B. Tamain, J. Quebert, Y.P. Viyogi, W.A. Friedman, and D.H. Boal. *Two-particle correlations at small relative momenta for* ^{40}Ar*-induced reactions in* ^{197}Au *at E/A=60 MeV. Phys. Rev.* C **35**, 1695 (1987).

[Pochodzalla *et al.*, 1994] J. Pochodzalla, J.C. Adloff, M. Begemann-Blaich, P. Bouissou, T. Hofmann, J. Hubele, G. Imme, I. Iori, J. Kempter, P. Kreutz, G.J. Kunde, W.D. Kunze, S. Leray, V. Lindenstruth, Z. Liu, U. Lynen, M. Mang, R.J. Meijer, U. Milkau, A. Moroni, W.F.J. Müller, C. Ngô, B. Ocker, C.A. Ogilvie, G. Raciti, F. Rosenberger, G. Rudolf, H. Sann, R. Scardoni, A. Schüttauf, W. Seidel, V. Serfling, L. Stuttge, W. Trautmann, A. Tucholski, A. Wörner, B. Zwieglinski. *Correlations and fluctuations in nuclear multifragmentation.* International Workshop on Dynamical Features of Nuclei and Finite Fermi Systems, Sitges, 13.-17 September 1993, edited by X. Vinas, M. Pi and A. Ramos, (World Scientific 1994), pp. 46.

[Pochodzalla, 1994] J. Pochodzalla. *Multifragmentation and the quest for the liquid-gas phase transition.* Nato Advanced Study Institute on Hot and Dense Nuclear Matter, Bodrum, 1993, NATO ASI Series B Vol 335, Plenum Press, New York, pp. 39.

[Pochodzalla *et al.*, 1995] J. Pochodzalla, T. Möhlenkamp, T. Rubehn, A. Schüttauf, A. Wörner, E. Zude, M. Begemann–Blaich, Th. Blaich, H. Emling, A. Ferrero, C. Groß, G. Imme, I. Iori, G.J. Kunde, W.D. Kunze, V. Lindenstruth, U. Lynen, A. Moroni, W.F.J. Müller, B. Ocker, G. Raciti, H. Sann, C. Schwarz, W. Seidel, V. Serfling, J. Stroth, W. Trautmann, A. Trzcinski, A. Tucholski, G. Verde, and B. Zwieglinski. *Probing the nuclear liquid-gas phase transition. Phys. Rev. Lett.* **75**, 1040 (1995).

[Pochodzalla *et al.*, 1996] J. Pochodzalla, T. Möhlenkamp, T. Rubehn, A. Schüttauf, A. Wörner, E. Zude, M. Begemann–Blaich, Th. Blaich, H. Emling, A. Ferrero, C. Groß, G. Imme, I. Iori, G.J. Kunde, W.D. Kunze, V. Lindenstruth, U. Lynen, A. Moroni, W.F.J. Müller, B. Ocker, G. Raciti, H. Sann, C. Schwarz, W. Seidel,

V. Serfling, J. Stroth, W. Trautmann, A. Trzcinski, A. Tucholski, G. Verde, and B. Zwieglinski. *Reply to [Moretto et al., 1996]. Phys. Rev. Lett.* **76**, 2823 (1996).

[Poggi *et al.*, 1995] G. Poggi, G. Pasquali, M. Bini, P. Maurenzig, A. Olmi, N. Taccetti, J.P. Alard, V. Amouroux, Z. Basrak, N. Bastid, I.M. Belayev, L. Berger, Th. Blaich, S. Boussange, A. Buta, R. Caplar, C. Cerruti, N. Cindro, J.P. Coffin, R. Dona, P. Dupieux, M. Dzelalija, J. Erö, Z.G. Fan, P. Fintz, Z. Fodor, L. Fraysse, R. Freifelder, S. Frolov, A. Gobbi, Y. Grigorian, G. Guillaume, N. Herrmann, K.D. Hildenbrand, S. Hölbling, A. Houari, S.C. Jeong, F. Fundt, J. Kecskemeti, P. Koncz, Y. Korchagin, R. Kotte, M. Krämer, C. Kuhn, M. Ibnouzahir, I. Legrand, A. Lebedev, C. Maguire, V. Manko, G. Mgebrishvili, J. Mösner, D. Moisa, G. Montarou, I. Montbel, P. Morel, W. Neubert, D. Pelte, M. Petrovici, F. Rami, V. Ramillien, W. Reisdorf, A. Sadchikov, D. Schüll, Z. Seres, B. Sikora, V. Simion, S. Smolyankin, U. Sodan, K. The, R. Tezkratt, M. Trzaska, M.A. Vasiliev, P. Wagner, J.P. Wessels, T. Wienold, Z. Wilhelmi, D. Wohlfarth, A.V. Zhilin, and P. Danielewicz. *Evidence for collective expansion in light-particle emission following Au+Au collisions at 100, 150 and 250 A·MeV. Nucl. Phys.* A **586**, 755 (1995).

[Porile *et al.*, 1989] N.T. Porile, A.J. Bujak, D.D. Carmony, Y.H. Chung, L.J. Gutay, A.S. Hirsch, M. Mahi, G.L. Paderewski, T.C. Sangster, R.P. Scharenberg, and B.C. Stringfellow. *Approach to criticality in the fragmentation of xenon by 1-19 GeV protons. Phys. Rev.* C **39**, 1914 (1989).

[Pouthas *et al.*, 1995] J. Pouthas, B. Borderie, R. Dayras, E. Plagnol, M.F. Rivet, F. Saint-Laurent, J.C. Steckmeyer, G. Auger, C.O. Bacri, S. Barbey, A. Barbier, A. Benkirane, J. Benlliure, B. Berthier, E. Bougamont, P. Bourgault, P. Box, R. Bzyl, B. Cahan, Y. Cassagnou, D. Charlet, J.L. Charvet, A. Chbihi, T. Clerc, N. Copinet, D. Cussol, M. Engrand, J.M. Gautier, Y. Huguet, O. Journiaux, J.L. Laville, P. Le Botlan, A. Leconte, R. Legrain, P. Lelong, M. Le Guay, L. Martina, C. Mazur, P. Mosrin, L. Olivier, J.P. Passerieux, S. Pierre, B. Piquet, E. Plaige, E.C. Pollacco, B. Raine, A. Richard, J. Ropert, C. Spitaels, L. Stab, D. Sznajderman, L. Tassan-got, J. Tillier, M. Tripon, P. Vallerand, C. Volant, P. Volkov, J.P. Wieleczko, and G. Wittwer. *INDRA, a 4π charged product detection array at GANIL. Nucl. Instrum. Methods* A **357**, 418 (1995).

[Pratt *et al.*, 1989] S. Pratt. *Nuclear thermometers for heavy-ion collisions. Phys. Rev.* C **40**, 168 (1989).

[Pratt *et al.*, 1995] S. Pratt, C. Montoya, and F. Ronning. *Balancing nuclear matter between liquid and gas. Phys. Lett.* B **349**, 261 (1995).

[Puri *et al.*, 1996] R.K. Puri, C. Hartnack, and J. Aichelin. *Early fragment formation in heavy-ion collsions. Phys. Rev.* C **54**, R28 (1996).

[Reichl, 1980] see for example L.E. Reichl. *A Modern Course in Statistical Physics.* University of Texas Press 1980, p.95ff.

[Reisdorf, 1994] W. Reisdorf. *Collective flow and cluster production in Au on Au collisions.* Proceedings of *International Workshop XXII on Gross Properties of Nuclei and Nuclear Excitations, Hirschegg, 1994*, edited by H. Feldmeier and W. Nörenberg (GSI, Darmstadt, 1994) p. 93.

[Renshaw Foxford *et al.*, 1996] E. Renshaw Foxford, K. Kwiatkowski, D.S. Bracken, K.B. Morley, V.E. Viola, N.R. Yoder, C. Volant, E.C. Pollaco, R. Legrain, R.G. Korteling, W.A. Friedman, J. Brzychczyk, and H. Breuer. *$4\,\pi$ studies of the 1.8-4.8 GeV $^3He+^{nat}Ag$, ^{197}Au reactions. II. Multifragmentation. Phys. Rev.* C **54**, 749 (1996).

[Sa *et al.*, 1990] Ben-Hao Sa, Yu-Ming Zheng, and Xiao-Ze Zhang. *Dependence of the phase transition on the mass number of hot nuclei before break-up. Nucl. Phys.* A **509**, 499 (1990).

[Satpathy *et al.*, 1989] L. Satpathy, M. Mishra, and R. Nayak. *Nuclear liquid-gas phase transition with finite range force. Phys. Rev.* C **39**, 162 (1989).

[Schüttauf *et al.*, 1996] A. Schüttauf, W.D. Kunze, A. Wörner, M. Begemann-Blaich, Th. Blaich, D.R. Bowman, R.J. Charity, A. Cosmo, A. Ferrero, C.K. Gelbke, C. Groß , W.C. Hsi, J. Hubele, G. Imme, I. Iori, P. Kreutz, G.J. Kunde, V. Lindenstruth, M.A. Lisa, W.G. Lynch, U. Lynen, M. Mang, T. Möhlenkamp, A. Moroni, W.F.J. Müller, M. Neumann, B. Ocker, C.A. Ogilvie, G.F. Peaslee, J. Pochodzalla, G. Raciti, F. Rosenberger, Th. Rubehn, H. Sann, W. Seidel, V. Serfling, L.G. Sobotka, J. Stroth, L. Stuttge, S. Tomasevic, W. Trautmann, A. Trzcinski, M.B. Tsang, A. Tucholski, G. Verde, C.W. Williams, E. Zude, and B. Zwieglinski. *Universality of spectator fragmentation at relativistic bombarding energies. Nucl. Phys.* A **607**, 457 (1996).

[Schüttauf, 1997] A. Schüttauf. *Untersuchung der Kernfragmentation.* PhD-thesis, Universität Frankfurt a.M. (1997).

[Schwarz *et al.*, 1993] C. Schwarz, W.G. Gong, N. Carlin, C.K. Gelbke, Y.D. Kim, W.G. Lynch, T. Murakami, G. Poggi, R.T. de Souza, M.B. Tsang, H.M. Xu, D.E. Fields, K. Kwiatkowski, V.E. Viola, Jr., and S.J. Yennello. *Emission temperatures from widely separated states in ^{14}N- and ^{129}Xe- induced reactions. Phys. Rev.* C **48**, 676 (1993).

[Schwarz *et al.*, 1997a] C. Schwarz, R. Bassini, M. Begemann-Blaich, A.S. Botvina, S. Fritz, S.J. Gaff, C. Groß, G. Immé, I. Iori, U. Kleinevoß, G.J. Kunde, W.D. Kunze, U. Lynen, V. Maddalena, M. Mahi, T. Möhlenkamp, A. Moroni, W.F.J. Müller, C. Nociforo, B. Ocker, T. Odeh, F. Petruzzelli, J. Pochodzalla, G. Raciti, G. Riccobene, F.P. Romano, Th. Rubehn, A. Saija, M. Schnittker, A. Schüttauf, W. Seidel, V. Serfling, C. Sfienti, W. Trautmann, A. Trzcinski, G. Verde, A. Wörner, Hongfei Xi, B. Zwieglinski. *Source Temperatures and Sizes in Central Collisions.* 35th International Winter Meeting on Nuclear Physics, Bormio, Italy, 26. Januar - 1. Februar, 1997, nucl-ex/9704001

[Schwarz *et al.*, 1997b] C. Schwarz, V. Serfling, R. Bassini, M. Begemann-Blaich, S. Fritz, S. Gaff, C. Groß , G. Imme, I. Iori, U. Kleinevoß , G.J. Kunde, W.D. Kunze, U. Lynen, V. Maddalena, M. Mahi, T. Möhlenkamp, A. Moroni, W.F.J. Müller, C. Nociforo, B. Ocker, T. Odeh, F. Petruzzelli, J. Pochodzalla, G. Raciti, G. Riccobene, F.P. Romano, A. Saija, M. Schnittker, A. Schüttauf, W. Seidel, C. Sfienti, W. Trautmann, A. Trzcinski, W. Wörner, H. Xi, and B. Zwieglinski. *Freeze out conditions for exploding nuclei.* (to be published).

[Serfling, 1996] V. Serfling. *Temperatumessungen in Au+Au Reaktionen bei Energien zwischen 50 und 200 AMeV.* PhD-thesis, Universität Frankfurt a.M. (1997).

[Siemens, 1983] P.J. Siemens. *Liquid-gas phase transition in nuclear matter. Nature* **305**, 410 (1983).

[Siemens, 1984] P.J. Siemens. *Nuclear fog. Nucl. Phys.* A **428**, 189c (1984).

[Soff *et al.*, 1995] S. Soff, S.A. Bass, C. Hartnack, H. Stöcker, and W. Greiner. *Disappearance of flow. Phys. Rev.* C **51**, 3320 (1995).

[Song and Su, 1991] H.Q. Song and R.K. Su. *Coulomb instability in hot nuclei with skyrme interaction. Phys. Rev.* C **44**, 2505 (1991).

[Stauffer and Aharony, 1992] D. Stauffer and A. Aharony. *Introduction to Percolation Theory.* Taylor & Francis, London (1992).

[Stöcker *et al.*, 1979] H. Stöcker, J. Maruhn, and W. Greiner. *On the possibility of detecting density isomers in high energy heavy ion collisions. Phys. Lett.* B **81**, 303 (1979).

[Sümmerer *et al.*, 1990] K. Sümmerer, W. Brüchle, D.J. Morrissey, M. Schädel, B. Szweryn, and Yang Weifan. *Target-fragmentation of Au and Th by 2.6 GeV protons. Phys. Rev.* C **42**, 2546 (1990).

[Tamagaki, 1993] R. Tamagaki. *Introduction. Prog. Theor. Phys. Suppl. No.***112**, 1 (1993).

[Trautmann *et al.*, 1993] W. Trautmann, U. Milkau, U. Lynen, J. Pochodzalla. *Systematics of the Power Law Parameter and Minimum Angular Momenta for Fragment Production. Z. Phys.* A **344**, 447 (1993).

[Tsang *et al.*, 1993] M.B. Tsang, W.C. Hsi, W.G. Lynch, D.R. Bowman, C.K. Gelbke, M.A. Lisa, G.F. Peaslee, G.J. Kunde, M.L. Begemann–Blaich, T. Hofmann, J. Hubele, J. Kempter, P. Kreutz, W.D. Kunze, V. Lindenstruth, U. Lynen, M. Mang, W.F.J. Müller, M. Neumann, B. Ocker, C.A. Ogilvie, J. Pochodzalla, F. Rosenberger, H. Sann, A. Schüttauf, V. Serfling, J. Stroth, W. Trautmann, A. Tucholski, A. Wörner, E. Zude, B. Zwieglinski, S. Aiello, G. Imme, V. Pappalardo, G. Raciti, R.J. Charity, L.G. Sobotka, I. Iori, A. Moroni, R. Scardaoni, A. Ferrero, W. Seidel, Th. Blaich, L. Stuttge, A. Cosmo, W.A. Friedman, and G. Peilert. *Onset of nuclear vaporization. Phys. Rev. Lett.* **71**, 1502 (1993).

[Tsang *et al.*, 1996a] M.B. Tsang, F. Zhu, W.G. Lynch, A. Aranda, D.R. Bowman, R.T. de Souza, C.K. Gelbke, Y.D. Kim, L. Phair, C. Williams, H.M. Xu, and W.A. Friedman. *Cross comparison of nuclear temperatures determined from excited states populations and isotope yields. Phys. Rev.* C **53**, R1057 (1996).

[Tsang *et al.*, 1996b] M.B. Tsang, W.G. Lynch, H. Xi, and W.A. Friedman. *Nuclear temperature thermometers from isotope yield ratios. Phys. Rev.* C (in print).

[Viola *et al.*, 1996] V.E. Viola, W.C. Hsi, K. Kwiatkowski, G. Wang, D.S. Bracken, E. Cornell, E. Renshaw Foxford, D. Ginger, K.B. Morley, N.R. Yoder, R.G. Korteling, H. Breuer, F. Gimeno-Nogues, E. Ramakrishnan, D. Rowland, S.J. Yennello, M.J. Huang, W.G. Lynch, M.B. Tsang, H. Xi, Y.Y. Chu, S. Gushue, L.P. Remsberg, R. Legrain, E.C. Pollacco, C. Volant, and J. Brzychczyk. *Probing the nuclear EOS with GeV light-ion beams.* Proceedings of Third International Conference on Nuclear Physics at Storage Rings STORI96, Bernkastel-Kues, Germany, 1996.

[Wales and Ohmine, 1993] D.J. Wales and I. Ohmine. *Structure, dynamics, and thermodynamics of model $(H_2O)_8$ and $(H_2O)_{20}$ clusters. J. Chem. Phys.* **98**, 7245 (1993).

[Wang *et al.*, 1997] G. Wang, K. Kwiatkowski, K.B. Morley, D.S. Bracken, E. Renshaw Foxford, W.A. Friedman, R.G. Korteling, R. Legrain, E.C. Pollacco, V.E. Viola, C. Volant. *Time dependence of multifragmentation in light-ion-induced reactions. Phys. Lett.* B **393**, 290 (1997).

[Warren *et al.*, 1996] P. G. Warren, S. Albergo, J. M. Alexander, F. Bieser, F. P. Brady, Z. Caccia, D. A. Cebra, A. D. Chacon, J. L. Chance, Y. Choi, S. Costa, J. B. Elliott, M. L. Gilkes, J. A. Hauger, A. S. Hirsch, E. L. Hjort, A. Insolia, M. Justice, D. Keane, J. C. Kitner, R. Lacey, J. Lauret, V. Lindenstruth, M. A. Lisa, H. S. Matis, R. L. McGrath, M. McMahan, C. McParlan, W. F. J. Müller, D. L. Olson, M. D. Partlan, N. T. Porile, R. Potenza, G. Rai, J. Rasmussen, H. G. Ritter, J. Romanski, J. L. Romero, G. V. Russo, H. Sann, R. P. Scharenberg, A. Scott, Y. Shao, B. K. Srivastava, T. J. M. Symons, M. L. Tincknell, C. Tuve, S. Wang, H. H. Wieman, T. Wienold, and K. Wolf. *The evolution of nuclear multifragmentation in the temperature-density plane.* nucl-ex/9610008 (1996).

[Warwick *et al.*, 1983] A.I. Warwick, H.H. Wieman, H.H. Gutbrod, M.R. Maier, J. Péter, H.G. Ritter, H. Stelzer, F. Weik, M. Freedman, D.J. Henderson, S.B. Kaufman, E.P. Steinberg, and B.D. Wilkins. *Breakup pd spectator residues in relativistic nuclear collisions. Phys. Rev.* C **27**, 1083 (1983).

[Wörner, 1995] A. Wörner. *Kritisches Verhalten in der Kernfragmentation.* PhD-thesis, Universität Frankfurt a.M. (1995).

[Xi *et al.*, 1996a] H. Xi, W.G. Lynch, M.B. Tsang, and W.A. Friedman. *Secondary decays and the helium lithium isotope thermometer. Phys. Rev.* C **54**, R2163 (1996).

[Xi *et al.*, 1996b] Hongfei Xi, T. Odeh, R. Bassini, M. Begemann-Blaich, A.S. Botvina, S. Fritz, S.J. Gaff, C. Groß, G. Immé, I. Iori, U. Kleinevoß, G.J. Kunde, W.D. Kunze, U. Lynen, V. Maddalena, M. Mahi, T. Möhlenkamp, A. Moroni, W.F.J. Müller, C. Nociforo, B. Ocker, F. Petruzzelli, J. Pochodzalla, G. Raciti, G. Riccobene, F.P. Romano, Th. Rubehn, A. Saija, M. Schnittker, A. Schüttauf, C. Schwarz, W. Seidel, V. Serfling, C. Sfienti, W. Trautmann, A. Trzcinski, G. Verde, A. Wörner, and B. Zwieglinski. *Breakup temperatures of target spectators in $^{197}Au+^{197}Au$ collisions at $E/A = 1000$ MeV.* (to be published).

[Xu *et al.*, 1989] H.M. Xu, W.G. Lynch, C.K. Gelbke, M.B. Tsang, D.J. Fields, M.R. Maier, D.J. Morrissey, T.K. Nayak, J. Pochodzalla, D.G. Sarantities, L.G. Sobotka, M.L. Halbert, D.C. Hensley. *Complex fragments emitted in particle stable states for the ^{32}S + ^{nat}Ag reaction at $E/A = 22.3$ MeV. Phys. Rev.* C **40**, 186 (1989).

[Yariv and Fraenkel, 1979] Y. Yariv and Z. Fraenkel. *Backward production of light ions in the interaction of 400 GeV protons with nuclei. Phys. Rev.* C **20**, 2227 (1979); Y. Yariv and Z. Fraenkel. *Intranuclear cascade calculations of high energy heavy ion collisions: effect of interactions between cascade particles. Phys. Rev.* C **24**, 488 (1981).

[Zabrodin, 1995] E.E. Zabrodin. *Vapor-liquid phase transition and multifragmentation. Phys. Rev.* C **52**, 2608 (1995).

[Zhang *et al.*, 1996] Yi-Jun Zhang, Ru-Keng Su, Hongqiu Song, and Fu-Min Lin. *Thermodynamical properties and Coulomb instabilities in hot nuclear systems with the Gogny interaction. Phys. Rev.* C **54**, 1137 (1996).